

---

**UNIVERSITY OF SZEGED, DOCTORAL SCHOOL OF GEOSCIENCES**

**INTEGRATED CHARACTERIZATION OF LOWER-NUBIAN  
HYDROCARBON RESERVOIRS, WITH SPECIAL EMPHASIS ON  
GEOSTATISTICAL UNCERTAINTIES**

---

**DOCTORAL (PhD) DISSERTATION**

**by**

**OMAR SLIMAN**

**Supervisor**

**Dr. Janos Geiger**

**associate professor**

**University of Szeged**

**Department of Geology and Paleontology**

**2011**

---

## Table of Contents

Table of Contents .....	1
List of Figures .....	6
List of Tables.....	10
1 INTRODUCTION .....	11
2 GENERAL OVERVIEW OF THE FIELD .....	12
2.1 LOCATION AND HISTORY OF DISCOVERY .....	12
2.2 GEOLOGICAL OVERVIEW .....	14
2.2.1 Stratigraphy.....	14
2.2.2 Structural makeup.....	16
3 METHODS.....	17
3.1 SEDIMENTOLOGICAL ANALYSES.....	17
3.1.1 Data preparation.....	20
3.1.2 Data analysis .....	21
3.1.2.1 Statistical description of continuous variables.....	22
3.1.2.2 Descriptive statistics .....	25
3.1.2.3 Categorical variable statistics .....	25
3.1.3 Well-log correlation .....	25
3.1.4 Core Porosity-Permeability correlation .....	26
3.2 PETROPHYSICS: GENERAL OVERVIEW.....	28
3.2.1 Deterministic approaches .....	29
3.2.2 Optimizing deterministic approach .....	30
3.2.3 Statistical approach.....	31
3.2.4 Statistical or deterministic lithology analysis?.....	31
3.2.5 What is the practical way of deterministic analysis?.....	32

3.2.6	Quantitative well log interpretation .....	33
3.2.6.1	Porosity definitions .....	34
3.2.6.1.1	Geological definition .....	34
3.2.6.1.2	Petrophysical definition .....	34
3.2.6.2	Permeability .....	34
3.2.6.2.1	Permeability definitions: .....	35
3.3	<i>GEOSTATISTICAL APPROACH FOR CHARACTERIZING THE DIFFERENT SPACES OF UNCERTAINTY</i> .....	35
3.3.1	The roots of uncertainty .....	36
3.3.2	Local and regional uncertainties .....	37
4	RESULTS .....	40
4.1	<i>SEDIMENTOLOGICAL CHARACTERIZATION OF THE FIELD</i> .....	40
4.1.1	Reservoir rock types .....	41
4.1.1.1	Base Unite: LNB .....	41
4.1.1.2	Middle Unite: LNM .....	42
4.1.1.3	Upper Unite: LNU .....	44
4.2	<i>FACIES ANALYSIS</i> .....	46
4.2.1	Braided Stream Association (BR)-Channel Facies .....	46
4.2.1.1	Channels in the LNU sequence .....	47
4.2.1.2	Channels in the LNM sequence .....	48
4.2.1.3	Channels in the LNB sequence .....	48
4.2.2	Braided Stream Association (BR)-Sand flat/Channel Abandonment Facies .....	48
4.2.2.1	Sand flat/Channel abandonment in LNU sequence .....	49
4.2.2.2	Sand flat/Channel abandonment in LNM sequence .....	49
4.2.3	Braided Stream Association (BR)-Abandoned Channel Facies .....	49
4.2.3.1	Abandoned channels in LNU sequence .....	50

4.2.3.2	Abandoned channels in LNM sequence .....	50
4.2.4	Estuarine/Deltaic Facies Association(ED) .....	50
4.2.4.1	Channel Deposits .....	50
4.2.4.2	Mouth bar deposits: .....	51
4.2.4.3	Abandoned Channel Deposits: .....	51
4.2.4.4	Channel /Bar Margin Deposits.....	52
4.2.4.4.1	Splay Deposits .....	52
4.2.4.4.2	Tidal Sand Flat Deposits .....	53
4.2.5	Fluvial Facies Association (FL) .....	53
4.2.5.1	Channel Deposits .....	53
4.2.5.2	Abandon Channel Deposits .....	54
4.2.5.3	Crevasse Splay Deposits .....	54
4.2.5.4	Lake/Overbank Deposits.....	54
4.2.6	Debris Flow Deposits Facies Association .....	55
4.3	<i>PETROPHYSICAL CHARACTERISTICS OF THE FACIESES</i> .....	55
4.3.1	Controls on Porosity and Permeability .....	56
4.3.1.1	Primary Controls: .....	56
4.3.1.2	Secondary or Diagenetic Controls: .....	57
4.4	<i>RESERVOIR ZONES BASED ON LATERAL CONNECTIONS OF SEDIMENTARY FACIESES</i> .....	59
4.4.1	Upper Unite.....	62
4.4.1.1	Reservoir Zone LNU9: .....	62
4.4.1.2	Reservoir Zone LNU8: .....	62
4.4.1.3	Reservoir Zone LNU7: .....	63
4.4.1.4	Reservoir Zone LNU6 .....	63
4.4.1.5	Reservoir Zone LNU5 : .....	64
4.4.1.6	Reservoir Zone LNU4 : .....	64



4.4.1.7	Reservoir Zone LNU3: .....	65
4.4.1.8	Reservoir Zone LNU2: .....	65
4.4.1.9	Reservoir Zone LNU1: .....	66
4.4.2	Middle Unite .....	66
4.4.2.1	Reservoir Zone LNM4: .....	66
4.4.2.2	Reservoir Zone LNM3: .....	67
4.4.2.3	Reservoir Zone LNM2: .....	67
4.4.2.4	Reservoir Zone LNM1: .....	68
4.4.3	Base Unite .....	68
4.4.3.1	Reservoir Zone LNB:.....	68
4.5	<i>CORED INTERVALS WITHIN THE ROCK BODY</i> .....	69
4.6	<i>PETROPHYSICAL RESULTS</i> .....	72
4.6.1	Depth shifts .....	75
4.6.2	Log Headings .....	76
4.6.3	Quantitative Interpretation Parameters.....	76
4.6.4	Quantitative evaluation of lithology in the Lower Nubian Formation .....	78
4.6.5	Evaluation of petrophysical properties in the Nubian formation.....	81
4.6.5.1	Selection of cutoff parameters.....	82
4.6.5.2	Distribution of the reservoirs into lithofacies and/or hydraulic units.....	83
4.7	<i>RESULTS OF WELL LOG CORRELATIONS</i> .....	87
4.7.1	Lower Nubian Formation: Stratigraphic succession and correlation .....	87
4.7.2	Flow-unite concept .....	90
4.7.3	Petrophysical zoning concept .....	91
4.7.3.1	Base and Middle units -Petrophysical layers package.....	92
4.7.3.2	Upper unite- petrophysical layers package .....	92
4.8	<i>GEOLOGICAL MODEL</i> .....	97

4.8.1	Model Grid .....	97
4.8.2	Layers .....	98
4.9	<i>RESULTS OF GEOSTATISTICAL APPROACHES</i> .....	99
4.9.1	Original data distribution .....	100
4.9.2	Modeling of experimental variograms .....	100
4.9.3	Stochastic realizations.....	103
4.10	<i>UNCERTAINTY APPROACH</i> .....	104
4.10.1	Uncertainty of porosity .....	104
4.10.2	Uncertainty of permeability.....	107
4.10.2.1	Regions with high level of uncertainty .....	108
4.10.3	Uncertainty of shale volume .....	112
4.10.3.1	Regions with high level of uncertainty .....	112
5	<i>DISCUSSION AND CONSLUSIONS</i> .....	114
5.1	<i>SEDIMENTARY CORE ANALYSIS</i> .....	114
5.2	<i>LOG ANALYSIS</i> .....	116
5.3	<i>UNCERTAINTY ANALYSIS</i> .....	117
6	<i>REFERENCES CITED</i> .....	118
7	<i>SUMMARY</i> .....	122
8	<i>SUMMARY in HUNGARIAN</i> .....	124

## **List of Figures**

Fig. 2.1-1 Study area location map (modified after Waha, 2007) .....	12
Fig. 2.2-1 General Stratigraphic column ( modified after Waha 2005).....	15
Fig. 3.1-1 Core description labels and indicators, lithology example .....	20
Fig. 3.1-2 Data base structure of the available data .....	21
Fig. 3.1-3. Histogram of permeability with a negatively skewed frequency distribution. ....	22
Fig. 3.1-4. Histogram of porosity following a multimodal frequency distribution .....	23
Fig. 3.1-5 Box-whisker plot of shale volume categorized by facies .....	24
Fig. 3.1-6 Scatterplot of porosity versus permeability coded by facies.....	24
Fig. 3.1-7 Categorical variable histogram. ....	25
Fig. 3.1-8 Porosity -Permeability correlation scatter- plot .....	27
Fig. 4.1-1: Location map with the cored wells (Note the scale is given in feet) .....	40
Fig. 4.1-2 : Frequency distribution of lithofacieses in LNB sequence of well 6J3 .....	42
Fig. 4.1-3: Frequency distribution of lithofacieses in LNM sequence of well 6J3 and 6J8 .....	43
Fig. 4.1-4: Frequency distribution of lithofacieses in LNM sequence of well 6J12.....	44
Fig. 4.1-5: Frequency distribution of lithofacieses in LNU sequence of well 6J14 and 6J6 .....	45
Fig. 4.1-6: Frequency distribution of lithofacieses in LNU sequence of well 6J12 and 6J8 .....	45
Fig. 4.2-1.: Lithological composition and grain-size characteristics of channels.....	47
4.2-2. Fig.: Lithological compositions and grain-size characteristics of braided sand flats.....	49
Fig. 4.2-3 Lithological compositions and grain-size characteristics of abandoned channels .....	49
Fig. 4.2-4 Lithological composition and grain-size characteristics of ED channel facies .....	51
Fig. 4.2-5 : Lithological composition and grain-size characteristics of mouth bars.....	51
Fig. 4.2-6 Lithology and grain size characteristics of estuarine\deltaaic abandoned channel facies .	52
Fig. 4.2-7 Lithology and grain-size characteristics of estuarine\deltaaic splay facies.....	52
Fig. 4.2-8 Lithology and Grain size characteristics of Esturian\Deltic Sand Flat Facies .....	53
Fig. 4.2-9 Lithology and grain-size characteristics of fluvial channel facies .....	53
Fig. 4.2-10 Lithology and grain-size characteristics of fluvial abandoned channel facies .....	54
Fig. 4.2-11 Lithology and grain-size characteristics of fluvial crevasse splay facies .....	54
Fig. 4.2-12 Lithology and grain-size characteristics of fluvial lake/overbank facies.....	55
Fig. 4.2-13 Lithology and grain-size characteristics of fluvial debris flow facies .....	55
Fig. 4.3-1 Porosity Permeability relationship Facies control .....	56

Fig. 4.3-2 Porosity Permeability relationship grain-size control .....	57
Fig. 4.3-3 Porosity Permeability relationship Lithology control .....	57
Fig. 4.3-4 Permeability reducing by Shale content .....	58
Fig. 4.3-5 Porosity reducing By Shale content .....	59
Fig. 4.4-1 Petrophysical characteristics of Lower Nubian Upper layer 9 .....	62
Fig. 4.4-2 Petrophysical characteristics of Lower Nubian Upper layer 8 .....	62
Fig. 4.4-3 Petrophysical characteristics of Lower Nubian Upper layer 7 .....	63
Fig. 4.4-4 Petrophysical characteristics of Lower Nubian Upper layer 6 .....	63
Fig. 4.4-5 Petrophysical characteristics of Lower Nubian Upper layer 5 .....	64
Fig. 4.4-6 Petrophysical characteristics of Lower Nubian Upper layer 4 .....	64
Fig. 4.4-7 Petrophysical characteristics of Lower Nubian Upper layer 3 .....	65
Fig. 4.4-8 Petrophysical characteristics of Lower Nubian Upper layer 2 .....	65
Fig. 4.4-9 Petrophysical characteristics of Lower Nubian Upper layer 1 .....	66
Fig. 4.4-10 Petrophysical characteristics of Lower Nubian Middle layer 4 .....	66
Fig. 4.4-11 Petrophysical characteristics of Lower Nubian Middle layer 3 .....	67
Fig. 4.4-12 Petrophysical characteristics of Lower Nubian Middle layer 2 .....	67
Fig. 4.4-13 Petrophysical characteristics of Lower Nubian Middle layer 1 .....	68
Fig. 4.4-14 Petrophysical characteristics of Lower Nubian Base .....	68
Fig. 4.5-1 Braided facies frequency and percentage controlled by well location .....	70
Fig. 4.5-2 Braided facies frequency and percentage controlled by well location .....	71
Fig. 4.5-3 Esturrian/Deltic facies frequency and percentage controlled by well location .....	71
Fig. 4.5-4 Fluvial facies frequency and percentage controlled by well location .....	72
Fig. 4.6-1 Density versus Neutron crossplot, coded by shale volume, used for picking the zone parameters of matrix and shale point .....	77
Fig. 4.6-2 Composite integrated log, consist of, input logs, core description, interpretation output, and reservoir zones .....	79
Fig. 4.6-3. Shale volume versus Porosity values used for the interpretation quality control .....	80
Fig. 4.6-4. Core porosity versus Core permeability used for calibrating the estimated permeability .....	81
Fig. 4.6-5. Core porosity versus log derived porosity used for calibrating the estimated porosity ...	82
Fig. 4.6-6 Equivalent pore height Cumulative frequency, used for determination of porosity cutoff value .....	83
Fig. 4.7-1 Total Lower Nubian Gross thickness distribution Map .....	88

Fig. 4.7-2 Lower Nubian Base Gross thickness distribution Map .....	88
Fig. 4.7-3 Lower Nubian Middle Gross thickness distribution Map.....	89
Fig. 4.7-4 Lower Nubian Upper Gross thickness distribution Map .....	89
Fig. 4.7-5 Well log correlation section hanged on PUK surface.....	91
Fig. 4.7-6 Well log correlation section hanged on Lower Nubian Middle-3 .....	93
Fig. 4.7-7 Well log correlation section hanged on Lower Nubian Upper-4 .....	94
Fig. 4.8-1 Cross-section generated from the stratigraphy model.....	98
Fig. 4.9-1 Histogram of the original data for permeability .....	100
Fig. 4.9-2 Histogram of the original data for porosity .....	100
Fig. 4.9-3 Histogram of the original data for shale fraction volume.....	100
Fig. 4.9-4 Experimental and model variogram surface of porosity .....	101
Fig. 4.9-5 Experimental and model variogram surface of shale volume .....	101
Fig. 4.9-6 Experimental and model variogram surfaces of permeability.....	101
Fig. 4.9-7 Modeling the lateral heterogeneity of porosity.....	102
Fig. 4.9-8 Modeling the lateral heterogeneity of shale volume .....	102
Fig. 4.9-9 Modeling the lateral heterogeneity of permeability .....	102
Fig. 4.9-10 Selected porosity stochastic realizations .....	103
Fig. 4.9-11 Selected shale volume stochastic realizations.....	103
Fig. 4.9-12 Two of stochastic realizations for permeability.....	104
Fig. 4.10-1 E-type estimation of well-averaged porosity.....	105
Fig. 4.10-2 Upper and lower bounding surfaces of E-type estimation for porosity (p=0.9).....	106
Fig. 4.10-3 Map of uncertainty for well-averaged porosity.....	106
Fig. 4.10-4 Uncertainty related to Fault traces as interpreted from 3D seismic.....	107
Fig. 4.10-5 Uncertainty related to Net thickness.....	107
Fig. 4.10-6 E-type estimation of well-averaged permeability.....	109
Fig. 4.10-7 Upper and lower bounding surfaces of E-type estimation for permeability (p=0.9) ....	109
Fig. 4.10-8 Map of uncertainty for well-averaged permeability.....	110
Fig. 4.10-9 Cross-plot of core permeability versus core porosity .....	110
Fig. 4.10-10 Core permeability correlation with shale volume .....	111
Fig. 4.10-11 Permeability values from production test in some locations.....	111
Fig. 4.10-12 E-type estimation of shale volume .....	113
Fig. 4.10-13 Upper and lower bounding surfaces of E-type estimation for shale volume (p=0.9) .	113

Fig. 4.10-14 Map of uncertainty for well-averaged shale volume.....	114
Fig. 4.10-15 Net to gross thickness ratio in well locations .....	114
Fig. 5.1-1 Porosity Permeability plots by facies .....	115
Fig. 5.1-2 Flow unite analysis using Lorenz plot.....	116
Fig. 5.1-3 Porosity permeability trends by flow units .....	116

## **List of Tables**

Table 3.1-1 GHE boundaries .....	27
Table 4.1-1 Stratigraphical positions of the formations .....	41
Table 4.2-1: The results of facies analysis.....	46
Table 4.4-1 Reservoir Zones in the Cored wells.....	60
Table 4.4-2 Cored Reservoir Layers by Facies and petrophysical parameters averages.....	61
Table 4.4-3 Cored Reservoir Layers by Facies and petrophysical parameters averages.....	61
Table 4.5-1: Depth intervals of the cores. ....	69
Table 4.5-2: The stratigraphical positions and thicknesses of the three facies associations .....	70
Table 4.6-1 Available Log and Core data .....	74
Table 4.6-2 Core to Log depth Shift .....	75
Table 4.6-3 Log heading information.....	76
Table 4.6-4 Summary of the selected reservoirs characteristics.....	84
Table 4.6-5 Summary of the selected reservoirs characteristics.....	85
Table 4.6-6 Summary of the selected reservoirs characteristics.....	86
Table 4.7-1 Lower Nubian(LNU) tops, measured depth from KB in feet.....	95
Table 4.7-2 Lower Nubian (LNM and LNB) tops, measured depth from KB in feet .....	95
Table 4.7-3 Lower Nubian layers, net and gross thicknesses measured in feet.....	96
Table 4.7-4 Lower Nubian layers, net and gross thicknesses measured in feet.....	97

## 1 INTRODUCTION

The main topic of this study to implement a geo-statistical characterization of the Lower Nubian Formation hydrocarbon bearing intervals, via the integrated study of all the available data (routine core analysis, log analysis, core description, etc) from two oil fields, namely North Gialo and Farigh . However, the focus will be mostly on **North Gialo (6J)** area, owned by Waha Oil Company.

The objective of the study to reveal and measure uncertainties associated with micro-, macro- and megascale reservoir heterogeneities by utilizing the application of geostatistics in clastic reservoir characterization.

To meet the above objective all cores recovered from the cored intervals were described in order to identify rock types building up the reservoir, interpret characteristic sedimentary structures and to identify the main depositional facies of the reservoir.

Conventional core measurements (porosity, permeability) were performed in several plug samples obtained from the available cored intervals of the subject wells. Geomathematical characters of the individual measurements by using maximum-likelihood methods, to avoid the effect of non-normal distributions, were established and compared to the above result obtained from the previously identified facies by using some non-parametric statistical tests.

Interrelations between and among core measurements by facies were analyzed. The obtained characterization and analysis will be given in results chapter.

Well log analysis was performed on all wells located in the study area and which penetrated the Lower Nubian sequences. All wells were quantitatively interpreted using deterministic PETROLOG approach. For selected wells with core data, log-derived porosity and permeability results were compared with core data, and were found to be in good agreement.

Well log correlations were performed utilizing the correlation program of PETROLOG. The Lower Nubian was divided in to LNU, LNM and LNB subunits. In addition these unites were distributed into zones or layers.

Correlation started by defining the main electro-facies by comparing well log shapes and sedimentological core descriptions in wells with (almost) total core recovery. Then lateral extensions of the different well log shapes (electro-facieses) were traced. Resistivity and gamma ray curves worked as excellent correlation markers.



The results of the stratigraphic and structural interpretation coming from log correlations, quantitative log interpretations and lithological core information for individual wells were input into 3D geological modeling of RockWorks software. 3D geological model was established for the study area comprising 3 reservoir units (total of 14 layers). Results of 3D modeling are depicted in cross sections, and maps, showing the distribution of Gross thicknesses.

The results of petrophysical log analysis were then stochastically modeled using Sequential Gaussian Simulation of the individual well log properties. For the sake of uncertainties E-type estimations were estimated which provides surfaces of probability intervals belonging to each grid-points. Finally, uncertainties were measured for each of the modeled properties.

## 2 GENERAL OVERVIEW OF THE FIELD

### 2.1 LOCATION AND HISTORY OF DISCOVERY

The Study area (North Gialo (6J) and Farigh field) is situated in the eastern portion of the Sirte Basin at the intersection of the Hameimat and Ajdabaiya troughs on the northern flank of the Gialo structural high (**Fig. 2.1-1**).

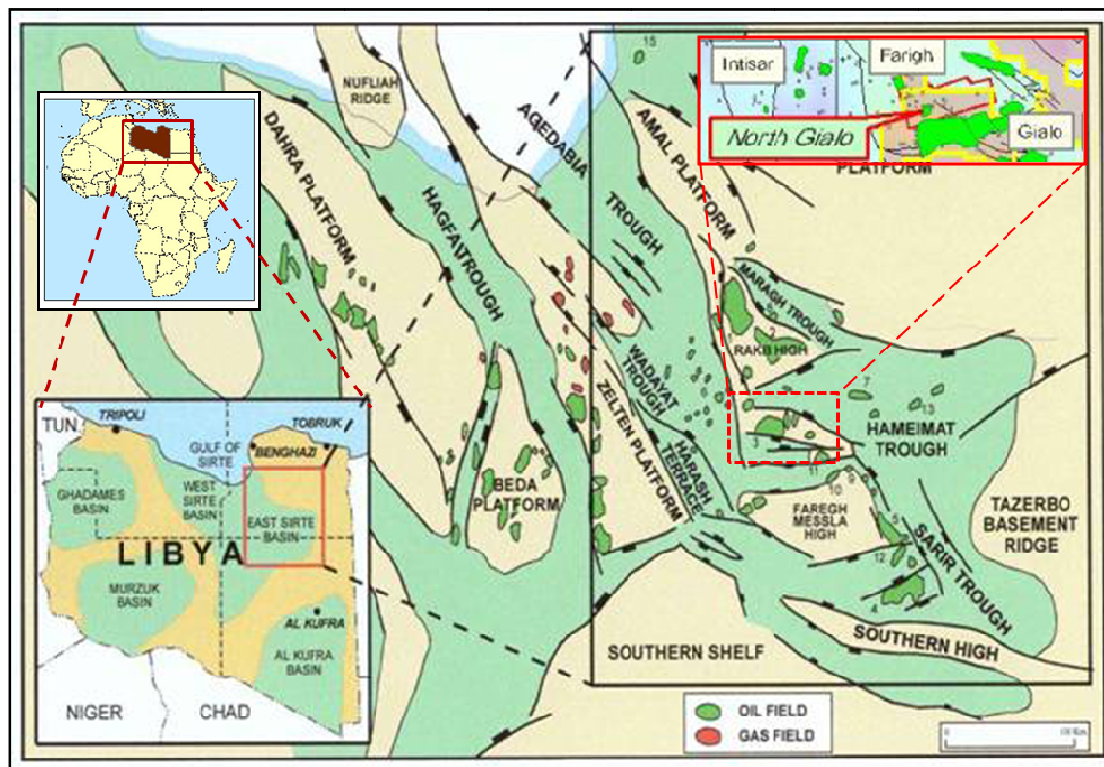


**Fig. 2.1-1 Study area location map (modified after Waha, 2007)**

The North Gialo field is about 18 km long and 7 km wide and covers an area of approximately 108 sq km.

Main pay of the field is the Pre-UK Nubian Sandstones. Secondary pay is basal UK Transitional/Etla sandstone. Other pay may be the fractured basement rocks (in 6J7-59). The top of Nubian sandstone is encountered at approximately 10,381 ft SS, 10,893 ft SS and 11,838 ft SS from southern to central, and to the northern part of the field, respectively. The gross thickness of the secondary pay, Trans./Etla sandstone varies from 50 -100 ft.

During the 1970's, four exploration wells were drilled on Waha acreage in an attempt to offset 1969 Farigh Field discovery in the Nubian Formation to the North. Three of the four wells tested the Nubian at uneconomic rates. The fourth well failed to encounter Nubian sand on what was termed a bald basement high. A new structural-stratigraphic play concept was developed by Waha in 1995 that led to the acquisition of a 3D seismic survey. Based on the interpretation of the 3D seismic data, the SE AA3-12 exploration well was proposed and drilled in early 2002.

This well proved to be the discovery well for the field and was. The well, later renamed as the 6J1-59 shown on was drilled to test the Nubian reservoir. The well was spud on November 1, 2002. The Nubian reservoir was encountered on December 10, 2001 at a depth of 11,258 ftKB and a 7" liner was run in the hole to 11,272 ft KB. After an additional 162 feet was drilled, drill stem test (DST) 2A was run which produced at 3,000 bopd of waxy 43<sup>0</sup> API oil with a gas oil ratio of 3,550 scf/bbl. The well continued to be drilled with a 6" hole and reached total depth of 13,370 ft KB on March 9, 2002. Five cores were drilled and open hole logs were run. On March 11, 2002, 6J1 was plugged back to 12,720 ft KB to isolate the open hole from the water aquifer.

During 2002-2004, the well intermittently, was put on production for a period of 83 days, producing 338 MBO over 129 days representing an average rate of 2,620 BOPD.

Then well 6J2 was drilled as an outpost to 6J1 to confirm the eastern extension of the Nubian formation. The well was spud on April 13, 2002 and had to be sidetracked three times before reaching total depth of 12,697 ft KB on September 5, 2002. The Etla and Nubian reservoirs were encountered in the open hole section.

Well A2-59D was drilled. A2-59D had produced oil rate of 10,170 bopd and was completed. It was the best producer in the field before the well was shut down.

An additional 17 appraisal wells were subsequently drilled to determine the extent of the field and define the characteristics of the reservoir. Successful well tests were recorded in all but two of the appraisal wells. The initial test rates of the appraisal wells exhibited a broad range of production rates from 200 to 10,000 BOPD suggesting a high degree of complexity within the reservoir. The two wells were both non-commercial. The 6J5 well encountered a bald basement high while the 6J7 well tested the Lower Nubian Base section at sub-economic rates. (**Fig. 4.1-1**) depicts all well locations (Waha Oil Co., 2004).

The reservoir rock is generally characterized by low average porosity (0.06v/v) and an overall low average permeability (1 mD), most likely the result of pervasive diagenetic changes to the rock.

## **2.2 GEOLOGICAL OVERVIEW**

### **2.2.1 Stratigraphy**

The primary reservoir in the North Gialo Field is Lower Cretaceous Nubian Sandstone. The overlying Transitional Beds are considered to provide additional reservoir potential to the field. The Transitional Beds (**TB**) are thought to be transgressive deposits overlying a marked unconformity, which defines the top of the Nubian section. The Pre-Upper Cretaceous unconformity (**PUK**) represents an erosional surface that truncates the Nubian progressively from the Northeast to the Southwest across the field (Waha Oil Company, 2005).

The maximum Nubian thickness in the field is present in the down-faulted blocks to the Northeast, Furthermore, the entire Nubian section is eroded on the upthrown basement block in the Southwest.

The Nubian, a series of primarily continental deposits, can be subdivided throughout the eastern Sirte basin into three zones: Upper Nubian (**UN**), Nubian Middle (**NM**), and Lower Nubian (**LN**). In North Gialo this usage is expanded by subdividing the Lower Nubian into three subunits: **LNU** (upper part of the lower Nubian), **LNM** (middle part of the lower Nubian), and **LNB** (base part of the lower Nubian). The sands in the overall Nubian section are primarily clean, quartz-rich sandstones generally attributed to braided stream deposits with a minor amount of overbank / lacustrine to marine influence. Pervasive quartz cementation appears to have had a profound negative effect on the reservoir quality of the sands by significantly reducing porosity and permeability (Waha Oil Company, 2005).



### 2.2.2 Structural makeup

The North Gialo Field is a complex structural/stratigraphic trap, incorporating dip closure and stratigraphic pinchout below the PUK. The field occupies a series of fault blocks stepping down towards the NNE from the culmination of the Gialo High in the south and southeast. The general structural orientation is NW-SE but includes several distinct domains. The western side of the field is dominated by NNW-SSE-trending faults, while the eastern side is dominated by faults trending WNW-ESE. The field is located in a transfer zone of wrench faulting across the arch that separates the Ajdabaiya and Hameimat troughs (Waha Oil Company, 2005).

Some structures have been inherited from late Paleozoic Hercynian deformation, but experienced maximum displacement during Tethyan rifting. Age of rifting varies throughout the basin, and may have begun in Jurassic or even Triassic time in some places. Maximum displacement took place in the Late Cretaceous in North Gialo. Reactivation and partial inversion occurred after the development of the PUK erosional unconformity, resulting in displacement of the PUK surface. The region remained passive after late Cretaceous, experiencing passive subsidence during the cooling phase of failed rifting in the Paleogene (Waha Oil Company, 2005).

Prior to the structural activity (uplift, faulting and erosional truncation) that was responsible for creating the current field geometry, the thick Nubian section (in excess of 2300 feet thick) is believed to have been deposited as primarily braided fluvial deposits over a wide-ranging area. The accumulation of Nubian sediments is postulated to have been generally uniform in thickness at the time of deposition. As uplift, faulting and erosion occurred, the field was dissected by numerous faults and fault blocks with various relative movements. The up-thrown fault blocks were subjected to major erosional truncation compared to the downthrown fault blocks. This has resulted in fault blocks containing highly variable thicknesses of Nubian section across the field.

The lateral seal for the reservoir sands are interpreted to be formed by impermeable, tight Nubian sections and/or impermeable granite basement (Waha Oil Company, 2005).



### 3 METHODS

#### 3.1 SEDIMENTOLOGICAL ANALYSES

For modeling spatial heterogeneity of a reservoir, to understand the reservoir geometry and recognize different geological bodies (reservoir architecture) which have an impact on subsurface flows, it is essential to reveal and identify the depositional environments. This aim can be achieved by complex analysis of different sedimentological scales. On a medium scale, core description studies can reveal the lithological and textural characters of depositional facies. Core measurements can show their petrophysical features. This information can then be extended by using well logs within a reservoir. On this larger scale there is another possibility for evaluation of the petrophysical content of the correlated vertical sequences.

Cores taken from five wells penetrating the Lower Nubian Unites in the study area were described according to the opinions and ideas of Waha Oil Company (Waha Oil Co., 2008), the observed reservoir sedimentology, architectural elements (facies) were quantitatively characterized using different conventional and indicator statistics tools to achieve their most important geological characteristics namely; grain size, (clay, silt and sand) content, sedimentary structures and thickness. Furthermore, their petrophysical characteristics have been measured on core plugs and estimated from well logs. These can, aid distinguishing different facies in the non-cored depth intervals to end up with vertical sequences laterally extended overall the studied area. Such sedimentary environment characterization is also very important for reservoir properties molding (stochastic molding), because horizontal and vertical variation of reservoir rock properties (eg. porosity and permeability) are partially controlled by deposition environments as well as diagenetic processes.

The cored intervals throughout the Lower Nubian Member in these wells, has been, divided into three facies groups. Namely: braided-stream facies association, estuarian/deltaic facies association and fluvial facies association, containing eight facies types. So we will now review the main characteristics of the facies which considered being good reservoir rocks.

**Channels fill sediments:** this facies was recognized in all the above mentioned environments. Among them braided stream shows the most favorable reservoir rocks because of its appreciable low fine sediment content (Friedman, G.M. and Sanders, J.E., 1978). The vertical sequence may consist of, coarse sandstone at base fining upward in texture well sorted, or sandstone intercalated

with shale. The lithology may vary according to the environment and on the location along the channel stream (Proximal, Mid, Distal), as mixture of conglomerate, sandstone, siltstone and shale, and almost any combination of clastic sedimentary types is possible. In general it shows dominantly of sand and are commonly conglomeratic. Silt and clay are volumetrically minor. Grain sorting ranges from poor to good (Galloway, W.E., Hobday, D.K., 1983). Because of the coarse grain nature of this facies, it has been given priority among the other facies to be a good reservoir rock for hydrocarbon depending on its primary petrophysical properties. Up to 30% porosity and thousands of milli-darcys, and a thickness of several hundred meters of sandstone with minor shales have been reported (Douglas, J.C., 1982). Despite channel geometry, reservoir continuity is good at least parallel to the channel body. When this facies is considered as potential hydrocarbon-bearing rock, then reservoir quality is controlled by the facies textural characteristics to a large extent. Permeability is believed to be primarily controlled by grain-size. A decrease in grain-size of such facies will dramatically reduce permeability values depending on whether this sequence was deposited in proximal or distal parts. However, sediments sorting play a major role in controlling porosity, permeability relationship. Whenever coarse grain sediments encountered, grain size control this relationship. However in the distal stream, when grain-size shows variation, sorting is the main control of this relationship (Clarke, R. H., 1979). Often the depositional facies alone did not determine the reservoir properties due to the diagenetic alteration of the primary reservoir properties. On the other hand if we consider the vertical variation of such reservoir properties within the channel facies, obviously the permeability will show distinctive trends which reflect the vertical textural trend. However, laterally the permeability values for example in braided fluvial environment can be oriented along the channel axis. At the same time reservoir properties even laterally along the channel axis can follow some trend in their values. Often it decreases downstream, where distal deposits are likely to be finergrained than the middle and proximal deposits (Bridge, J.S., 2003)

### **Well logs signature**

In wire line logs when applied to identify this facies, resistivity and gamma ray futures frequently reveal bell-shaped profile. Moreover, the separation distance between the density and neutron log overlay and thorium, potassium log overlay, reflect relatively large width in the first case, while it is small in second case, This separation is determined by the fraction volume of the clay minerals and the fluid type occupying the sandstone pores network. These log features vary according to

cut and fill of the channel. Grain-size variation (upward-fining) alone often did not give the final log shape but indicated an intercalation of fine-grained sediment units with coarse grain sediments. Furthermore, fluvial channels often have clay and shale clasts near the base which will modify the mentioned typical log shapes. This makes the reorganization of such facies from wire line log patterns somewhat confusing (Serra, O., 1989).

### **Crevasse splay facies**

It is an overbank deposit or channel margin facies. Regarding the hydrocarbon potential, this facies is considered to be in second rank. These deposits form isolated lobes of sand within the floodplain muds up to 10 km long and 5 km width and 2-6 m in thickness. The volume of these sands may be small but economically important as hydrocarbon-bearing reservoir rocks (Galloway, W.E., Hobday, D.K., 1983). Moreover, geometry and dimensions of the crevasse splay sandstone body within overbank sequences may give important information about the related fluvial channel sandstones, where probably the channelized proximal part of a crevasse splay lobe have large thickness close to the fluvial feeder channel margin and thins rapidly toward the distal part of the lobe (Mjos, R., Walderhaug, O. and Prestholm, E., 1993). Crevasse splay facies is characterized by thin beds of sand with fining-upward section near the channel and coarsening upward sequence towards the edge of this lobe (Bjorlykke, K., 1989). Lithology of this facies may consist of fine- to medium-grained sandstone and interbedded laminae of siltstone with mudstone. Grain size laterally decreases away from the main source channel towards the outer edge of the splay (Miall, A.D.). Relating the lateral grain-size variation to fluvial feeder channel location can also help to estimate the apart distance where the sand/silt fraction can reveal this relation in short distances. However, the silt/clay fraction can serve better for illustrating this relationship in larger distances from the feeder channel (Guccione, M.J., 1993). Vertical variation in grain-size within the crevasse splay facies looked to be minor but in general is composed of coarsening upward sequences of sands and muds (Farrell, F.G., 2001).

Considering reservoir heterogeneity obviously heterogeneity is present on different scales within the reservoir (Eaton, T., 2006). Practically core description information is considered to be related to macro-scale reservoir heterogeneity. However, this information needs to be compared with other data sources, like reservoir properties derived from wire line logs (mega-scale) and lab-core measurements (micro-scale). These data can be differentiated depending on their vertical



continuity as continuous and discrete ones. Even they can be point data or interval data. Moreover, these data can be handled statistically as indicators or quantities. In reservoir characterizations the results of core description studies should be linked to the analyses of logs and core plugs in order to determine the factors affecting the reservoir quality. These data coming from five cored wells having penetrated the Lower Nubian Formation, was organized in such way, which made their statistical analysis possible.

### 3.1.1 Data preparation

The very first step was the matching core depth intervals to that of the corresponding wire line logs. The values of depth shifting were determined by overlaying the core-gamma and total gamma ray logs.

In the next step, the geological information coming from sedimentary core descriptions was transformed to specific indicators using (SPSS) software. The different lithofacies, grain size classes and depositional facieses were coded by a special set of labels expressing their hierarchy (**Fig. 3.1-1**)

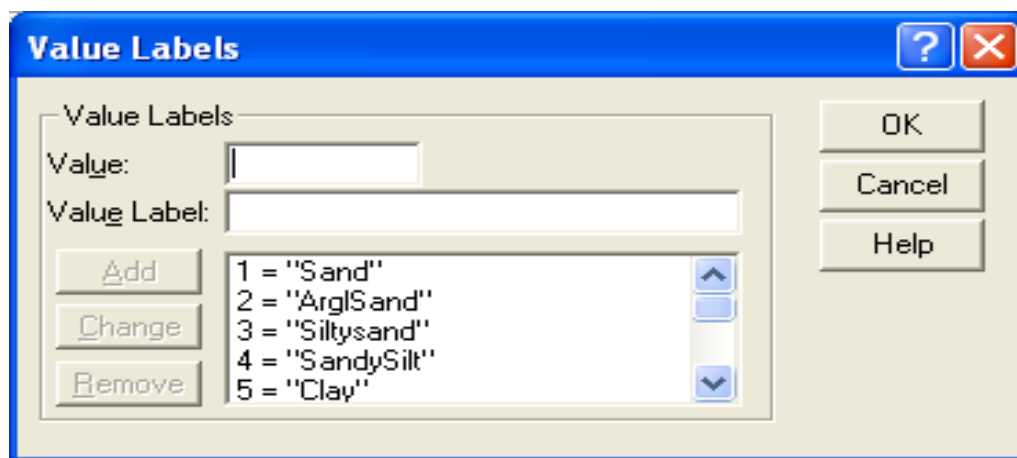
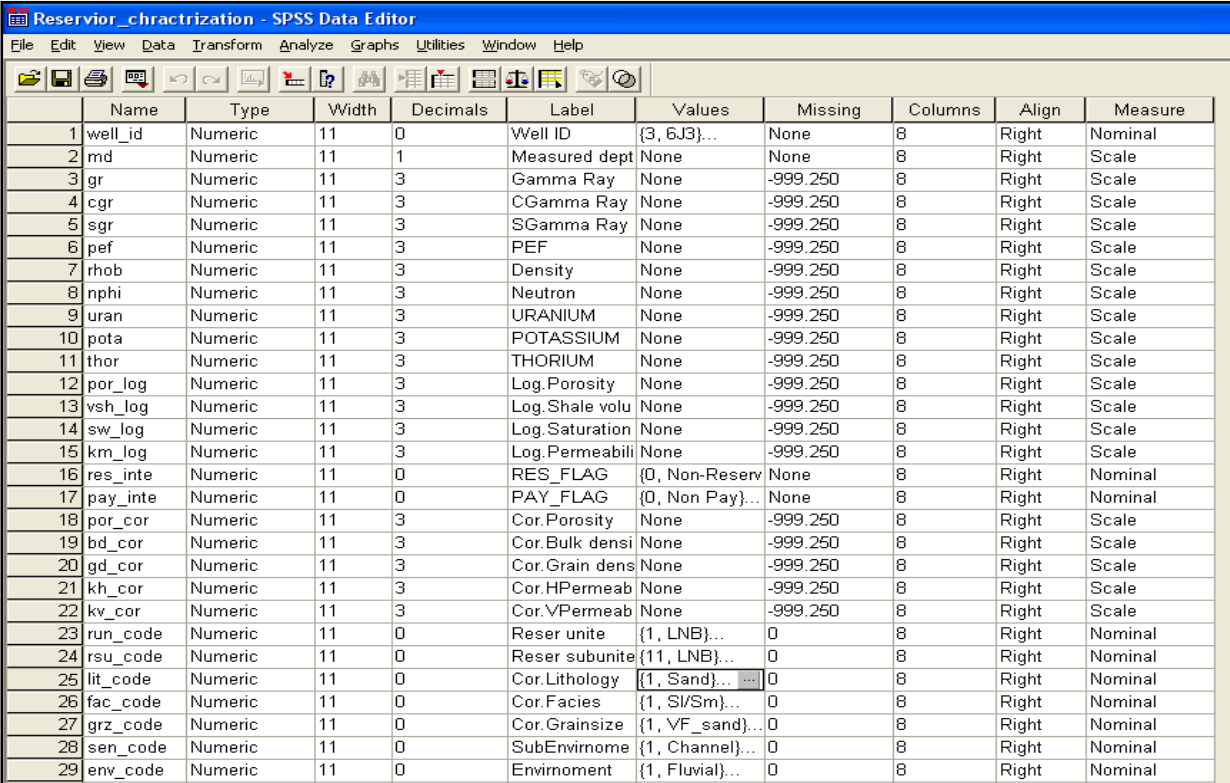


**Fig. 3.1-1** Core description labels and indicators, lithology example

All the data available from core description, core analysis, raw logs measurements and log interpretation results, were inserted into the data base of SPSS (**Fig. 3.1-2**), STATGRAPHICS and STRATER software, where each of them will be used for specific purpose.



	Name	Type	Width	Decimals	Label	Values	Missing	Columns	Align	Measure
1	well_id	Numeric	11	0	Well ID	{3, 6J3}...	None	8	Right	Nominal
2	rmd	Numeric	11	1	Measured dept	None	None	8	Right	Scale
3	gr	Numeric	11	3	Gamma Ray	None	-999.250	8	Right	Scale
4	cgr	Numeric	11	3	CGamma Ray	None	-999.250	8	Right	Scale
5	sgr	Numeric	11	3	SGamma Ray	None	-999.250	8	Right	Scale
6	pef	Numeric	11	3	PEF	None	-999.250	8	Right	Scale
7	rhob	Numeric	11	3	Density	None	-999.250	8	Right	Scale
8	nphi	Numeric	11	3	Neutron	None	-999.250	8	Right	Scale
9	uran	Numeric	11	3	URANIUM	None	-999.250	8	Right	Scale
10	pota	Numeric	11	3	POTASSIUM	None	-999.250	8	Right	Scale
11	thor	Numeric	11	3	THORIUM	None	-999.250	8	Right	Scale
12	por_log	Numeric	11	3	Log.Porosity	None	-999.250	8	Right	Scale
13	vsh_log	Numeric	11	3	Log.Shale volu	None	-999.250	8	Right	Scale
14	sw_log	Numeric	11	3	Log.Saturation	None	-999.250	8	Right	Scale
15	km_log	Numeric	11	3	Log.Permiability	None	-999.250	8	Right	Scale
16	res_inte	Numeric	11	0	RES_FLAG	{0, Non-Reserv	None	8	Right	Nominal
17	pay_inte	Numeric	11	0	PAY_FLAG	{0, Non Pay}...	None	8	Right	Nominal
18	por_cor	Numeric	11	3	Cor.Porosity	None	-999.250	8	Right	Scale
19	bd_cor	Numeric	11	3	Cor.Bulk densi	None	-999.250	8	Right	Scale
20	gd_cor	Numeric	11	3	Cor.Grain dens	None	-999.250	8	Right	Scale
21	kh_cor	Numeric	11	3	Cor.HPermeab	None	-999.250	8	Right	Scale
22	kv_cor	Numeric	11	3	Cor.VPermeab	None	-999.250	8	Right	Scale
23	run_code	Numeric	11	0	Reser unite	{1, LNB}...	0	8	Right	Nominal
24	rsu_code	Numeric	11	0	Reser subunite	{11, LNB}...	0	8	Right	Nominal
25	lit_code	Numeric	11	0	Cor.Lithology	{1, Sand}...	0	8	Right	Nominal
26	fac_code	Numeric	11	0	Cor.Facies	{1, Sl/Sm}...	0	8	Right	Nominal
27	grz_code	Numeric	11	0	Cor.Grainsize	{1, VF_sand}...	0	8	Right	Nominal
28	sen_code	Numeric	11	0	SubEnvironme	{1, Channel}...	0	8	Right	Nominal
29	env_code	Numeric	11	0	Environment	{1, Fluvial}...	0	8	Right	Nominal

Fig. 3.1-2 Data base structure of the available data

### 3.1.2 Data analysis

The main task of this stage is, to characterize the recognized facies by the petrophysical parameters, textural properties, lithofacies, and by locations (well number). This was established by using descriptive methods of univariate and bivariate description. The first step is the data exploration by utilizing the conventional statistics tools , histograms, box-plot and scatter plots, which will provide summary statistics, and also can give information about the data quality by revealing abnormal values which can be measurement errors or real extremes(outliers). Petrophysical properties are handled as continuous variables, while other information obtained from core description is handled as categorical variables(Isaaks, E.and Srivastava, R., 1989) , (Webster, R. and Oliver, M., 2007), (Deutch, C., 2002), (Goovaerts, P., 1997) and (Jensen, J.L., Lake, L.W., Corbett, P.W.M., and Goggin, D.J., 2000).

### 3.1.2.1 Statistical description of continuous variables

The summary statistics of the continuous variables, in our case porosity, permeability and shale volume, was achieved using univariate description approach, by applying histograms. These are not else than, graphical presentation of the variable frequency distribution within a certain interval for a given data set. Specifically histograms of such mentioned properties were built for each facies type observed by the core description. The histogram is defined by classes of frequencies in form of bars. The height of each bar is proportional to the number of class value counted within the investigated data set. Several frequency distribution proprieties can help in characterizing the facies, by range values (minimum, maximum) and averages (mean, median, and mode) of the particular parameter. Permeability values often followed an asymmetrical frequency distribution with negative skewness caused by extreme values or outliers (**Fig. 3.1-3**). In such cases, to reduce the influence of extremes, the variable values should be transformed to log normal values. However, porosity values may show heavily peaked (multimodal) distributions (**Fig. 3.1-4**). This is clear evidence that the data set is not homogeneous. In other words some class values do not belong to the same facies.

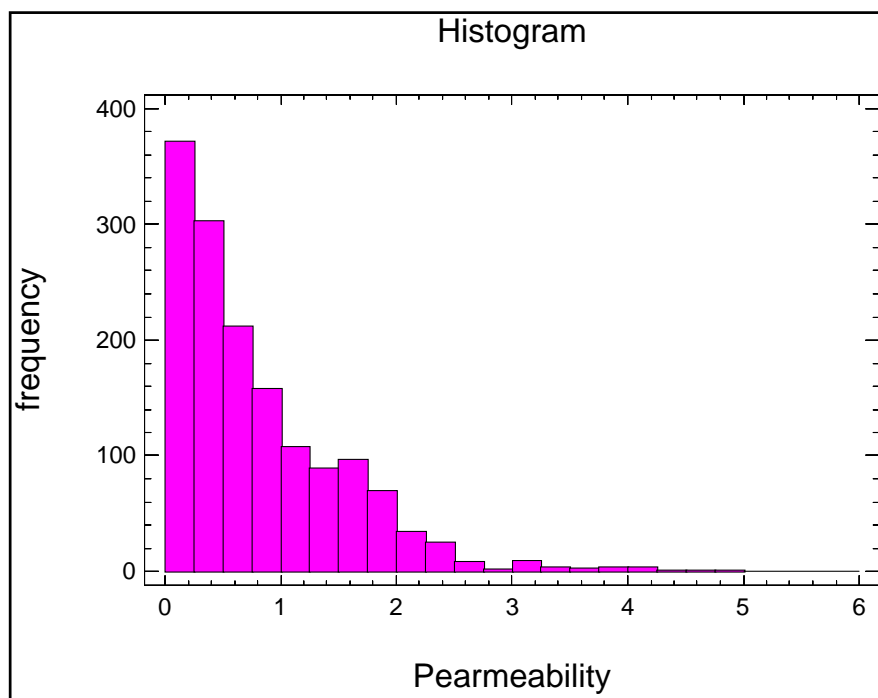


**Fig. 3.1-3. Histogram of permeability with a negatively skewed frequency distribution.**

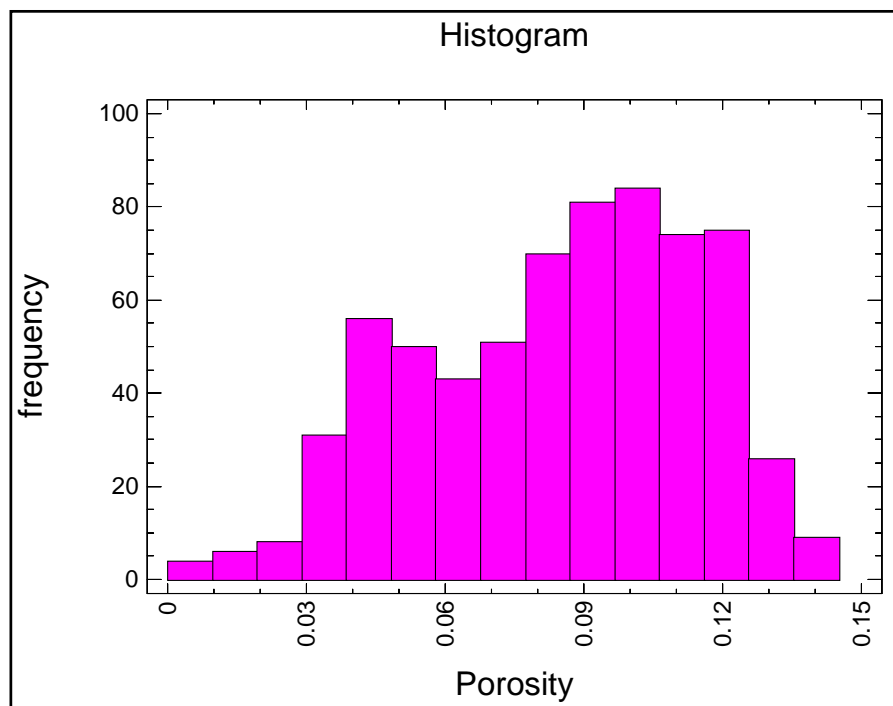


**Fig. 3.1-4. Histogram of porosity following a multimodal frequency distribution**

Another technique used for describing frequency distribution is box-plot. This graphical tool consists of boxes bounded with interquartile values ( $Q_1$  and  $Q_3$ ) and in-between the median ( $M$ ). Across the boxes the whisker line signals to the extreme values. This approach enables us to compare the same variable belonging to different data sets, for example comparing the shale volume distribution for the distinguished facies (**Fig. 3.1-5**).

Often continuous variables, which are in our case represented by petrophysical parameters, either derive from log-analysis or measured in core plugs and recorded versus depth. Each depth point defined by multiple records, where a pair or more continuous variables are measured simultaneously, must be studied to reveal the relationships and dependencies of such variables. A powerful tool for bivariate description is scatterplot. It represents two variables as a cloud of points arranged in a two-dimensional plane. The position of each point is determined by the value of one variable along the horizontal X-axis and by the value of the other variable along the vertical Y-axis. Different colors and marks (e.g. square, circle, and cross) can be applied for different categories of points. Regression of the second variable on the first variable can be computed and the regression line displayed on the plot, with elementary statistics of the variables (such as mean, variance, minimum etc.). The correlation of two variables is suitable for investigating the reservoir quality. For example scatterplot of permeability versus porosity, coded by facies or any other

geological attribute (**Fig. 3.1-6**). The quality of this correlation is determined by the correlation coefficient value given by the scatterplot.

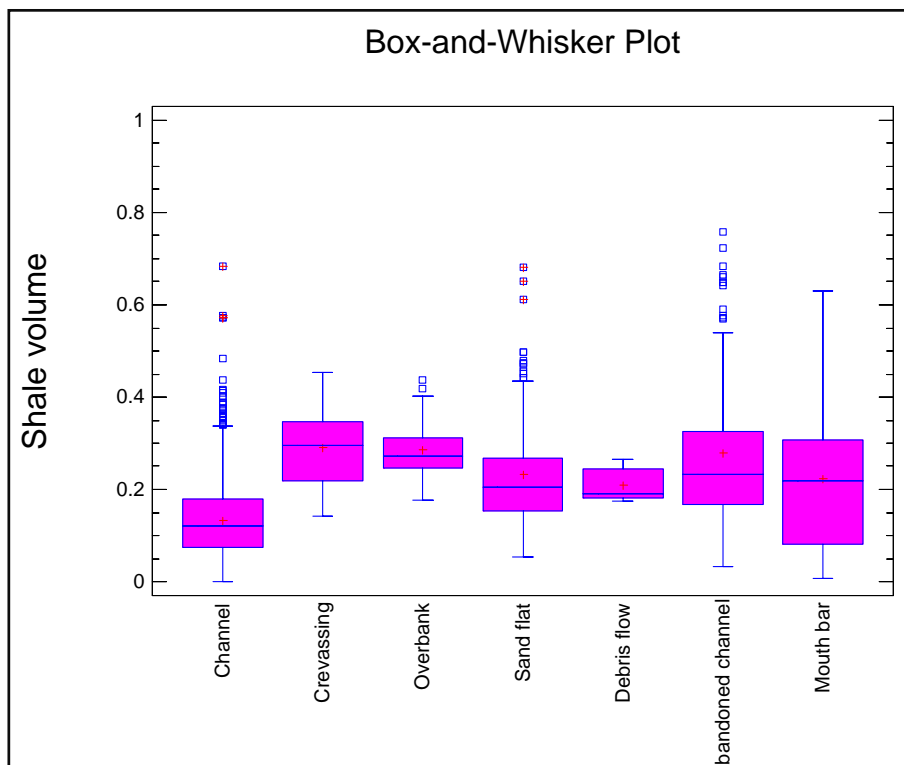


Fig. 3.1-5 Box-whisker plot of shale volume categorized by facies

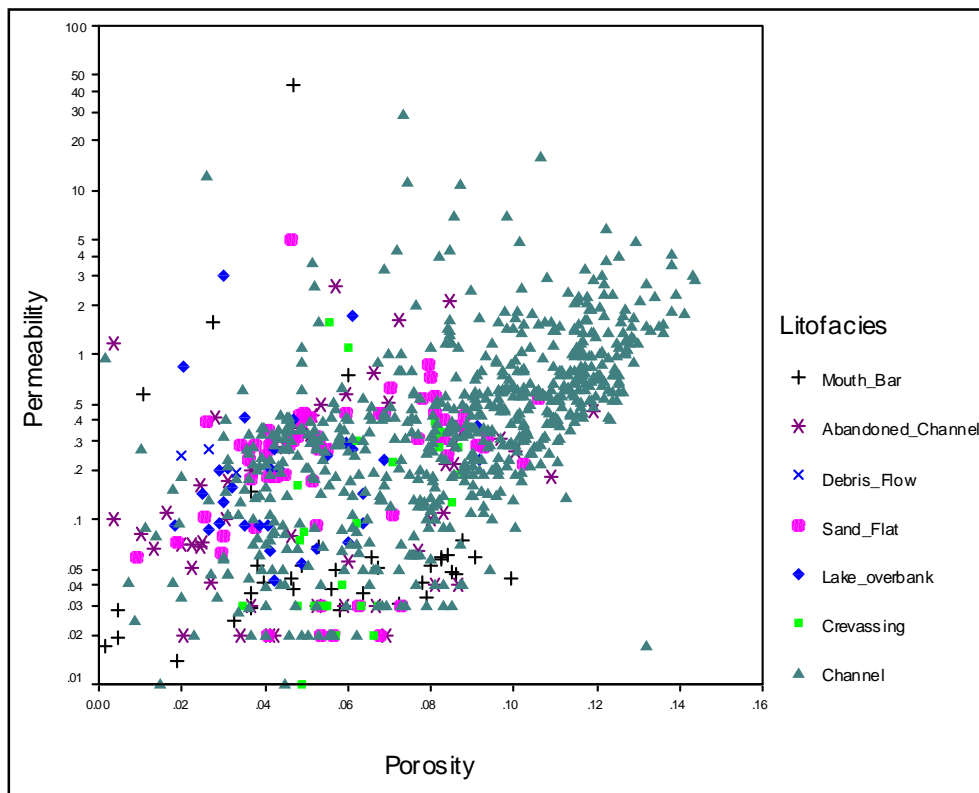


Fig. 3.1-6 Scatterplot of porosity versus permeability coded by facies

### 3.1.2.2 Descriptive statistics

Tables with elementary statistics of the variables by case processing summary, and descriptive summary (mean, median, Std. Deviation, minimum and maximum) allow us to compare the different variables, and for the same variable data sets belonging to different geological environments or properties. Arithmetic averages which are determined by the mean, are sensitive to extreme values. The median, which is determined by M value at which cumulative percentage is 50%, is sensitive to gaps in the middle of the distribution. M-Estimators were applied to overcome such shortages

### 3.1.2.3 Categorical variable statistics

The discrete or indicator variables such as grain-size categories, facies and lithofacies were described using frequency distribution histograms, defined by case bars. The height is proportional to the presence of each category within the processed data set. It enabled us to characterize the facies by another indicator variable like the lithofacies or any other (**Fig. 3.1-7**)

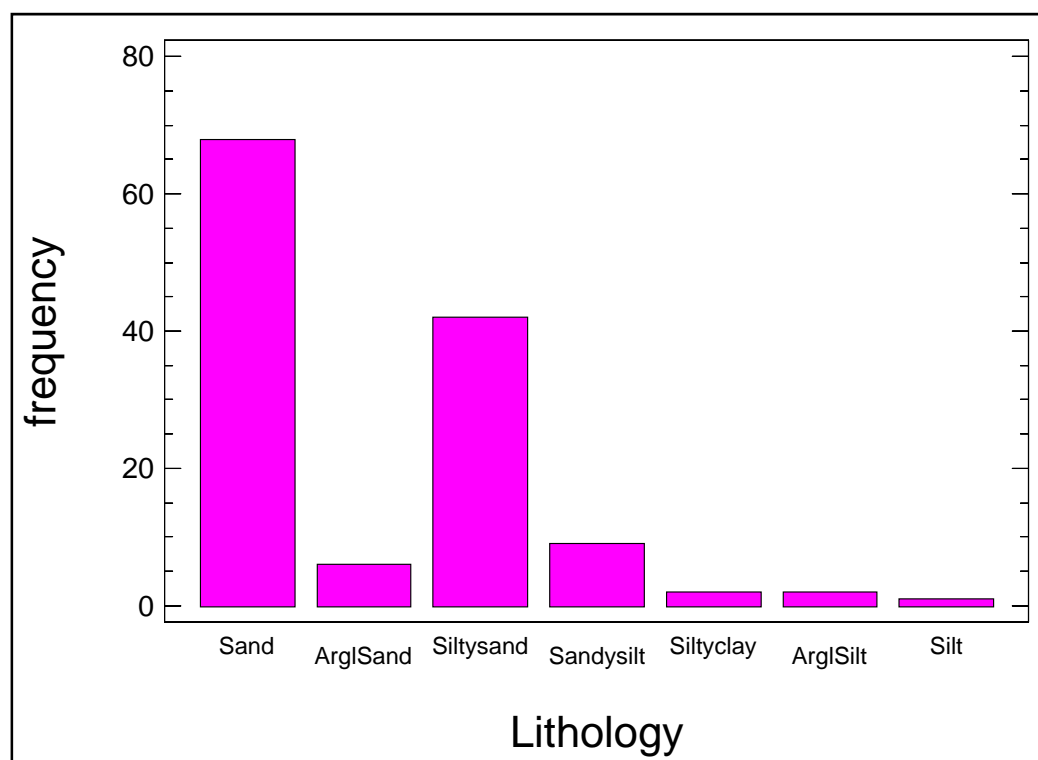


**Fig. 3.1-7 Categorical variable histogram.**

### 3.1.3 Well-log correlation

The original plane for performing the stratigraphic correlation was by integrating the well logs and core description. Typical gamma-ray, response log shape for all the distinguished facies was

compared in the cored intervals from five wells, penetrating the lower Nubian sequence. Once done, these log response shapes should be extended laterally to investigate the lateral continuity of each facies overall the studied area through the log correlation approach. Unfortunately this scenario was not successful, because log response shape was not only controlled by rock texture, but in addition the strong diagenetic alteration and tectonic activity, which later deformed the typical log features of the different facies. Instead a stratigraphic framework was built by using specific marker layers, which could be observed and picked, from well-log correlation. The Lower Nubian sequence was divided into several flow unites, and petrophysical zones (Arkinson, C.D., McGowen, J.H., Bloch, S., Lundell, L.L. and Trumbly, P.N., 1990). This was carried out by three steps, first starting with a general framework where the top and bottom depth of the Lower Nubian was picked easily by correlating the gamma ray and resistivity logs., Then the flow unites and barriers can be recognized and their tops picked by using, the separation distances, from both the density neutron overlay and thorium potassium logs overlay. Finally each flow unite was divided into petrophysical zones (Murray, C., 1994) by utilizing the results of quantitative wireline log analysis, namely porosity, permeability, and shale volume. All the picked tops were inserted into the Rock Work software data base, and a 3D onlap stratigraphic model was constructed. Consistency of the used tops was examined. Several stratigraphic cross-sections could be extracted in different directional trends. Moreover the porosity, permeability, and shale volume, averages were (3D) deterministically modeled. The distribution of thickness and petrophysical properties was established and presented as vertical cross-sections and in form of 2D maps. It should be noted that no structural 3D model could be built by using only the log-correlation because of pinching out phenomena caused by a regional Pre-Upper Cretaceous unconformity (PUK) surface

#### **3.1.4 Core Porosity-Permeability correlation**

In practical reservoir analysis the relationship between the core permeability and porosity shows poor correlation (**Fig. 3.1-8**) due to the heterogeneity of lithology, grain-size, facies, and heterogeneity of pore geometry (Gardiner, S., Thomas, D, Bowering, D. and McMinn, L., 1990). To investigate the impact of such heterogeneities on the porosity/permeability relationship, several semi-log scatterplots were built for porosity versus permeability, coded by each of mentioned influence factors. All of them was provided by the core description (Thomeer, J., 1983), but the pore geometry factor influence was determined by global hydraulic element approach, by which

the reservoir rocks is distributed into petro-types (hydraulic unites) (Corbett, P., Ellabad, Y., and Mohamed, K., 2001) and (Corbett, P., and Mousa, N., 2010). This was performed by several steps.

First calculating the reservoir quality indicator (RQI) by utilizing the core porosity ( $\phi_e$ ) and core permeability ( $\kappa$ ) values using this equation:  $RQI = 0.0314 \sqrt{\frac{\kappa}{\phi_e}}$

Next step calculating the normalized porosity ( $\phi_z$ ) using this expression:  $\phi_z = \left[ \frac{\phi_e}{1 - \phi_e} \right]$

Then computing the flow zone indicator (FZI) using this formula:  $FZI = \frac{RQI}{\phi_z} = 0.0314 \frac{\sqrt{\frac{\kappa}{\phi_e}}}{\left[ \frac{1}{1 - \phi_e} \right]}$

Finally the processed interval is distributed into hydraulic unites according to the boundaries determined by global hydraulic element (GHE) boundaries shown **Table 3.1-1**.

**Table 3.1-1 GHE boundaries**

FZI	GHE
0.0938	1
0.1875	2
0.375	3
0.75	4
1.5	5
3	6
6	7
12	8
24	9
48	10

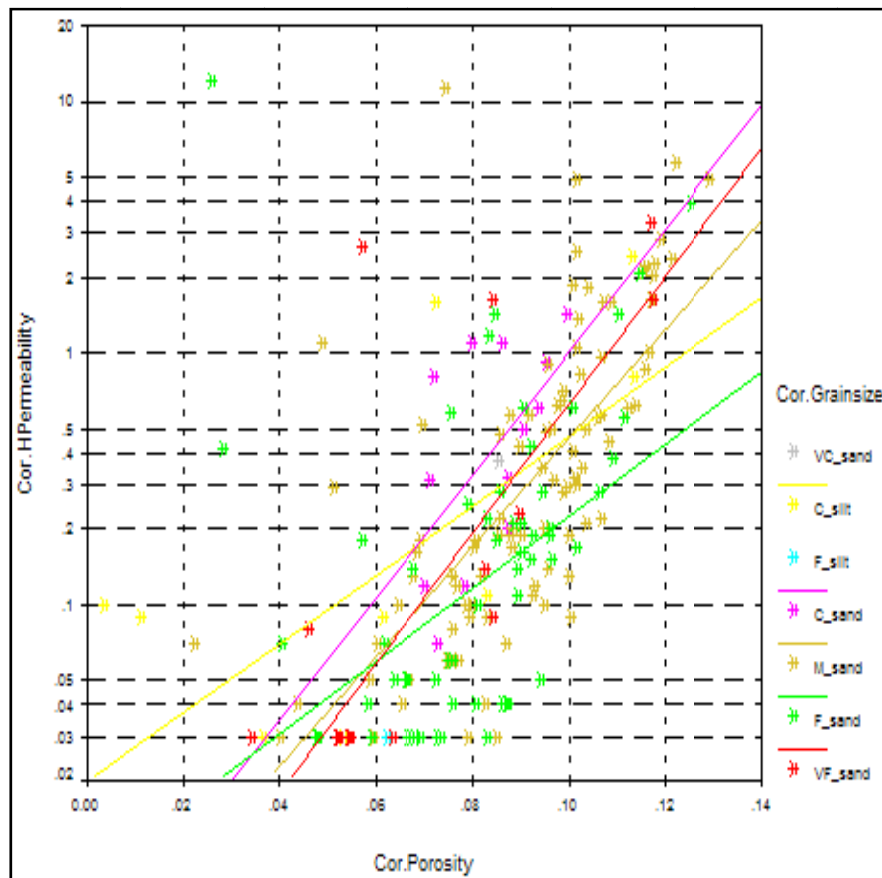


**Fig. 3.1-8 Porosity -Permeability correlation scatter- plot**



### **3.2 PETROPHYSICS: GENERAL OVERVIEW**

Model generation for reservoir simulation requires accurate input of petrophysical parameters such as porosity, permeability and water saturation. These parameters are necessary to optimize reservoir development. These properties can be measured in cores and also derived from wireline logs. The certainty of such information is essential for reservoir modeling because the local errors committed during the measurement or determination of the subject properties can be propagated into the spatial distribution or stochastic simulation processing (Jia, L., Ross, C.M and Kovscek, A.R., 2005). Such errors can occur during the coring and handling of the core and also through the measuring procedures. Core analysis data vary in accuracy depending on the techniques employed and the precision of the equipment used. Furthermore during the logging operation and the interpretation of the well- logs. The log-derived petrophysical reservoir parameters are often obtained with level of uncertainty depending on the used logs availability, quality (Kelemen, Z., 2000) and on the interpretation methodology (Kennedy, J., Cox, A. and Aldred, R., 2010), Integration process between core and log data are necessary in order to achieve reliable accurate reservoir parameters. In addition such combination can lead the identification of depositional features (electrofacies) through the available logs (Everett, R., Herron, M. and Pirie, G., 1983). Quantitative determination of these parameters usually involves costly coring programs, plus extensive laboratory effort to conduct the measurement of these parameters under reservoir conditions. Thanks to the development of sophisticated logging techniques however, the in situ determinations of porosity and under favorable conditions the hydrocarbon saturation are now conducted within reasonable accuracy. The determination of permeability on the other hand, still requires coring or drill-stem testing (Timur, A., 1968),

In the field of the formation evaluation activity the core analysis data are frequently considered to be as hard data for the reservoir porosity, permeability and fluid saturations measurements. despite its availability and the vertical distribution viruses of the well axis(discrete data). However, well log data, which are the result of continuous (0.5 feet increment) measurements of the physical properties of the solid part and the fluid or gas occupying the pore space of the reservoir hydrocarbon-bearing rocks by running different logging tools(resistivity, density , neutron, sonic, gamma and imagery ) in the well borehole as single or combination , each tool characterized by its own physical theory and (vertical, horizontal) resolution, the recorded measurements can reveal the same reservoir properties as that obtained from the cores. In addition it can be used for

estimating the mineral composition of the solid(matrix) portion of the reservoir rocks. Namely the lithology in volume fraction quantities such as shale, sand and silt volumes (Serra, O., 1989). In order to obtain these results from log data, the well logs are usually handled by the analyst in several mathematical and probabilistic processes mentioned as log analysis methodology either deterministic or probabilistic(Serra, O. and Abbot, H.T, 1980)and (Barlai, Z., 2000).

Logging tools are perpetual in evolution to improve their characteristics and consequently improve the data quality measured, long way since Schlumberger brothers put the first electrical log measurements onto paper in 1927. (Crain, E.R., 2000),

In the following we will review the main processes and methods used in well logs formation evaluation to gain the lithology and petrophysical reservoir characteristics. The common way of quantitative log analysis (petrophysical evaluation) methodology was established by G. E. Archie in 1942. He related porosity and formation water resistivity to formation resistivity and water saturation (Archie, G. E, 1952). In 1944 H. Guyod determined resistivity from lateral and normal curves. In early days of well-log analysis, only porosity, water saturation and sometimes permeability were calculated from the logs. Somewhat later well-log analysis methods and approaches for lithology, petrophysical and facies interpretation were developed by a number of authors (Barlai, Z., Czegledi, I. and Muller, P., 1973) , (Mayer, C. and Sibbit, A., 1980), (Hietala, R.W. and Connolly, E.T., 1984), (Quirein, J., Kimminau, S., LaVigne, J., Singer, J. and Wendel, F., 1986), (Cannon, D.E. and Coates, G.R., 1990) and (Hietala, R.W., 1990).

The main tasks of well-log analysis are:

1. lithology determination including shale volume
  2. Porosity and petrophysical determination including fluid saturation and permeability,
- These tasks can be established by several log analysis methods.

### **3.2.1 Deterministic approaches**

The traditional method followed by a petrophysicist is sequential deterministic approach where the petrophysical parameters can be obtained in sequence stepwise calculations. It starts with calculating the shale volume from several log response equationsfor example using gamma ray log. Then the porosity is calculated using sonic, neutron, and density response equations dependent on the shale volume previously calculated. The last step is calculation of water

saturation utilizing the results of porosity and shale volume already determined from the previous steps. This deterministic solution cannot give the quality of the analysis because the relation between the measured value and the answer of the used log response is not reflected. The given answers are often doubted with level of uncertainty. Potential source of errors causing this uncertainty may be for example during the selection of shale zone parameters when implementing natural total gamma ray log for computing the shale volume in interval. Here beside the presence of the shale, thorium-bearing silt or uranium-bearing limestone or maicaciuoes sandstone can present the maximum (GR) and the minimum (GR) as erroneous values. To overcome the drawbacks of this log analysis method the obtained results of shale volume, porosity and water saturation values should be calibrated using outside information coming from core analysis, drilling stem test and other geological data.

### **3.2.2 Optimizing deterministic approach**

In 1980, Mayer and Sibbit, presented a new approach of well-log analysis in a paper titled "Global, a New Approach to Computer-Processed Log Interpretation". They present the idea of the relation between the measured log values and the theoretical answer expressed by the response formula stated for each log, where the log response equation is considered as mathematical equation consisting of known values and unknown values. The log analyst can set up the known component by his area geological knowledge about the basic lithology (sandstone, shale, limestone, dolomite) and the mineral composition of such lithology (quartz, calcite, clay minerals), plus the fluids type filling the pore space (water base mud filtrate, oil base mud filtrate). Furthermore, by entering the log response properties of such minerals and fluids (matrix zone properties, shale zone properties and fluid properties) into the mathematical response equations of the used logs which composed also with unknowns expressed by fraction volumes( $v/v$ ) of minerals(shale, quartz, calcite, etc) and fluids(porosity). These volumes can be obtained by simultaneously solving the mathematical response equations of the used logs. The derived fraction volumes were adjusted to give the optimum and as a consequence to get good match of the measured log reading and the predicted log reading for the reservoir interval has been processed. Unlike the previous deterministic method, with the optimized deterministic method all unknown volume fractions are computed simultaneously, so the complete forms of response functions are used (e.g. in the previous example effect of porosity on gamma ray measurement is not ignored). Furthermore, it can

monitor the quality of the predicted answers by handling of constraints on the accepted range of volume fractions.

### **3.2.3 Statistical approach**

In 1986, (Quireine et. Al), in a paper titled "A Coherent Framework for Developing and Applying Multiple Formation Evaluation Models" , introduced well log analysis to statistical interpretation by involving more logging tools expressed by their mathematical response equations in form of models in such way, that in each depth site we will have several lithology models. Each model is composed of certain number of minerals in addition to the porosity. The number of the model components are controlled by the number of the used logs Response equations will be built according to the components of each model in this way: multiple rock models are defined; in each of them the number of equations(log response equation) should be greater than the number of components(minerals and porosity). The obtained system of equations at each depth site will be solved applying over-determined mathematical solution. In this case there is no single unique solution, only a most likely solution. The alternative solution is done through a least squares approach on an error formulation. First the difference between measured log and answered log values are determined for all used logs and expressed as interpretation error which will have different value and unite related to each log. These error terms then should be normalized with measured log uncertainty according to each used log. Finally each single normalized error value squared up, the least squares approach achieved by summing all the (normalized squared) interpretation errors this function is called incoherence function. Measuring this function between the estimated log value and the recorded log data will lead the selection of the most likely reliable solution. At each depth site with each model, the set of volume fractions which minimizes the incoherence is accepted as the solution. At each depth site where multiple models are applied, the model with the least incoherence is selected and by which the best fit between the measured and answered log can be obtained.

### **3.2.4 Statistical or deterministic lithology analysis?**

It is well known that statistical log analysis is superior to the deterministic system since the former has an intrinsic quality control and standard errors of the results can be also estimated. However, application possibility of the statistical lithology evaluation is limited. Namely, a minimal number of input well logs is required, and the composition of suite of the available well logs is also

restricted. An adequate suite of well logs for statistical evaluation is the following: Density, neutron limestone, photoelectric adsorption index and gamma ray logs.

Spectral gamma ray instead of the single total gamma ray is more advantageous along with thorium and potassium concentration logs as they are free of uranium effect what is sometimes highly destructive first of all in carbonates. There are sometimes marginal cases between applicability of the statistical system. Here is a classical example: three input logs are available; namely gamma ray, neutron and sonic( $\Delta t$ ). In this case three-component rock composition model for statistical analysis could be mathematically applied. However, the uncertainty of the output results would be too high along with high output errors, since the involved two porosity-following logs, the neutron and the sonic, are affected similarly by the rock composition, namely by the porosity and the shaliness. Both log quantities are increased by increasing porosity and by increasing shaliness. According to the above, deterministic analysis is more prosperous in this case. Obviously, only deterministic analysis can be applied when two lithological logs are available such as gamma ray and neutron, or gamma ray and sonic  $\Delta t$ , or gamma ray and density. In these cases the minimal rock-buildup model embedding porosity, basic lithology, shaliness can be applied.

### **3.2.5 What is the practical way of deterministic analysis?**

It is not advantageous to apply a linear system of equations with three unknowns; i.e. porosity, basic lithology, shale volume and to solve this system of equations in simultaneous direct mathematical way. Uncertainties of the relevant zone parameters are regularly too high. This is true especially for the zone parameters of the shale. Uncertainties of zone parameters may result in high output errors. Instead of the simultaneous solutions of the three unknowns, it is more prosperous to apply serial solution logic. First to estimate the shaliness from the gamma ray, and second by inserting the obtained shale volume into the response equation the density, response equation of the neutron and into the response equation of the sonic( $\Delta t$ ). Then to evaluate the effective porosity from the neutron, density and sonic. Finally, the obtained effective porosities  $\Phi_D$ ,  $\Phi_n$  and  $\Phi_s$  will provide the effective porosity  $\Phi$  as an arithmetic mean. It is important to mention that the cases presented above are the most frequent in the practice of deterministic log analysis.

### 3.2.6 Quantitative well log interpretation

Reservoirs exist principally in sedimentary rocks either detrital origin (clastic: sandstone and conglomerates), or of chemical or biochemical origin (nonclastic: limestones and dolostones), or in a mixture of these rock types. However, pyroclastic rocks (breccias, tuffs, weathered or fractured volcanic rocks) may have reservoir characteristics as well. In addition plutonic or metamorphic rocks may constitute hydrocarbon reservoirs under typical conditions: important fracturing and leaching. For rocks to be oil or gas reservoirs two essential characteristics are required: capacity to store fluid, called **porosity**, and connectivity of pore space allowing fluid flow through the rock, **permeability** which is a measure of rocks specific flow capacity and is related to the connectivity and continuity of pore space. Porosity and permeability playing critical roles in the evaluation and management of oil reservoirs. Their understanding is essential for the following:

1. **Determination of oil initially in place:** The task of the hydrocarbon reserve estimation is to calculate the total volume of the oil related to the effective porosity of the reservoir rocks. A necessary condition is the knowledge of effective porosity value. Using of well log analysis such as (PETROLOG software methods) and core analysis measurements in an integrated form could be helpful to establish a method for the determination of the effective porosity for different rock environments.
2. **Pore system characterization, its impact on the well productivity, production optimization and recovery** (Coskun, S.B., Wardlaw, N.C. and Haverslew, B., 1993): The reservoir rocks consist of an interconnected pore network made up of many different pore types and pore sizes. While details of pore geometry may seem to be of little immediate practical significance for petroleum exploration purpose (Pettijohn, F., Potter, P. and Siever, R., 1972), they are of vital importance for production. The rate, at which a non-wetting fluid like oil can be produced from reservoir rock, and the efficiency of the oil recovery as a percentage of the oil in the reservoir, are determined by fluid properties and the characteristics of the pore system (Dullien, F., 1979). That is why it is necessary to study the relation between porosity and hydraulic fluid permeability and to have continuous information about permeability of the reservoir rocks. These cannot be obtained from core analysis neither from well tests, the only source of it are the well logs.

### **3.2.6.1 Porosity definitions**

#### **3.2.6.1.1 Geological definition**

The pore systems contained in reservoir rocks (the bulk volume percentage of voids or pores within a rock) are controlled by primary factors which are related to depositional processes (facies, texture, grain size/sorting, detrital clay content) and by secondary factors related to diagenetic processes (autogenetic clay content, cementation, compaction, and dissolution of soluble grains or fracturing). (Brayshaw, A.C., Davies, G.W. and Corbett, P.W.M., 1996) The pore systems can be classified as: Primary porosity comprises the intergranular spaces between grains before modification of the pore system by diagenetic processes. And secondary porosity as a consequence of the following processes: fracturing, shrinkage, dissolution (Laresn, G. and Chilingar, G., 1979). In turn it can be subdivided into macroporosity or microporosity depending on whether pores are  $>$  or  $<20\mu\text{m}$  in diameter.

#### **3.2.6.1.2 Petrophysical definition**

Total porosity: The total void volume related to the bulk rock volume.

Bound water porosity: That part of void volume which is filled up with bound water (associated with clays and silts), related to the bulk rock volume.

Effective porosity: Interconnected pore volume occupied by free fluids (movable part of the water in the effective pore space), and capillary water (occupies capillary pore throats; it is retained by capillary forces).

Useful porosity: Is the effective porosity which contributes to the permeability during the production such as open fractures, large size vugs, and small size vugs.

### **3.2.6.2 Permeability**

Permeability is a measure of the ability of porous material to transmit fluid. The unit of measurement is the darcy, named after a French scientist who investigated flow of water through filter beds in the year 1856. The permeability is a function of the size, shape, and distribution of pore channels in the rock. These relationships were investigated for clean sands by Slichter in 1889 and Kozeny in 1927, and related to grain sizes and packing arrangement. Based on Kozeny-Carman relation, many other models relating permeability to porosity, pore geometry and other

petrophysical and petrological parameters were evolved (Allen, D., Coates, G. and Muller, P., Ayoub, J., et al, 1988)

#### 3.2.6.2.1 Permeability definitions:

Specific permeability: This refers to permeability with one fluid present at 100 percent saturation.

Effective permeability: When a second or third phase is introduced, the resulting permeability to each phase is called effective permeability which is the hydraulic conductivity of each phase at specific saturation.

Relative permeability: The concept of relative permeability provides an extension of Darcys Law to the presence and movement of more than a single fluid within the pore space. It represents the ratio of effective permeability to the specific permeability.

### **3.3 GEOSTATISTICAL APPROACH FOR CHARACTERIZING THE DIFFERENT SPACES OF UNCERTAINTY**

Effective management of petroleum reservoirs regularly requires detailed spatial models/descriptions of basic lithological units and their porosity, permeability and saturation characters. Because spatial heterogeneity of these properties is commonly complicated and the available information is limited, it is impossible (even unrealistic) to build any deterministic models that represents the actual heterogeneity of the reservoir. By accepting and understanding these limitations it becomes sensible to translate the imperfect knowledge into a probabilistic framework. In general uncertainty can be interpreted as imperfectness of our knowledge.

From the early 90's considerable amount of efforts were taken to several issues of uncertainty. For example, about its objective assessment Srivastava (1994) emphasized that any work focusing on uncertainty relied on the 'belief' that outcomes could fairly sample the space of uncertainty. Wingle and Poeter (1993) recognized that using only a single semivariogram model, there is no way to take all the uncertainty into account. Journel (1999) acknowledged that geostatistics could not provide a fully objective assessment of uncertainty, since its probability statements strongly depended on both the decision taken on *a priori* probability distribution and the algorithm used to express the uncertainty. Later Goovaerts concluded that both the models of uncertainty and the



subsequent risk assessment were affected by the (1) choice of conceptual model; (2) simulation algorithm and (3) inference of the parameters of the random function model (Goovaerts, 2006).

### **3.3.1 The roots of uncertainty**

The conceptual model of any kind of probabilistic framework is that of random variable or random function. This model allows making uncertainty assessment about an imperfectly known attribute or variable. A random variable is a variable that can take a series of possible outcomes, each with a certain probability (frequency) of occurrence (Goovaerts, 1997, Deutsch and Journel 1998). In the discrete case, to each outcome  $z_i$  is attached a probability value of the following form:

$$p_i = P(Z = z_i) \in [0,1], \text{ where } \sum_{i=1}^n p_i = 1 \quad (1)$$

In the continuous case, the distribution of probability values can take two forms of a cumulative or a probability density function. The former one is pictured as cumulative histogram, while the latter one is shown as histogram.

A cumulative distribution function (cdf) gives the probability of not exceeding a special cut-off. From a probability density function (pdf) one can derive probability intervals. For a probabilistic interpretation of a random variable, modeling of the distribution function (cdf or pdf) is an essential task. It is worth emphasizing, that such modeling does not mean necessarily fitting a parametric function. That distribution function can be built up by a series of classes with attached probabilities (frequencies). This dense histogram can then provide all the information that is needed for quantifying the uncertainty about the actual outcome.

The above explanations account for the popularity of geostatistics. Geostatistics is not simply the application of statistical methods to geology-driven spatial distributions. It also provides a conceptual framework for making inferences from Earth sciences data including hydrocarbon reservoirs. At the root of this framework the term of regionalized variable can be found. Regionalized variable is a complex term. Regionalized variables are locally random variables, as many as the number of locations available. But these random variables are connected by a multidimensional function in space. That is one can say that a regionalized variable is a multidimensional probability distribution, where the number of dimension equals to the number of locations. By accepting the above thoughts of uncertainty, one can argue that all predictive geostatistics amounts to the determination of a probability distribution model above a particular

region. That is why geostatistics is an outstanding approach for modeling uncertainty (Goovaerts, 1997, Chiles and Delfiner, 1999).

### **3.3.2 Local and regional uncertainties**

In the characterization of petroleum reservoirs Goovaerts (2006) has defined local, regional and response uncertainty. Local uncertainties are uncertainties about the value of a petrophysical attribute at an unsampled location. Spatial uncertainties are joint uncertainties about values at several locations taken together. Finally, response uncertainties arise about production forecasts. These latter ones are not the scope of this work.

The probabilistic way to model uncertainty about a continuous attribute  $z$  at  $u$  location views the unknown value  $z(u)$  as the realization of a random variable  $Z(u)$ . It makes possible drawing the conditional cumulative distribution function of  $Z(u)$ .

$$F(u; z|n) = P\{Z(u) < z(u)\} \quad (2)$$

In the above equation the notation “ $|n$ ” expresses conditioning to the local information, say  $n(u)$  neighboring porosity values. According to the above explanation, cumulative distribution function of type (2) fully models the uncertainty at location  $u$ .

This modeling approach can be performed in a parametric (i.e. Gaussian approach) or in nonparametric ways. In the first case, determination of ccdf used to draw back to normal distribution, which is fully determined by its mean (expected value) and variance. Multi-Gaussian kriging (VERLY, 1986) capitalizes this property of the multi-Gaussian model, when determines the mean and variance by the simple kriging estimate and variance. In case of skewed, or spike distribution some data transformations (for instance log or square root transformation, etc) are necessary for stabilizing the variance. Doubtless, the most powerful way is the normal score transformation. These procedures usually do not introduce additional uncertainty in the analyses.

Remy et al. (2009) pointed out, that neither the most often used moments, expected value and variance suffice by themselves to define a distribution unless it is a Gaussian one. Also in case of Gaussian related distribution, the problem is that errors associated to the various data integration processes involved in spatial interpolation are almost never Gaussian distributed as opposed to direct errors due to measurement devices. Hence applying probability intervals in the form of (3) is a general solution in the case of nonparametric description.

$$P\{Z \in (a, b)\} = F(b) - F(a) = \int_a^b f(z) dz \quad (3)$$

Unlike the Gaussian based approach, nonparametric algorithms do not assume any particular shape or analytical expression for the conditional distribution. Instead, the  $F(u)$  function is determined by a series of  $K$  threshold values discretizing the range of variation of  $z$ .

The nonparametric geostatistical estimation of  $F(u)$  values (Journel, 1983) is based on the interpretation of conditional probability (1) as the conditional expectation of an indicator random variable given the information  $(n)$ . That is

$$F(u; z|n) = E\{I(u; z_l)|(n)\}, \text{ where } I(u; z_l) = \begin{cases} 1, & \text{if } Z(u) < z_l \\ 0, & \text{otherwise} \end{cases} \quad (4)$$

Consequently, values of a conditional cumulative distribution can be estimated by least-squares (kriging) interpolation of indicator transforms of data. This procedure usually requires the estimation and modeling of an indicator semi-variogram for each threshold (cut-off). It must be noted that this indicator approach is much more demanding than the multi-Gaussian one both in terms of variography and computer requirements.

From the above outline it may be clear, that for characterizing the local uncertainty the random variable nature of regionalized variables is used. For describing the field of regional uncertainty the multidimensional distribution character of these variables is the traditionally applied approach. Multidimensional distributions are functions of many parameters which are different from one location to another.

The analytical expression of such multidimensional distribution is impractical on a grid. Just as a single random variable can be defined by a finite set of simulated realizations, a multidimensional distribution is displayed and used through its realizations (Goovaerts, 1997, Chiles and Delfiner, 1999, Deutsch and Journel 1998). In practice these realizations take the form of a finite number  $L$  of simulated maps. Each of them provides an alternative, equally probable representation of the unknown 'true' map. These can be regarded to be a numerical model of the possible distribution in space of the  $z$  values. From the set of  $L$  realizations (grids) one can derive the following:

The probability distribution of the unknown  $z(u)$  at any particular locations  $u$  can be built up by the  $L$  simulated values  $z^{(l)}(u)$  at that same location  $u$ . It is worth noting that in a spatial interpolation setting, the cumulative distribution function of the  $L$  simulated error values  $([z^{(l)}(u) - z^*(u)], l=1,2,...,L)$  takes definitely different shapes depending on the data environment of location  $u$ . Also, these shapes do not resemble of Gaussian distribution.

The probability that two nearby unknown  $z(u)$  and  $z(u')$  be simultaneously greater than any given threshold  $z_0$  can be evaluated by the proportion of the  $L$  realizations displaying high simulated values at these locations.

The probability that a connected path of high  $z$ -values exists between two distant locations  $u$  and  $u'$  can be similarly evaluated by the proportion of simulated realizations displaying such connected paths.

Since the  $L$  simulated realizations are equiprobable, their point-wise arithmetic average provides a single estimated value in the sense of least square error. It is called E-type estimated value (Goovaerts, 1997, Deutsch and Journel, 1998). It is also worth mentioning that E-type maps are usually 'smoother' than any one of the  $L$  simulated realizations.

From the above mentioned 'equiprobability' one can point-wise probability intervals defined by (3). The upper and lower data bounds form two surfaces surrounding the E-type estimations. The thinner the data range between the upper and lower quartiles, the less uncertainty about the expected value. That is the width of these probability intervals directly expresses the uncertainty about the E-type estimation.

These are those thoughts which were applied in the geostatistical analysis of the uncertainty of spatial distributions of well-averaged porosity, permeability and shale volume properties coming from quantitative well log interpretations.

## 4 RESULTS

### 4.1 SEDIMENTOLOGICAL CHARACTERIZATION OF THE FIELD

This chapter is intended to report on sedimentological characteristics of the sequences appearing in the cored intervals of the Lower Nubian series, in well 6J3, 6J4, 6J6, 6J8, and well 6J12 (**Fig. 4.1-1**).

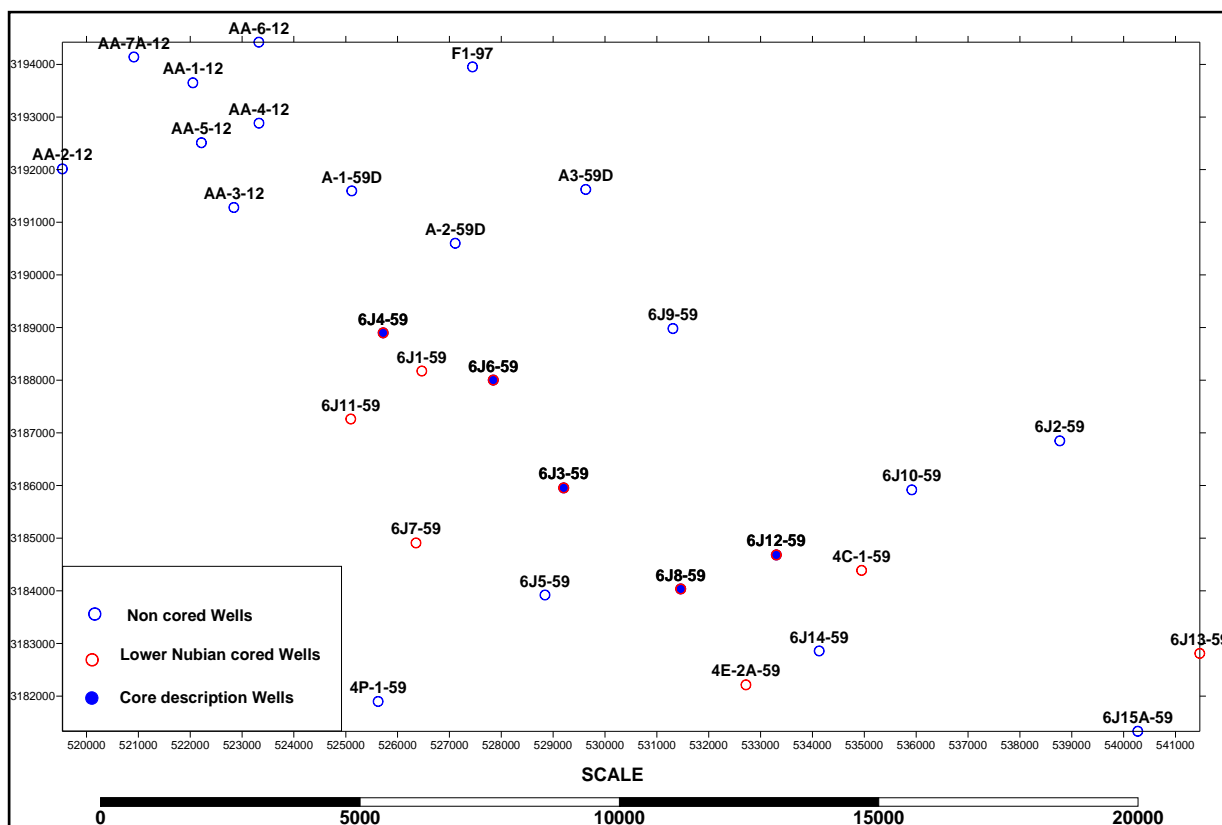


**Fig. 4.1-1: Location map with the cored wells (Note the scale is given in feet)**

These sequences represent the Lower Nubian Base (**LNB**), Middle (**LNM**) and Upper Unite (**LNU**). The corresponding depth intervals and thicknesses are collected in **Table 4.1.-1**.

A detailed core description study performed by Waha Oil Company (Waha, 2008) was the basis of interpretations, which are summarized and presented along with the correlated core analysis data, log analysis input curves and output results **Appendix 1** (**Fig1-1 to Fig1-5**, scale 1:200)

**Table 4.1-1 Stratigraphical positions of the formations**

Well Name	Formation Unite	Start Depth Ft	End Depth ft	Thickness Ft	Remarks
6J3	LNM	11258	11475.5	217.5	
	LNB	11475.5	11736	260.5	
6J4	LNU	11982.5	12750	767.5	
6J6	LNU	12163	12771	608	
6J8	LNU	10740	11033	293	
	LNM	11033	11373	340	
	LNB	11373	11403.5	30.5	not cored
6J12	LNU	11113.5	11351.5	238	
	LNM	11351.5	11674.5	323	
	LNB	11674.5	11854.5	180	not cored

#### 4.1.1 Reservoir rock types

##### 4.1.1.1 Base Unite: LNB

This unit consists of predominantly medium-grained, but locally pebbly sandstone with thin conglomerate beds (**Fig. 4.1-2**). Scattered pebbly layers interbedded by gray and brown sandstone clasts with possibly extra formational origin can also be characteristic.

Faint and cross-lamination are present. Some laminae are partially stylolitized. Sandstones from this unite reflect deposition by a high energy braided channel system (**Fig.4.1-2**).

Sandstones are tightly cemented by quartz. There is little or no visible porosity. Subsequent pervasive quartz cementation is noticeable and is in contrast with the overlying Lower Nubian Middle section (LNM).

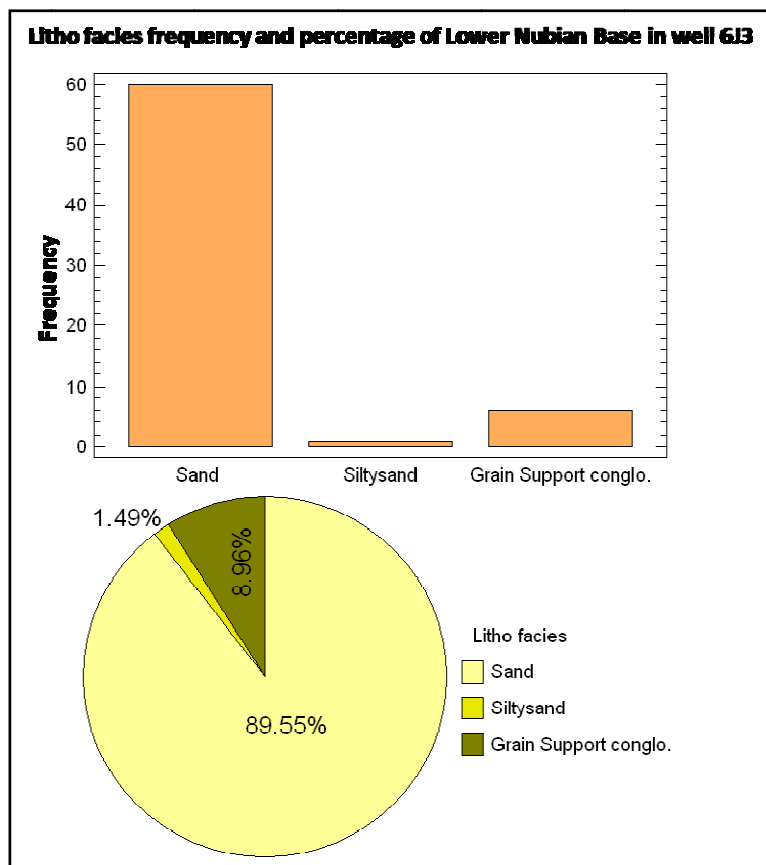


Fig. 4.1-2 : Frequency distribution of lithofacies in LNB sequence of well 6J3

#### 4.1.1.2 Middle Unite: LNM

Predominantly fine to medium-grained sandstones (commonly pebbly and some locally silty), with subordinate siltstones and minor conglomerates play important role in building up this sequence. The latter two rock types are present in 6J3, at the base of the section in 6J3. Overall, the LNM zone exhibits higher silt content than the units being above (LNU) and below it (LNB).

Horizontal lamination is prevalent throughout, with cross-bedding observed locally. The silty constituents are in the form of laminated siltstone and laminated to massive silty fine sandstone. Sandstone is generally massive or laminated or cross-bedded, with a minor amount of ripple bedding. Some indistinct bioturbation is present, noticeably in the silty interval of 6J12 from 11454 to 11471 feet, (**Appendix 1 (Fig1-5)**). This interval is also distinguished by thin wavy bedding with alternations of sandstone and muddy siltstone. Sandstones near the base of LNM in 6J3 (11460-11470 feet)

In 6J3, just above the upward cleaning basal section, sandstones are locally coarse with pebble lags, in crudely fining-upward cycles of 5 to 10 foot thickness.

In 6J12, near the middle of LNM, about a foot of thin-bedded conglomerate of angular sandstone pebbles was observed. The cored section from 6J12 is similar but shows somewhat more contrast between porous and well-cemented units.

Slightly higher in 6J3 (11450- 11455 feet), cross-bedded sandstones have distinct and coalescing spots of reddish-brown cement, probably siderite oxidized to hematite.

Sandstones in the cored interval of 6J3, after an initial pulse of coarse-grained conglomeratic debris flows, reflect the progradation of a fluvial and subsequent braided channel system. This initially coarsens upwards, with later localized marginal sand flat and rarer silty overbank deposition. LNM unit are also recognized in 6J8 and 6J12, where moderately silty successions of splays and overbank facies may represent marginal sedimentation in the former, and a bioturbated estuarine/deltaic section in the latter, in addition to channelized (braided) environments (**Fig.4-1.3 and Fig.4-1.4**).

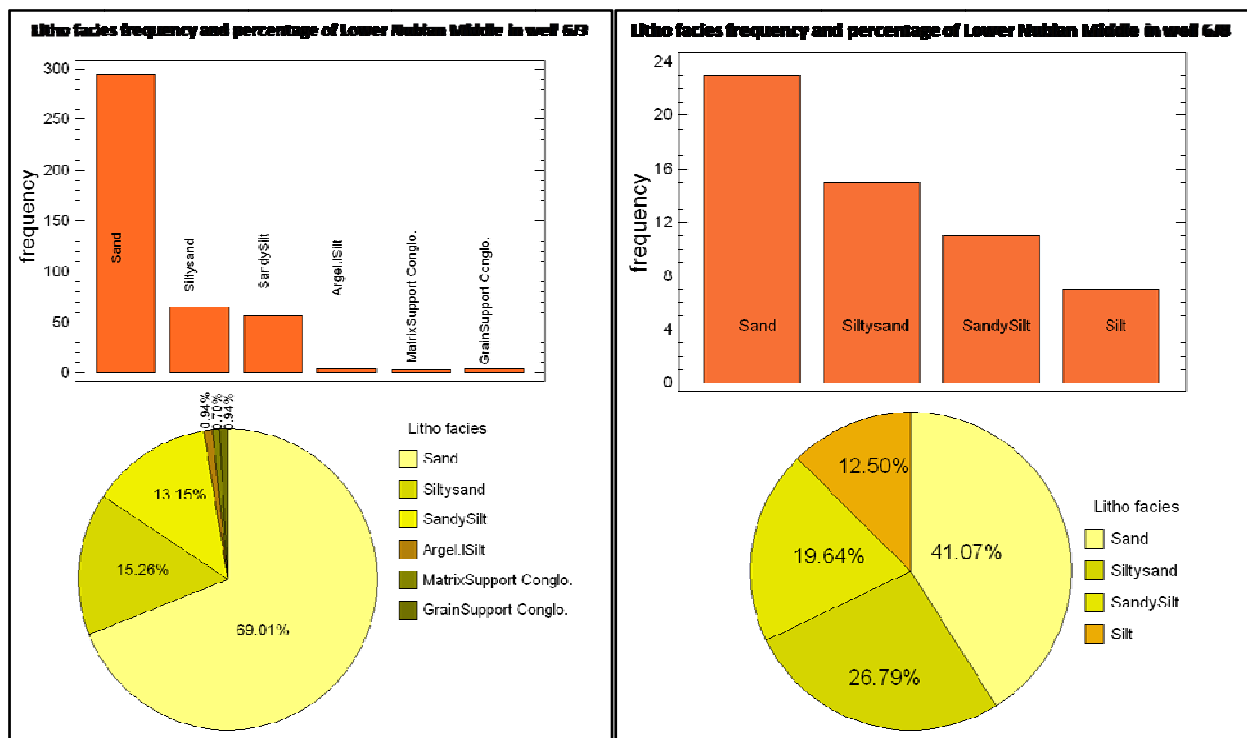


Fig. 4.1-3: Frequency distribution of lithofacies in LNM sequence of well 6J3 and 6J8



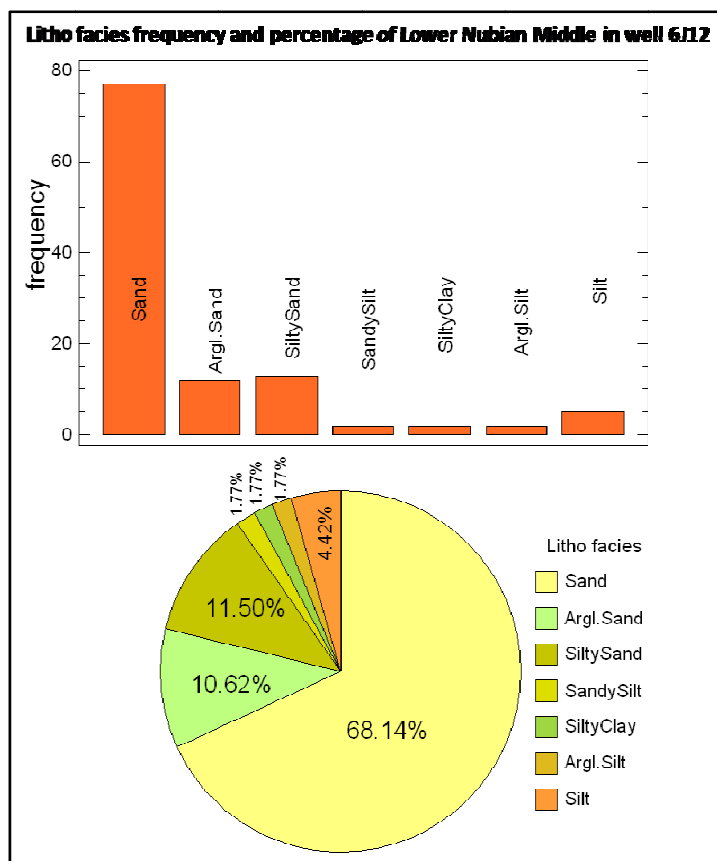


Fig. 4.1-4: Frequency distribution of lithofacies in LNM sequence of well 6J12

#### 4.1.1.3 Upper Unite: LNU

The predominant lithofacies of this unite are fine- to medium-grained sandstones with some very fine and coarse intervals. The siltstone and silty shale beds are up to a few feet thick.

Individual beds are defined by cross-bedding sets and co-sets, and planar-laminated to low-angle cross-stratified intervals. Pebble lags are scarce and mainly consist of tabular claystone intraclasts. Mudstones are predominantly gray, silty, and slightly bioturbated. Sandstones are well- cemented and variably oil-stained. (**Fig.4.1-5, 4.1-6**)

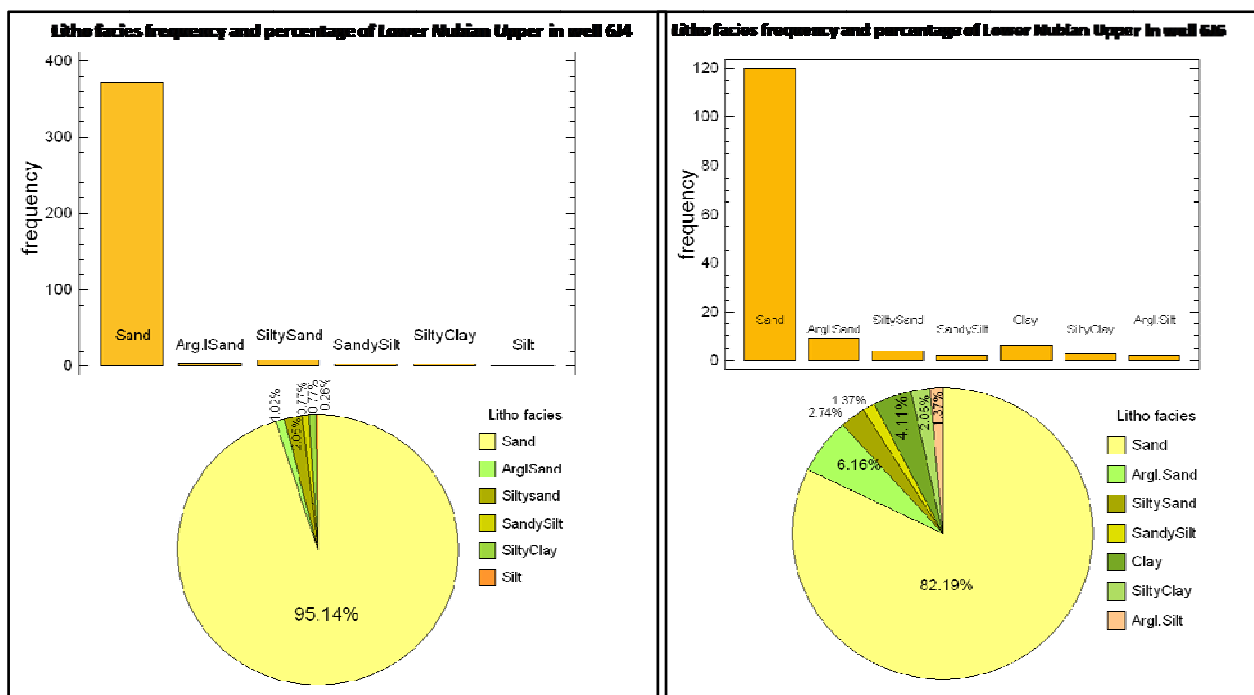


Fig. 4.1-5: Frequency distribution of lithofacieses in LNU sequence of well 6J14 and 6J6

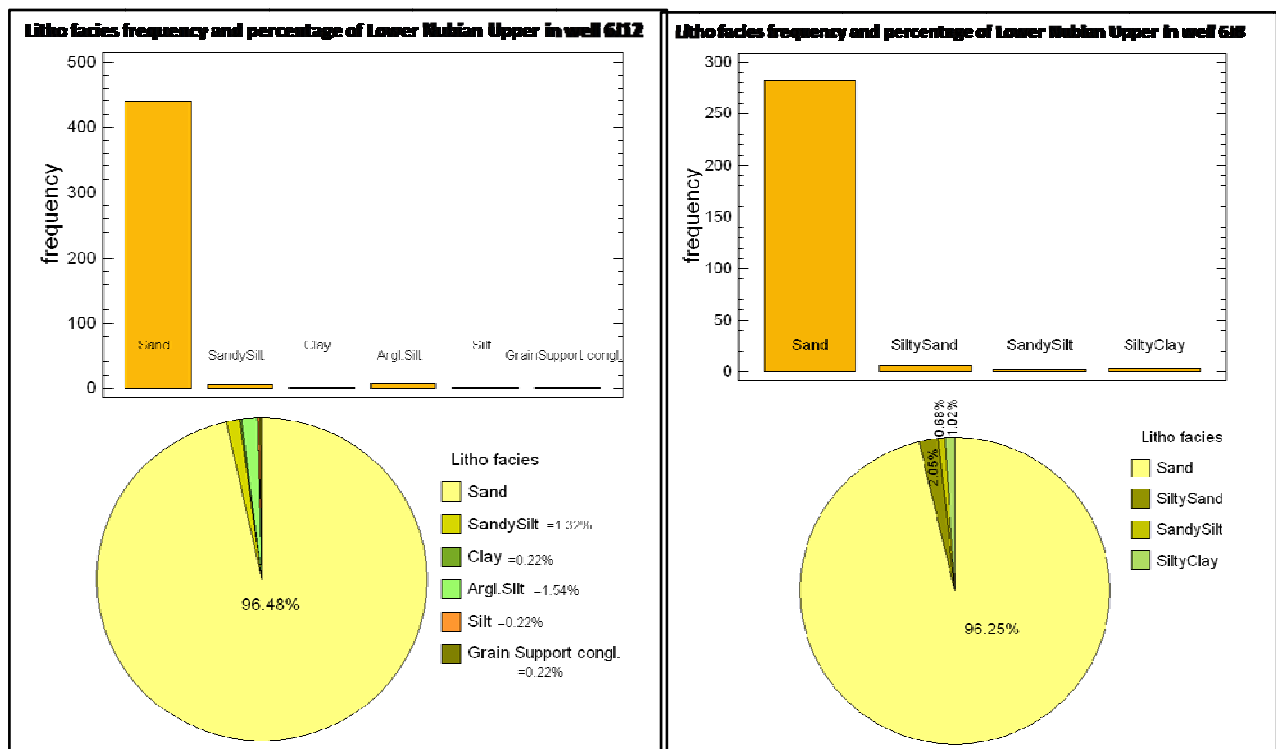


Fig. 4.1-6: Frequency distribution of lithofacieses in LNU sequence of well 6J12 and 6J8

## 4.2 FACIES ANALYSIS

In the cored wells the Lower Nubian sequence has been subdivided into three groups of facieses containing eight facies types. The groups of facieses are summarized in **Table 4.2-1**. Each facies represents a distinct association of lithology, grain-size, and sedimentary structures. Wire line Log characteristics is shown by type log diagram reported in the **Appendix 1 (Fig2.1 to Fig2-7)**.

**Table 4.2-1: The results of facies analysis**

Facies Group	Facies	Thickness Range (ft)	Facies Description
Braided Stream (BR)	Channel	4-137	Channel sandstones mostly medium grained, clean to slightly silty, planar cross-bedding, massive to fining upwards
	Sand Flat	2.5-11.5	Sandstone of this facis is mostly very fine grained, highly silty, laminated planar and cross-bedded fine grained sandstone.
	Abandon Channel	2-5	Abundant channel sandstone is very fine grained; variably silty to argillaceous dominated by horizontally laminated, bioturbated when it is silty or argillaceous.
Esturian/Deltic (ED)	Channel	7.5-8	Fine- to medium-grained sandstone, clean to slightly argillaceous, cross bedding to wavy laminated.
	Mouth bar	1-21.5	Coarsening upward succession, massive to laminated mudstone with very fine to fine grained sandstone, clean, massive to wavy lminated and biouturbated
	Abandon Channel	3-4	Fining upward succession, with fine to medium grained sand stone, massive to gross bedded. And massive mudstone.
	Channel/Bar Margin	6.5-13	Fine grained sandstone, clean to slightly argillaceous, bioturbated. With laminated siltstone and massive mudstone.
Fluvial (FL)	Channel	2-8	Fine to medium grained, cross bedded sandstone, clean to silty, massive to silty laminated.
	Lake/Overbank	1.5-4.5	Very fine grained sandstone, highly silty, dominated by lamination.
	Abandon Channel	1-3	Very fine sandstone horizontal to rhythmical silty laminated
	Crevasse splays	1.5-9.5	Crevasse splay sandstones, very fine to medium grained, slightly to highly silty, dominated by lamination, arranged in upwards coarsening sequences.
	Debris Flow	4	Corse to very coarse sandstone, slightly silty, massive to granular with matrix supported conglomerate.

### 4.2.1 Braided Stream Association (BR)-Channel Facies

This facies represents the **LNU** in wells 6J4 and 6J12; the **LNM** in wells 6J3, 6J8 and 6J12; and **LNB** in well 6J3. (**Fig. 4.2-1**)

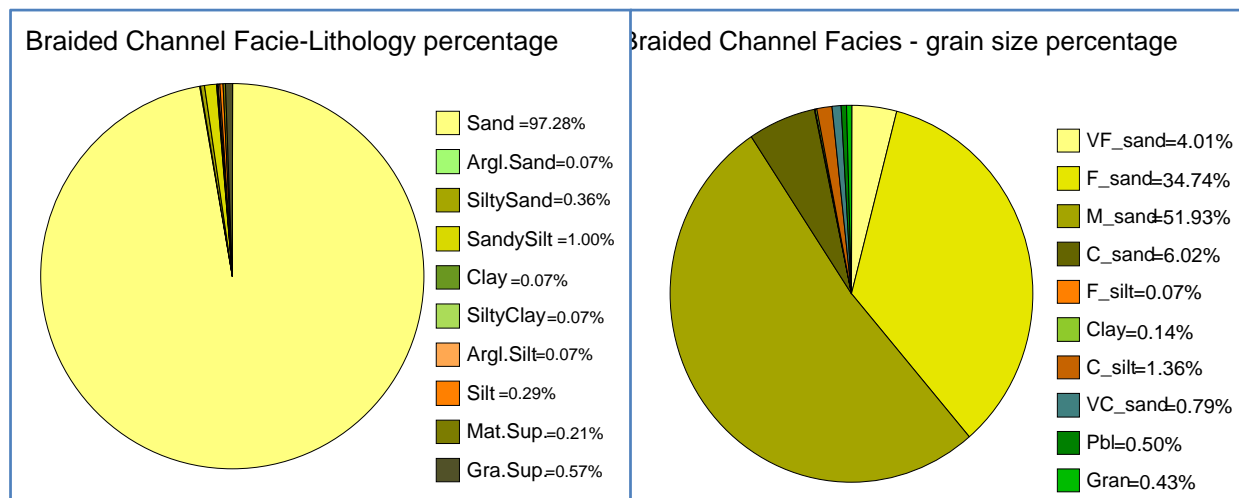


Fig. 4.2-1.: Lithological composition and grain-size characteristics of channels.

#### 4.2.1.1 Channels in the LNU sequence

**In 6J4** this facies appears by appreciable thickness at (12657.5 to 12741.5ft), it is characterized by fine to medium grained massive sandstones (**sm**) above which faintly cross-bedded sandstone(**sp/sm**) then fine to medium grained cross-bedded sandstone(**sx**), and finally very fine to fine grained, horizontally laminated sandstone (**sl**) appears **Appendix 1 (Fig1-2)**. In this fining upward sequence very fine grained, rhythmically laminated sandstone (**szl**), and fine to medium grained, faintly laminated to massive sandstone (**sl/sm**) may also be characteristics.

**In 6J12** this facies appears at two stratigraphic intervals. Between 11132.5 and 11194ft it consists of massive sandstone(**sm**) above which locally coarse, but generally fine- to medium-grained faintly cross-bedded sandstone (**sp/sm**) has been settled. Fine- to medium grained, planar cross-bedded sandstone (**sp**), and fine grained, horizontally laminated sandstone (**SL**) is also characteristics. They often rhythmically change each other **Appendix 1 (Fig1-5)**.

From 11199 to 11336ft, this facies is built up by a series of fine to medium grained massive sandstone(**sm**), fine to medium grained cross-bedded sandstone (**sx**), and fine- to medium-grained, horizontally laminated sandstone (**sl**). However, silty, laminated sandstone (**szl**), planar cross-bedded sandstone (**sp**) can also be characteristic (**Appendix 1 (Fig1-5)**).

#### **4.2.1.2 Channels in the LNM sequence**

These channels are revealed by the cored intervals of **6J3, 6J8 and 6J12**.

**In 6J3** it consists of planar cross-bedded (sp), faintly laminated to massive (sl/sm) and more typical massive sandstones (sm). However, coarse to very coarse-grained (Sgran) trough cross-bedded (St), and horizontally laminated sandstones (sl) can also be found. At the bases of the channels matrix (Gms) – and clast supported conglomerates (Gcs) appear. The channels are regularly terminated in laminated siltstones (zl). In general after an initial coarsening upward sequence a gentler fining-upward trend is observed. These units unit broadly represents a rapidly fining-upward braided fluvial channel (**Appendix 1 (Fig1-1)**).

**In 6J8** the channels consist of faintly cross bedded sandstone (sp/sm). These intervals comprises silts, very fine- and fine-grained sandstones that are arranged in thin units which commonly display small-scale coarsening upward profiles (**Appendix 1 (Fig1-4)**).

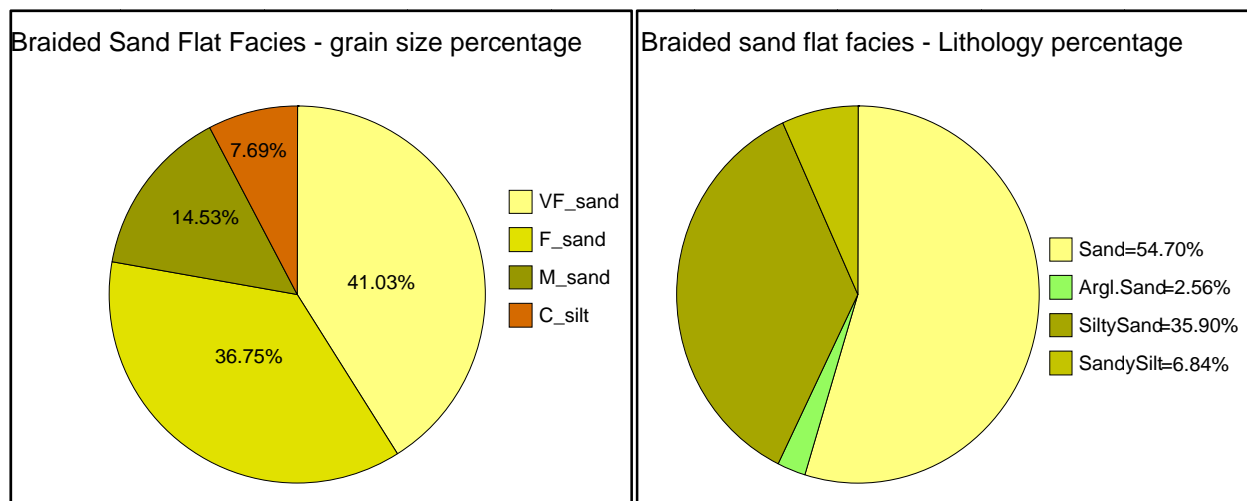
The channels appearing **in 6J12** (11479-11538ft) are built up of medium to very coarse grained, cross-bedded granular sandstone (Sp/Sgran). The intervals are terminated by finer sediments showing bioturbation/churning, which has been interpreted as localized abandonment of braided channel deposition (**Appendix 1 (Fig1-5)**).

#### **4.2.1.3 Channels in the LNB sequence**

These ones have only been revealed by the cored interval of **6J3**. The channel bases are characterized by medium grained matrix supported conglomerates (Gms). Later trough cross-bedded and faintly laminated to massive sandstone series become characteristics. Because of these features, sandstones of these series are thought to reflect deposition by high energy braided channel system (**Appendix 1 (Fig1-1)**).

#### **4.2.2 Braided Stream Association (BR)-Sand flat/Channel Abandonment Facies**

This facies represents the LNU in well 6J4 and LNM in wells 6J3, 6J8. Their lithological, compositions and grain size features are shown on (**Fig. 4.2-2**)



4.2-2. Fig.: Lithological compositions and grain-size characteristics of braided sand flats

#### 4.2.2.1 Sand flat/Channel abandonment in LNU sequence

In **6J4**, it consists of silty and horizontally laminated sandstones (**SI**). As it has been pointed out earlier, this finer-grained interval represents minor abandonments or sand flat deposition.

#### 4.2.2.2 Sand flat/Channel abandonment in LNM sequence

In **6J3** horizontally laminated sandstone (**SI**), laminated (often rhythmically) siltstone (**ZI**), and heavily bioturbated siltstone (**Zb**) are comprised in this series (**Appendix 1 (Fig1-1)**).

Silty, laminated (**SZI**), fine-grained, planar cross-bedded sandstone (**Sp**) and laminated claystones (**MI**) play important role in the sand flats appearing in **6J8 (Appendix 1 (Fig1-4))**.

#### 4.2.3 Braided Stream Association (BR)-Abandoned Channel Facies

This facies represents the LNU in well 6J4, LNM in wells 6J3, 6J8, and 6J12 (**Fig. 4.2-3**).

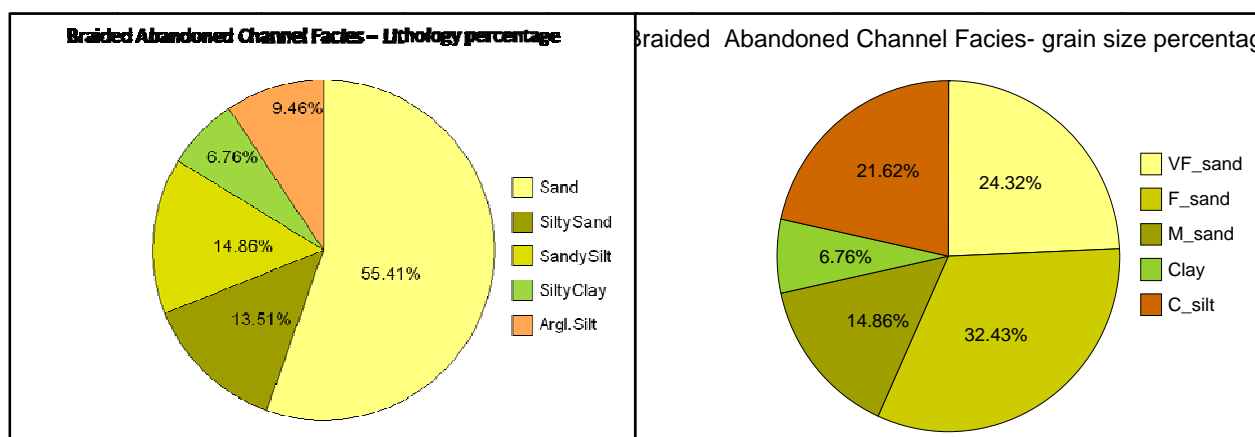


Fig. 4.2-3 Lithological compositions and grain-size characteristics of abandoned channels

#### **4.2.3.1 Abandoned channels in LNU sequence**

This fining upward series appearing above the typical channel lag deposits consists of horizontally laminated sandstone (**SI**), and often rhythmically laminated very fine sandstone (**SZI**) in 6J4. The siltstones of these units often show internal lamination. Bioturbation is also very characteristic (**Appendix 1 (Fig1-2)**).

#### **4.2.3.2 Abandoned channels in LNM sequence**

In 6J3 this series is very similar to that of 6J4. However, in 6J8 this appears in the form of laminated claystone (**MI**) (**Appendix 1 (Fig1-4)**)

Silty laminated (**SZI**), faintly cross bedded (**Sp/Sm**) and horizontally laminated sandstone (**SI**) above which heavily bioturbated argillaceous sandstone (**Sba**) and siltstone (**ZIb**) appear prove the existence of abandon channels in 6J12 between 11502 and 11524ft (**Appendix 1 (Fig1-5)**).

#### **4.2.4 Estuarine/Deltaic Facies Association(ED)**

In 6J6 it is dominated by fine- and medium-grained sandstones, but also contains finer silty sandstones and rarer coarse-grained units. Siltstone and mudstone are present but subordinate. Sedimentary structures include cross-bedding and horizontal lamination. The most striking feature is the moderate to high degree of bioturbation. Together with some subtle coarsening upward trends noted, the degree of bioturbation is thought to reflect a degree of marine influence, perhaps in an estuarine or prograding deltaic setting. The possible development of localized coarsening-upward, prograding mouth bars are predicted, although the overall sequence might be transgressive. This section represents the following facies type:

##### **4.2.4.1 Channel Deposits**

This facies consists of cross-bedded sandstone (**Sx**), fine- to medium-grained, locally coarse, intraclasts-rich sandstone (**Si**), and fine- to medium-grained and wavy laminated sandstone (**Sw**) (**Fig.4.2-4**).

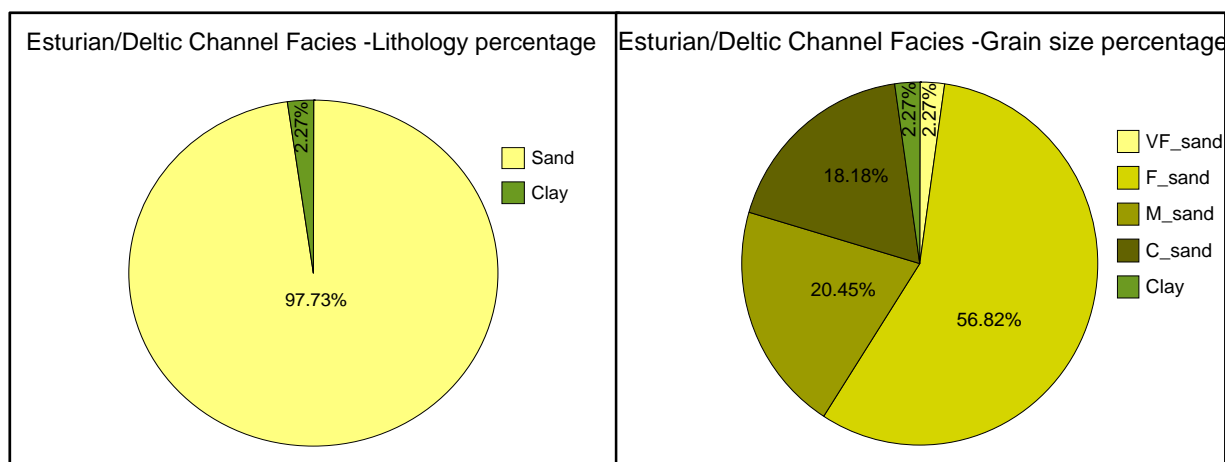


Fig. 4.2-4 Lithological composition and grain-size characteristics of ED channel facies

#### 4.2.4.2 Mouth bar deposits:

The coarsening upward sequence of this facies is built up (from bottom to top) by massive claystone(**Mm**), laminated claystones(**MI**), heavily bioturbated clean sandstone(**Sb**), very fine- to fine-grained, massive sandstone (**Sm**), and wavy laminated sandstone(**Sw**), (**Fig. 4.2-5**).

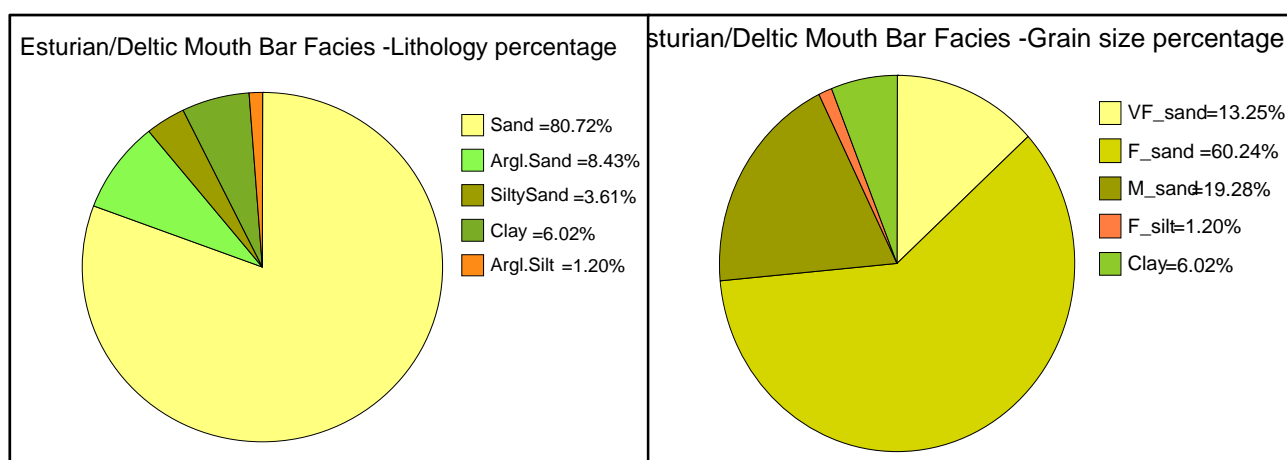


Fig. 4.2-5 : Lithological composition and grain-size characteristics of mouth bars

#### 4.2.4.3 Abandoned Channel Deposits:

At the base of this facies massive sandstone (**Sm**) has been deposited, above which generally fine- to medium-grained, locally coarse, cross-bedded sandstone (**Sx**), then massive claystone (**Mm**) comes (**Fig. 4.2-6**).



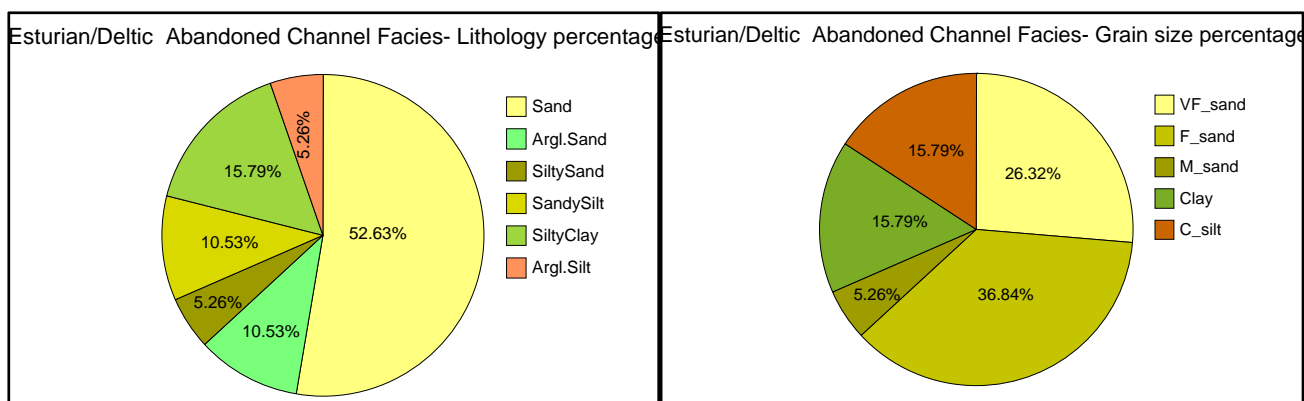


Fig. 4.2-6 Lithology and grain size characteristics of estuarine\deltaaic abandoned channel facies

#### 4.2.4.4 Channel /Bar Margin Deposits

This facies consists of heavily bioturbated clean sandstone (**Sb**), which shows a gradational transition to usually fine-grained, heavily bioturbated, argillaceous sandstone (**Sba**). Then, after laminated siltstone (**Zl**), heavily bioturbated siltstone (**Zb**), and massive claystone (**Mm**) was deposited

In 6J12 (11480- 11499.5ft) this section represented by generally finer-grained and silty facies. In this latter one bioturbation is very common. This section represents two sub facieses: splay and tidal sand flat deposits (Appendix 1 (Fig1-5)).

##### 4.2.4.4.1 Splay Deposits

In such sequences above the basal faintly laminated to massive sandstone unit (**Sl/Sm**), laminated sandstone (**SZI**), heavily bioturbated argillaceous sandstone (**Sl/Sm**) and laminated siltstone have been deposited (Fig. 4.2-7).

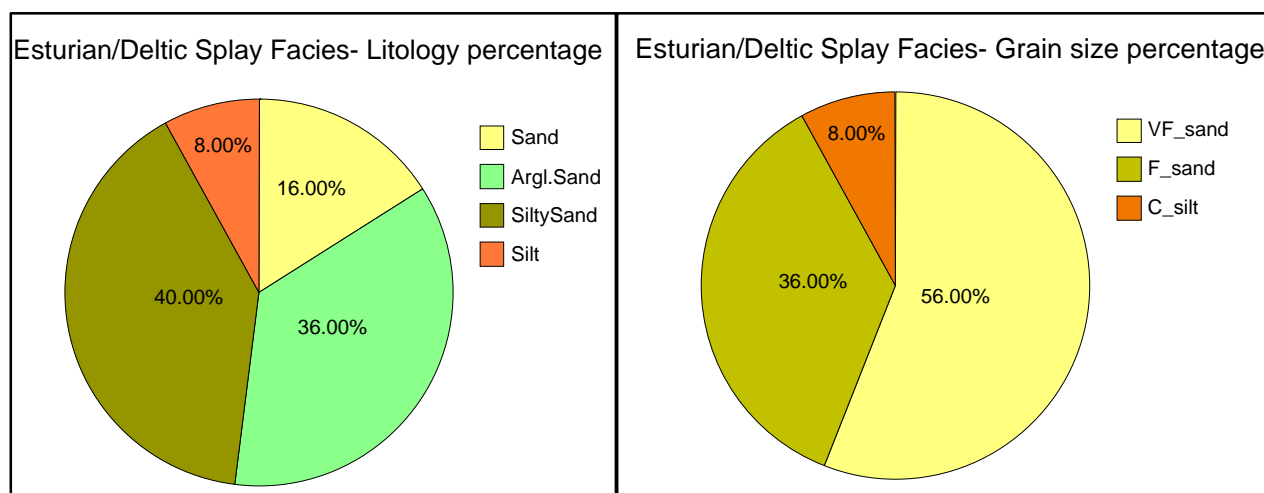


Fig. 4.2-7 Lithology and grain-size characteristics of estuarine\deltaaic splay facies

#### 4.2.4.4.2 Tidal Sand Flat Deposits

This facies consists of ripple laminated sandstone (**Sr**), and very fine- to fine-grained, silty, laminated sandstone (**SZI**) (**Fig. 4.2-8**).

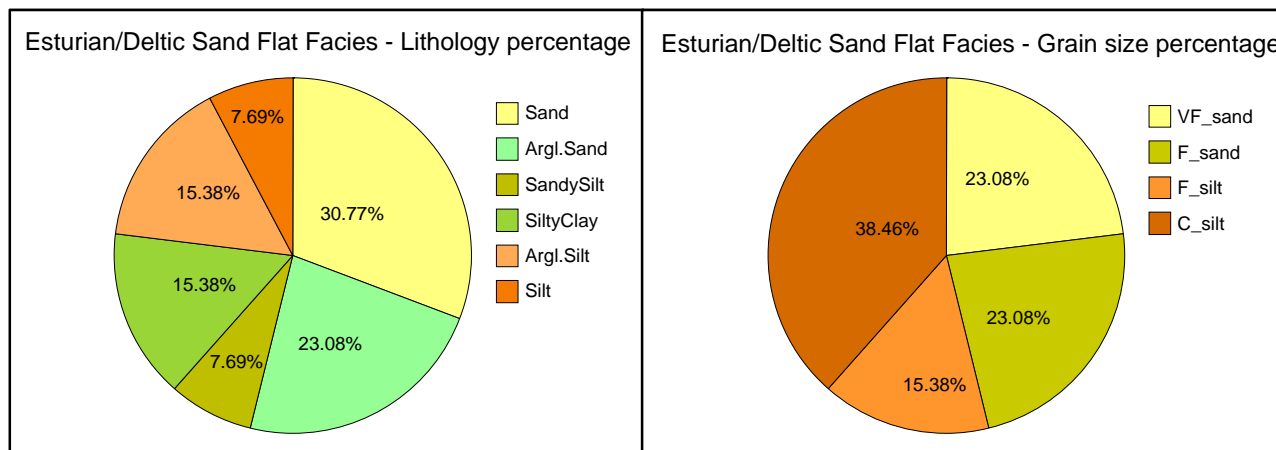


Fig. 4.2-8 Lithology and Grain size characteristics of Esturian\Deltic Sand Flat Facies

#### 4.2.5 Fluvial Facies Association (FL)

This facies represents the LNM in well 6J3 by more distal channel and adjacent overbank deposition. The more granular facies are representative of channels, while the moderately silty successions reflect splays and overbank facies. The coarse-grained conglomeratic debris flows expresses the progradation of a fluvial system.

##### 4.2.5.1 Channel Deposits

In the typical sequence of this depositional facies, above the faintly laminated to massive sandstone (**SI/Sm**) fine- to medium grained, cross bedded sandy series have deposited. This one is followed by horizontally laminated (**SI**) and finally a silty laminated sandstone (**SZI**) series

(**Fig. 4.2-9**).

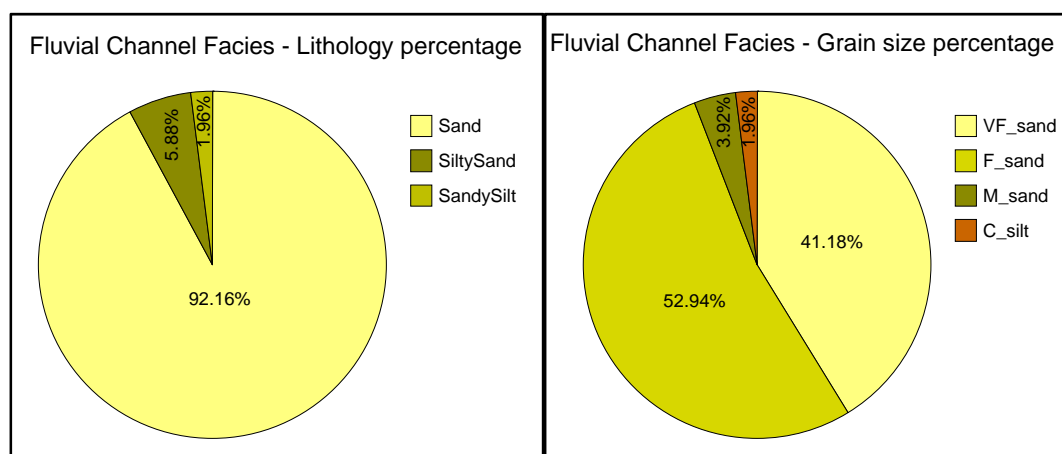


Fig. 4.2-9 Lithology and grain-size characteristics of fluvial channel facies

#### 4.2.5.2 Abandon Channel Deposits

As in any other situation, this sequence appears laminated (**SZI**) or very fine grained, horizontally laminated sandstone (**SI**) at the base which is replaced by often rhythmically laminated siltstone (**ZI**), (**Fig. 4.2-10**).

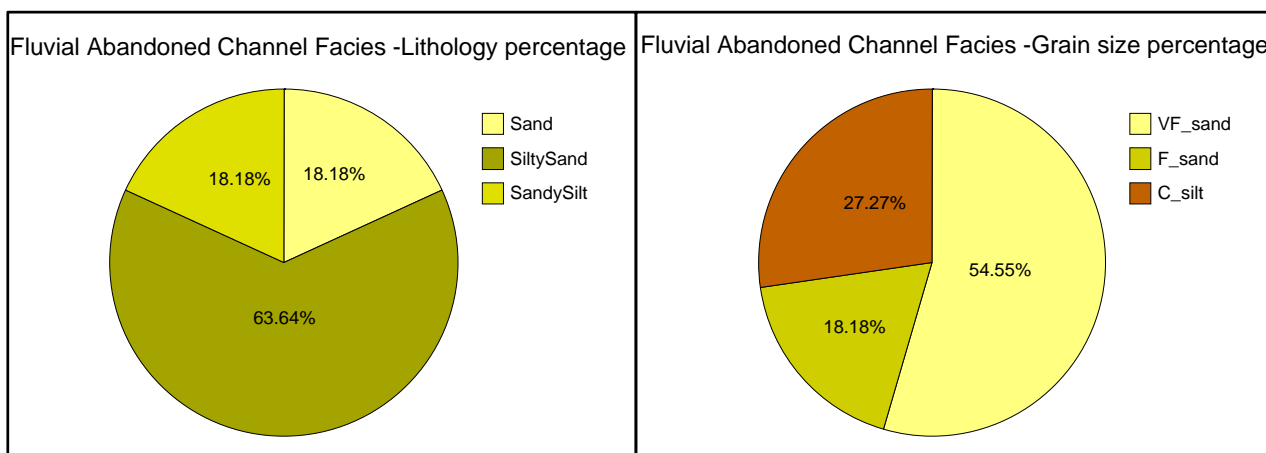


Fig. 4.2-10 Lithology and grain-size characteristics of fluvial abandoned channel facies

#### 4.2.5.3 Crevasse Splay Deposits

With a very fast 'progradation' a massive sandstone unit appears above the flat plain deposits. Above this one often rhythmically, horizontally laminated sandstone (**SI**), and finally bioturbated siltstone build up this facies (**Fig. 4.2-11**).

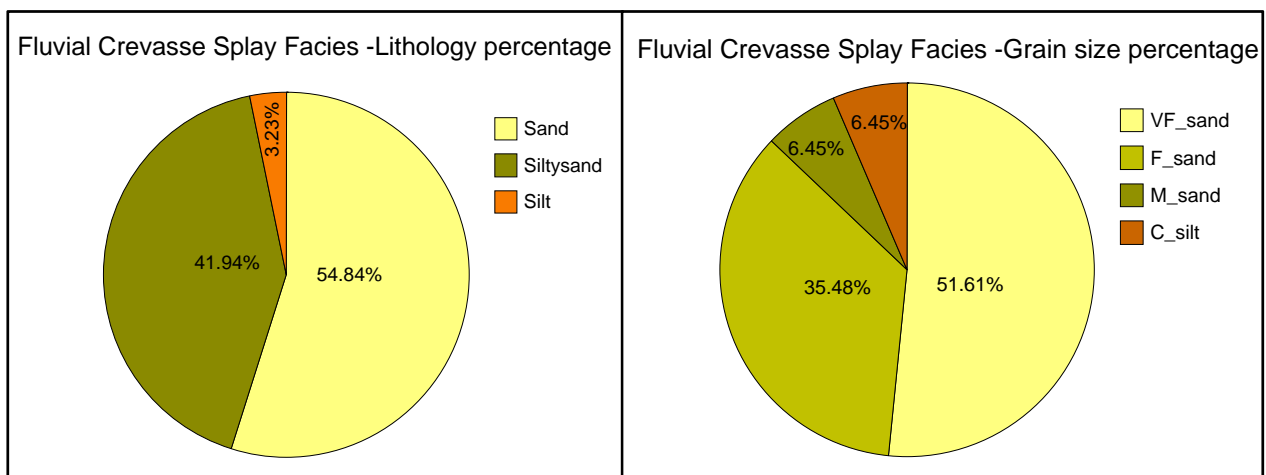


Fig. 4.2-11 Lithology and grain-size characteristics of fluvial crevasse splay facies

#### 4.2.5.4 Lake/Overbank Deposits

In **6J3** this facies is represented by very fine grained laminated sandstone (**SZI**), above which laminated siltstone (**ZI**) appears (**Fig. 4.2-12**).

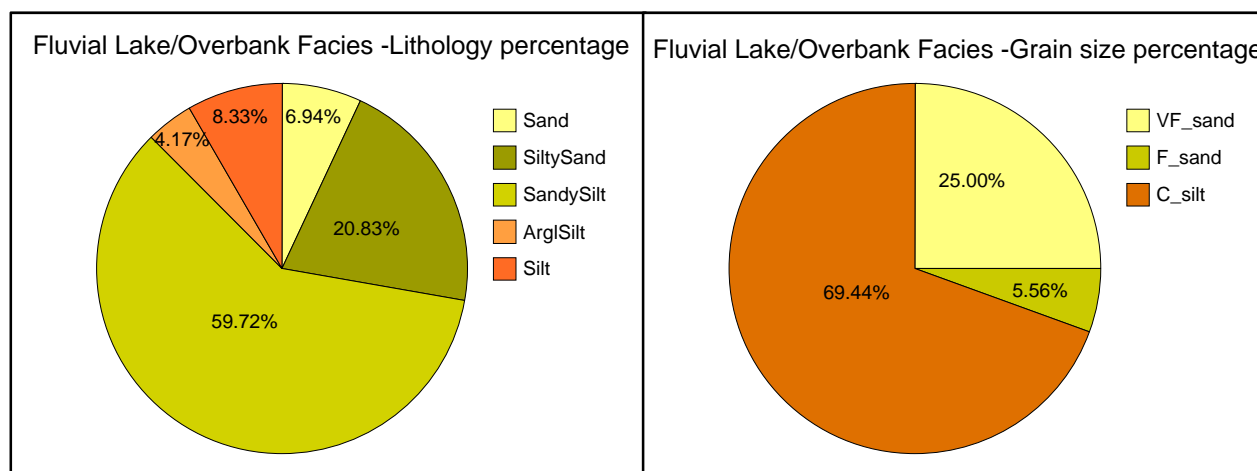


Fig. 4.2-12 Lithology and grain-size characteristics of fluvial lake/overbank facies

#### 4.2.6 Debris Flow Deposits Facies Association

In LNM sequence of **6J3** this facies is presented by matrix-supported conglomerate (**Gms**), coarse to very coarse-grained sandstone (**Sgran**) with common granules, and massive sandstone (**Sm**), (**Fig. 4.2-13**).

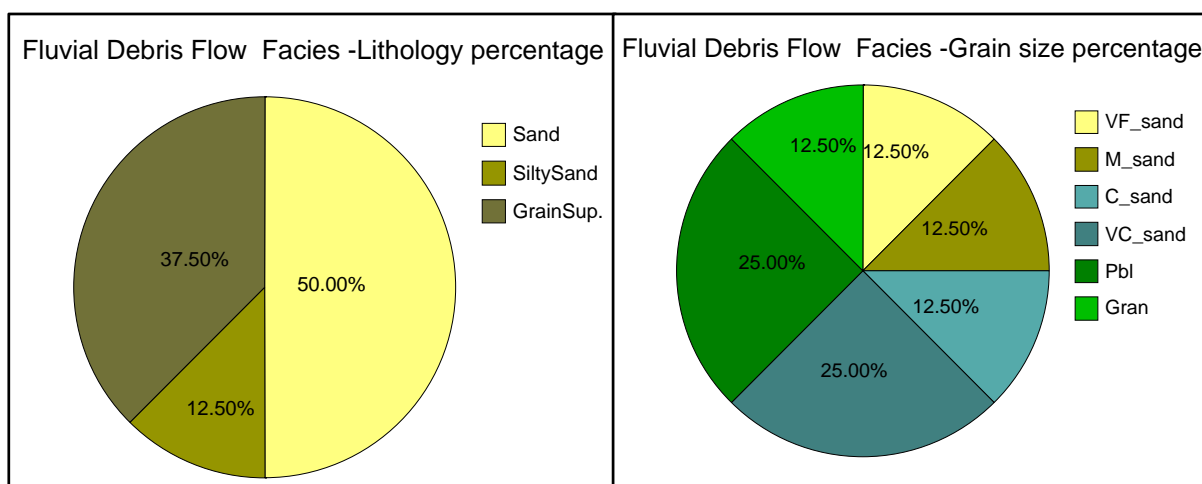


Fig. 4.2-13 Lithology and grain-size characteristics of fluvial debris flow facies

### 4.3 PETROPHYSICAL CHARACTERISTICS OF THE FACIESES

The reservoir characteristics of the studied rock body are discussed in terms of their Petrophysical characteristics (observed from deterministic log analysis and core measurements), sand body geometry and reservoir zonation. These properties are summarized in **(Appendix 1 (Fig1-5))**. For each of the nine reservoir zones of the Upper Unite (LNU), four reservoir zones of the Middle Unit (LNM) unite and one reservoir zone of the basal unite (LNB) .

### 4.3.1 Controls on Porosity and Permeability

#### 4.3.1.1 Primary Controls:

Primary textural characteristics (grain size, sorting and detrital clay content) play the major controls on the lateral and vertical distribution of primary porosity and permeability characteristics of most sandstone reservoirs (Beard and Weyl, 1973). In general, the better sorted the sediments, the more porous it is and the better sorted and coarser grained, the larger the pore throats and the more permeable it is. In the wells studied, despite of a strong diagenetic overprint, primary textural characteristics (i.e. facies type) remain an important control on porosity and permeability variations, as it is illustrated by the relationship between facies and porosity and permeability data (**Fig. 4.3-1**). In these wells, the most significant textural controls on porosity and permeability are sorting, detrital clay content and grain size (**Fig. 4.3-2, 4.3-3**). The highest mean porosities and permeabilities belong to the good and better sorted, and generally coarse-grained sandstones of braided facies sequences (Porosity mean= 0.067 v/v, Permeability mean= 0.52 mD). In marked contrast, estuarine/deltaic facies sediments are more argillaceous (Porosity mean= 0.061 v/v, Permeability mean= 0.21 mD), more poorly sorted and the grain size generally smaller. That is why their average permeabilities are significantly smaller than that of the former cases.

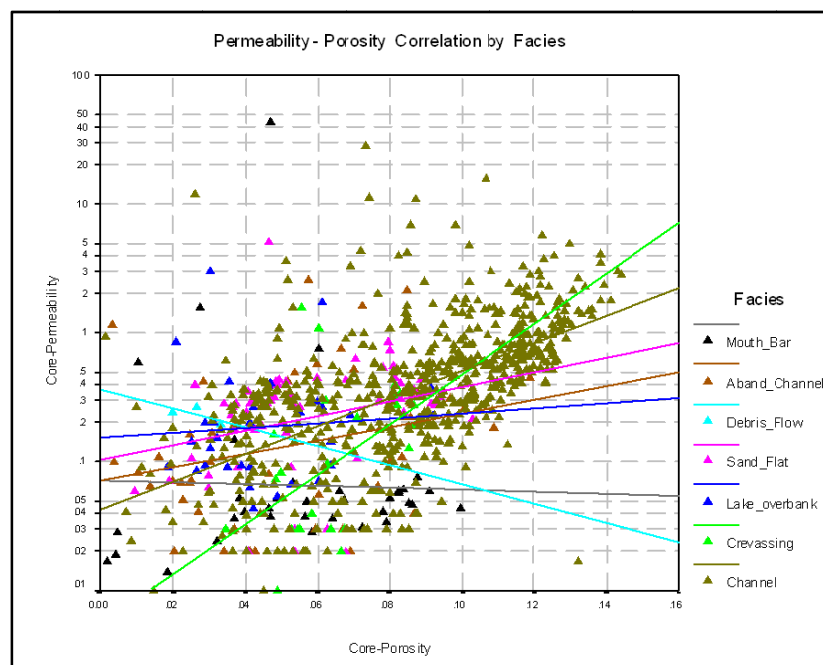


Fig. 4.3-1 Porosity Permeability relationship Facies control

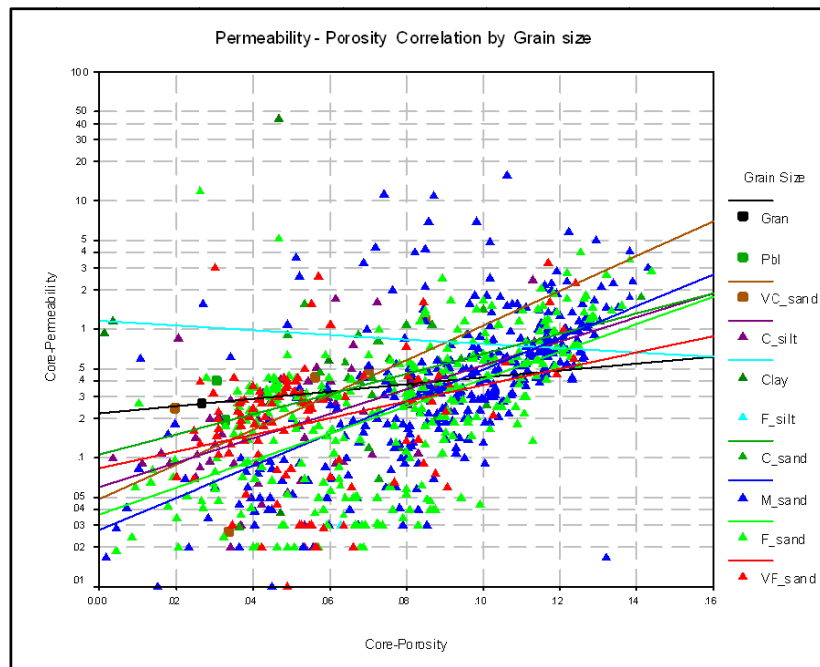


Fig. 4.3-2 Porosity Permeability relationship grain-size control

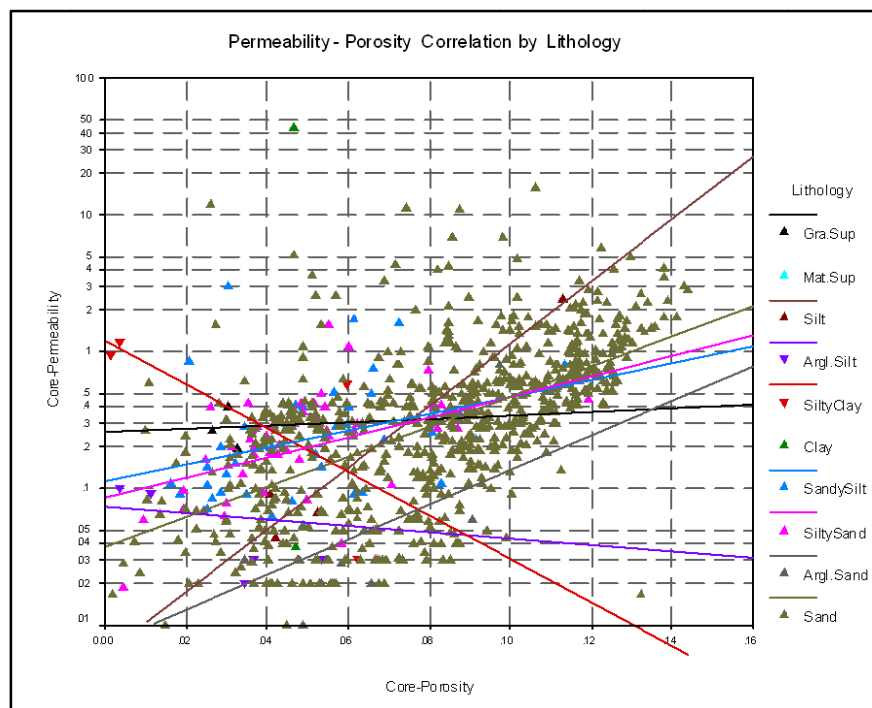


Fig. 4.3-3 Porosity Permeability relationship Lithology control

#### 4.3.1.2 Secondary or Diagenetic Controls:

Porosity reduction by cement precipitation, pore throat narrowing and choking by clays, represents an important diagenetic overprint on the primary porosity and permeability in these wells. According to the core description, four secondary effects have been responsible for reducing initial porosity and permeability: compaction, cementation, formation of autogenic (in situ) clay minerals and fracturing.

Compaction: core observations suggest that porosity loss through burial-related compaction is important as reflected in the localized development of quartz over growth. Permeability has also been reduced by pore throat narrowing and squeezing of detrital clay.

Cementation: In these sandstones, there is a strong relationship between increased cementation and porosity loss both within individual facies and the sequences as a whole. The major cement type's correlation between cementation and porosity loss are quartz, this impact can be seen in the LNB section.

Authigenic Clays: In these sandstones, there is a clear relationship between volume of clay and porosity and permeability (**Fig. 4.3-4, 4.3-5**).

Fracturing: Within the cored interval, fracturing is locally extensive. The main type of fractures recognized in these wells according to the core description studies are as follows: cemented, partly cemented and closed cemented. Locally, there appears to be a significant effect on permeability.

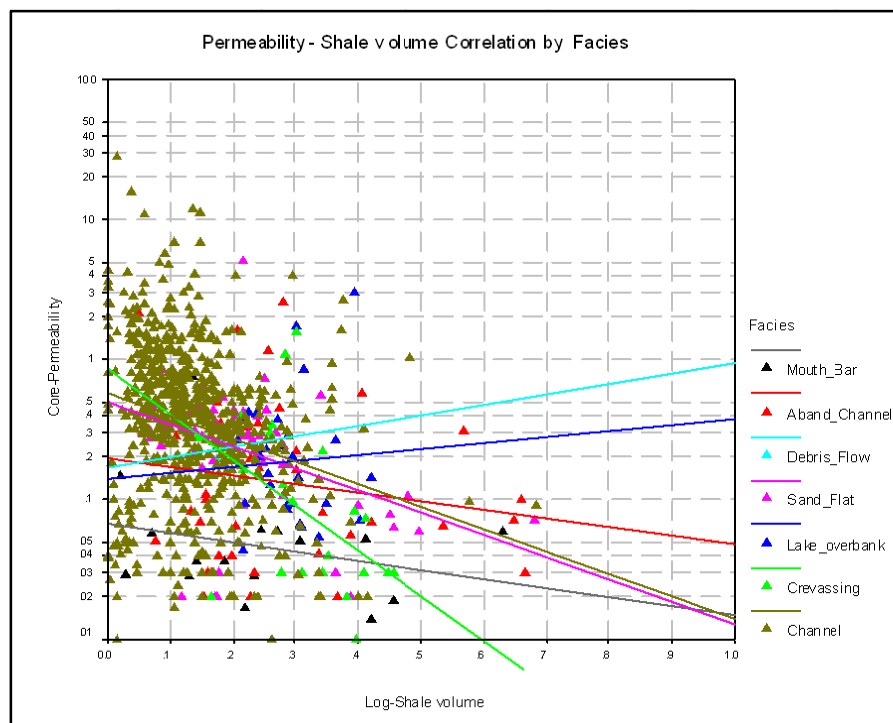


Fig. 4.3-4 Permeability reducing by Shale content

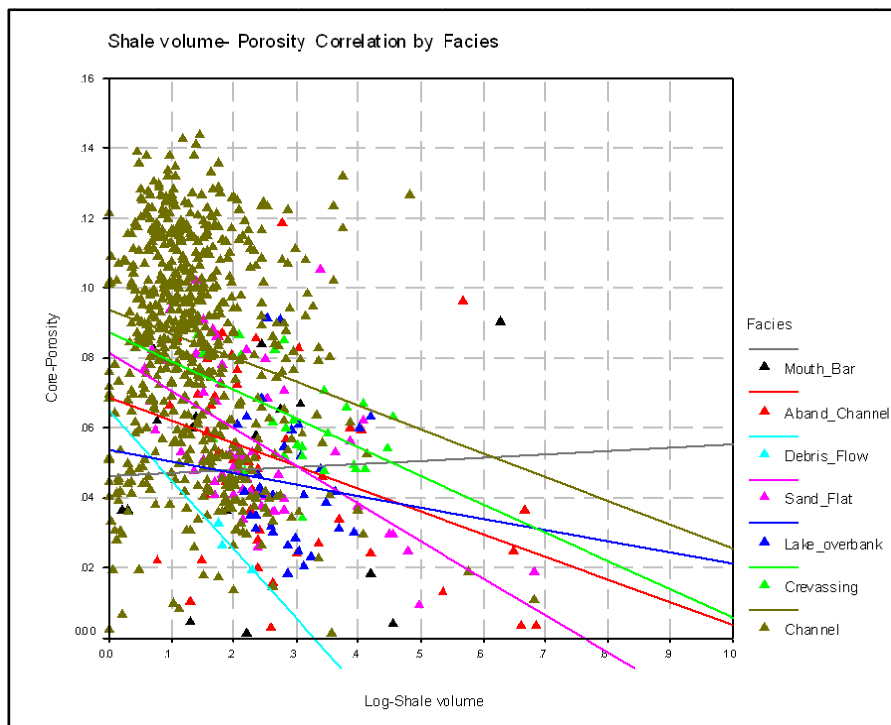


Fig. 4.3-5 Porosity reducing By Shale content

#### 4.4 RESERVOIR ZONES BASED ON LATERAL CONNECTIONS OF SEDIMENTARY FACIESES

This section briefly discusses the reservoir characteristics of the lower Nubian upper; Middle and Base unite reservoir zones. Reservoir zones have been delineated on the basis of their petrophysical characteristics and the facieses contained. Summary of porosity and permeability for each cored zone are present in **Table 4.4-2, 4.4-3**. Porosities and permeabilities quoted in this section are estimated from the logs and measured on cores.



Table 4.4-1 Reservoir Zones in the Cored wells

Well name	Unite Name	Layer Name.	Start Depth ft	End Depth ft	Gross thickness ft	Core d intervals Ft	Cored thickness ft
6J3	LNM	LNM3	11258	11340.5	82.5	11259.5-11340.5	81
		LNM2	11340.5	11436.5	96	11340.5-11436.5	96
		LNM1	11436.5	11475.5	39	11436.5-11475.5	39
	LNB	LNB	11475.5	11736	260.5	11475.5-11508	32.5
6J4	LNU	LNU9	11982.5	12080	97.5		
		LNU8	12080	12175.5	95.5		
		LNU7	12175.5	12287	111.5		
		LNU6	12287	12323	36		
		LNU5	12323	12443.5	120.5	12376.5-12424	47.5
		LNU4	12443.5	12547.5	104		
		LNU3	12547.5	12657	109.5	12585.5-12657	71.5
6J6	LNU	LNU2	12657	12750	93	12657-12747.5	90.5
		LNU9	12163	12250	87	12163-12183	20
		LNU8	12250	12345.5	95.5		
		LNU7	12345.5	12441	95.5		
		LNU6	12441	12467	26		
		LNU5	12467	12587	120	12535-12587	52
		LNU4	12587	12675.5	88.5	12587-12593-	6
6J8	LNU	LNU3	12675.5	12771	95.5		
		LNU3	10740	10832	92	10754-10832	78
		LNU2	10832	10941	109	10832-10905	73
	LNM	LNU1	10941	11033	92		
		LNM4	11033	11116.5	83.5	11095-11116.5	21.5
		LNM3	11116.5	11222	105.5	11116.5-11125	8.5
		LNM2	11222	11323	101		
LNM1	11323	11373	50				
6J12	LNU	LNB	11373	11403.5	30.5		
		LNU3	11113.5	11130.5	17	11113.5-11130.5	17
		LNU2	11130.5	11247.5	117	11130.5-11247.5	117
	LNM	LNU1	11247.5	11351.5	104	11247.5-11328	80.5
		LNM4	11351.5	11409	57.5		
		LNM3	11409	11501.5	92.5	11450-11501.5	51.5
		LNM2	11501.5	11595.5	94	11501.5-11538	36.5
		LNM1	11595.5	11674.5	79		
	LNB	LNB	11674.5	11854.5	180		

**Table 4.4-2 Cored Reservoir Layers by Facies and petrophysical parameters averages**

Well name	Strata name.	Channel				Crevassing				Lake overbank			
		Log P v/v	Core P v/v	Log K md	Core K md	Log P v/v	Core P v/v	Log K md	Core K md	Log P v/v	Core P v/v	Log K md	Core K md
6J3	LNM3	.049	.052	.137	.259					.042	.052	.138	.259
	LNM2	.060	.057	.236	.405								
	LNM1	.073	.077	.348	.348	.056	.077	.167	.282	.070	.067	.282	.250
	LNB	.042	.042	.108	.108								
6J4	LNU5	.081	.077	.634	3.65								
	LNU3	.088	.090	.543	.872								
	LNU2	.109	.112	1.113	.968								
6J6	LNU9												
	LNU5	.046	.045	.124	.726								
	LNU4	.069		.307									
6J8	LNU3	.121	.106	1.773	.790								
	LNU2	.120	.108	1.633	.733								
	LNM4	.051	.067	.137	.059	.043	.066	.121	.114	.046	.047	.132	.495
	LNM3					.064	.069	.249	.552				
6J12	LNU3	.090	.077	.678	.228								
	LNU2	.104	.093	1.01	.866								
	LNU1	.086	.077	.545	.741								
	LNM3					.057	.055	.181	.027				
	LNM2					.089	.070	.603	.031				

**Table 4.4-3 Cored Reservoir Layers by Facies and petrophysical parameters averages**

Well name	Strata name.	Sand Flat				Mouth Bar				Aband. Channel			
		Log P v/v	Core P v/v	Log K md	Core K md	Log P v/v	Core P v/v	Log K md	Core K md	Log P v/v	Core P v/v	Log K md	Core K md
6J3	LNM3	.038	.047	.088	.326					.043	.048	.106	.300
	LNM2	.067	.062	.305	.374					.059	.066	.216	.465
	LNM1	.079	.074	.424	.384								
	LNB												
6J4	LNU5	.042	.045	.104	.783								
	LNU3	.070	.072	.309	.320								
	LNU2												
6J6	LNU9						.060		2.31				
	LNU5					.047	.048	.157	.085	.031	.039	.077	.250
	LNU4												
6J8	LNU3	.049	.030	.133	.071								
	LNU2	.090	.048	.924	.106								
	LNM4												
	LNM3												
6J12	LNU3									.046	.053	.121	.328
	LNU2									.072	.054	.318	.488
	LNU1												
	LNM3	.054	.058	.162	.024								
	LNM2									.073	.065	.323	.030

**Log P=** Log derived Porosity, **Core P=** Core measured Porosity,

**Log K =** Log derived Permeability, **Core K=** Core measured Permeability

**V/V =** Volume fraction unite, **md=** Millie Darcy unite

#### 4.4.1 Upper Unite

##### 4.4.1.1 Reservoir Zone LNU9:

This uppermost zone of the Lower Nubian upper unite is cored, only in well 6J6 by 20 ft thick section (**Table 4.4-1**), which represents Esturian/Deltic Mouth bar sediments. It exhibits zone porosity average value (.06 v/v) and permeability average value (2.31md). (**Fig. 4.4-1**).

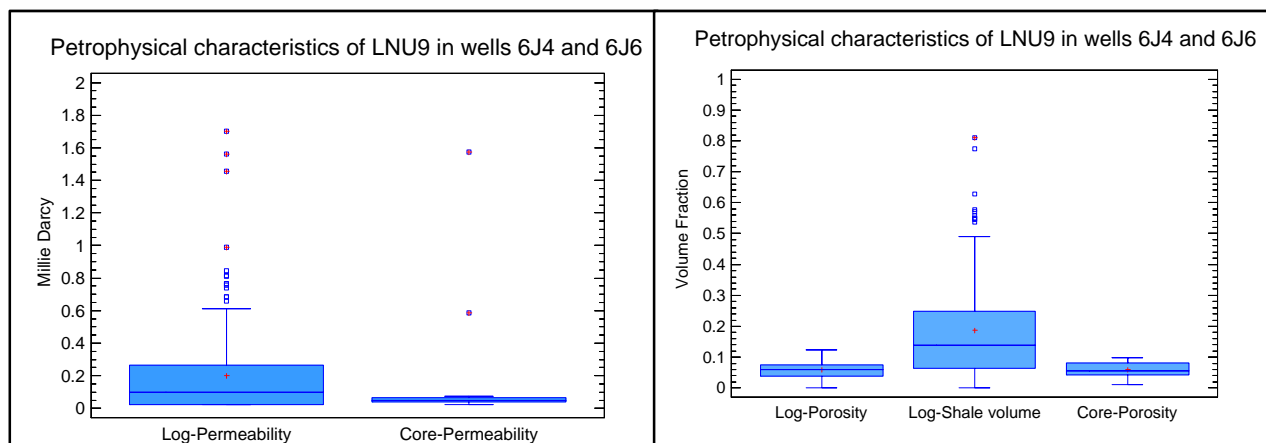


Fig. 4.4-1 Petrophysical characteristics of Lower Nubian Upper layer 9

##### 4.4.1.2 Reservoir Zone LNU8:

This zone is penetrated in two wells 6J4 and 6J6 (**Table 4.4-1**) but it is not cored in any of them, it characterized by porosity average (094v/v), permeability average (4.2 md) and average shale volume (.15v/v). The petrophysical characteristics, shale volume are well log derived in well 6J6. (**Fig. 4.4-2**).

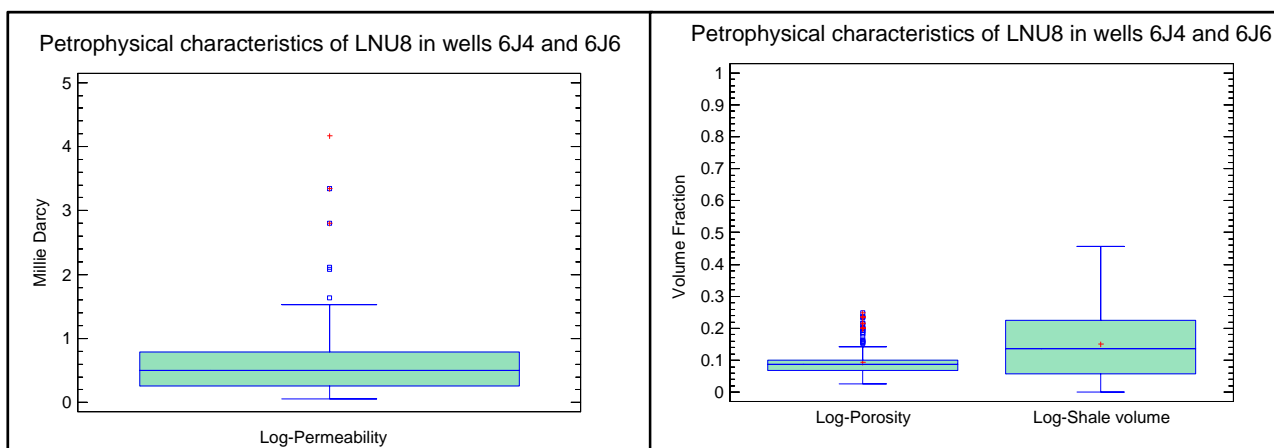


Fig. 4.4-2 Petrophysical characteristics of Lower Nubian Upper layer 8

#### 4.4.1.3 Reservoir Zone LNU7:

The LNU7 is encountered but not cored in wells, 6J4 and 6J6, with 111.5ft and 95.5ft thick (**Table 4.4-1**). In well 6J6 shows porosity average of (.084v/v) and permeability average of (.56 md). It is comprised of a sequence of sandstones, determined by a combination, of the petrophysical characteristics and shale volume. This sandstone (generally clean to moderately shaly), average Shale volume (.11v/v) (**Fig. 4.4-3**).

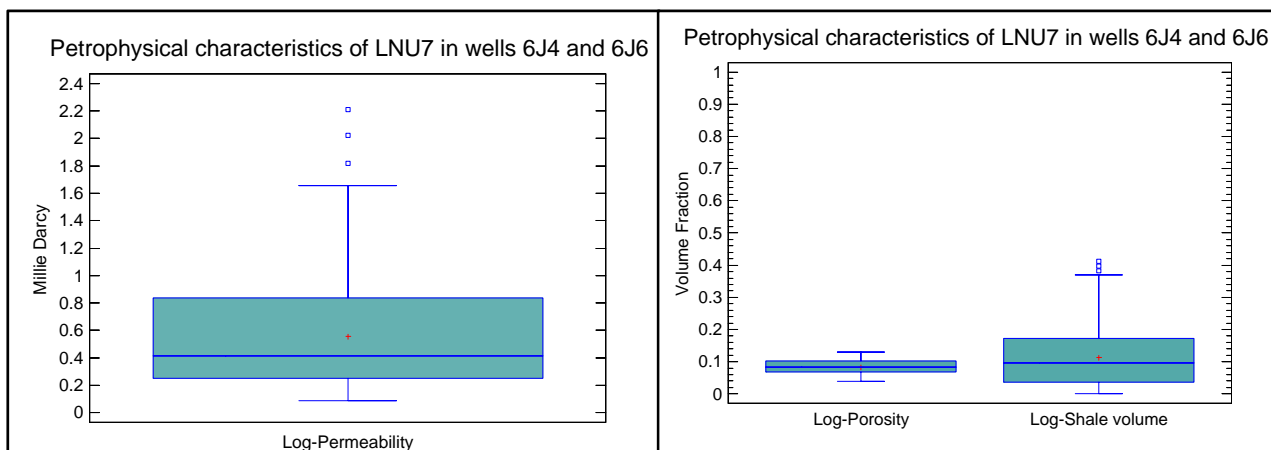


Fig. 4.4-3 Petrophysical characteristics of Lower Nubian Upper layer 7

#### 4.4.1.4 Reservoir Zone LNU6

The depth interval belonging to this zone is not cored .It is characterized by a zonal porosity of (.085 v/v) and a permeability of (.46 md). It consists of thin sequence of sandstone, with 36 ft thick in well 6J4 and 26ft thick in well 6J6, locally shows average shale volume (.098 v/v). (**Fig. 4.4-4**)

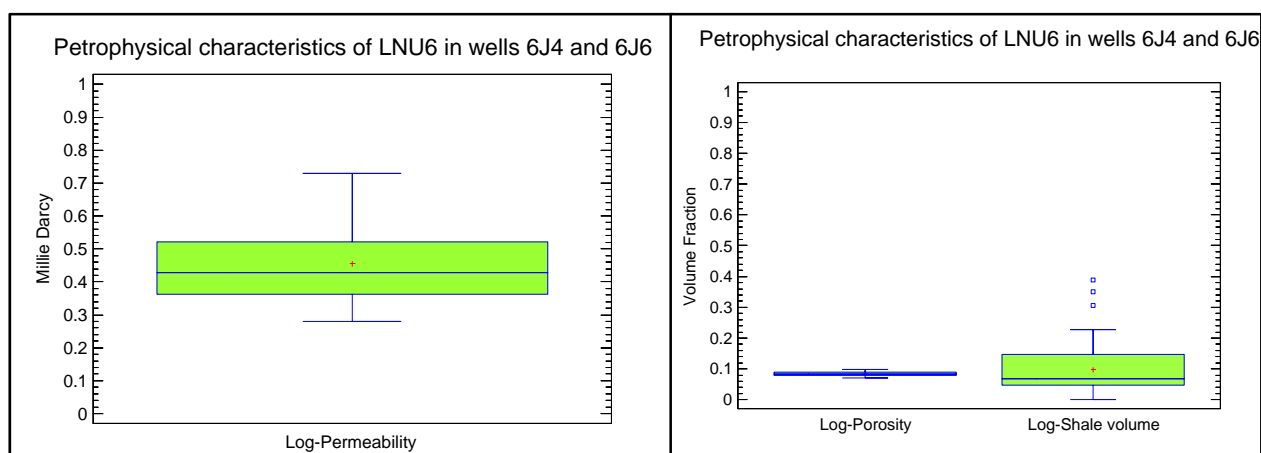


Fig. 4.4-4 Petrophysical characteristics of Lower Nubian Upper layer 6

#### 4.4.1.5 Reservoir Zone LNU5 :

This zone has thickness of 120ft in both wells 6J4 and 6J6 (**Table 4.4-1**). It is characterized by channel zonal core porosity of (.077%), core permeability of (3.65 md) and average shale volume of (.14v/v). It consists of 47.5 ft thick-bedded braided sandstones in well 6J4, and 52ft thickness of estuarine/deltaic sandstones in well in 6J6 (**Fig. 4.4-5**).

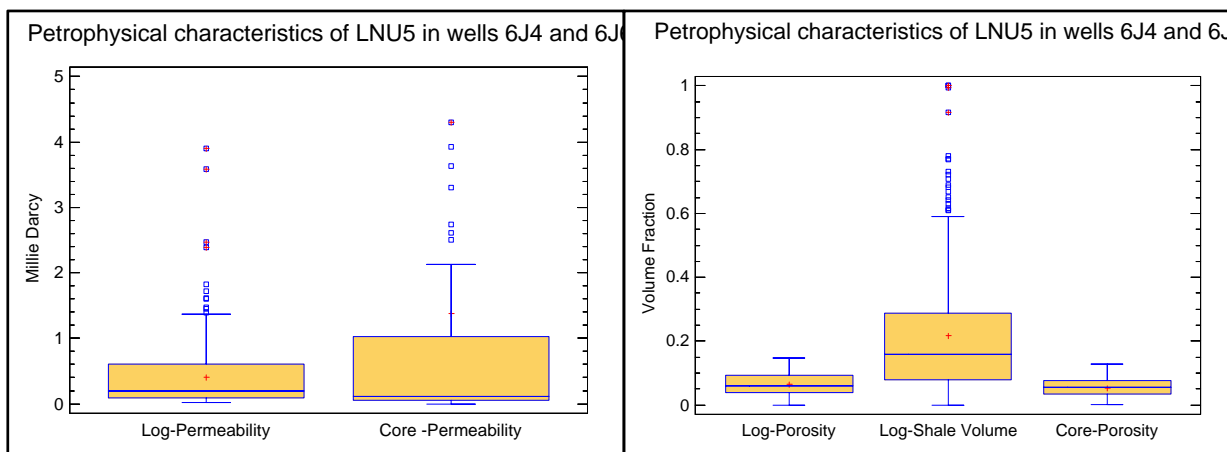


Fig. 4.4-5 Petrophysical characteristics of Lower Nubian Upper layer 5

#### 4.4.1.6 Reservoir Zone LNU4 :

Zone LNU4 cored in well 6J6 by 6 ft thick. It represents channel sediments of estuarine/deltaic environment. In non-cored interval of the well 6J4 It forms a relatively thick sequence with 104 ft thickness (**Table 4.4-1**), dominated by sandstones, which characterized by average porosity of (.07v/v) and average permeability of (.4 md). It is determined by a combination of petrophysical characteristics and shale volume (**Fig. 4.4-6**).

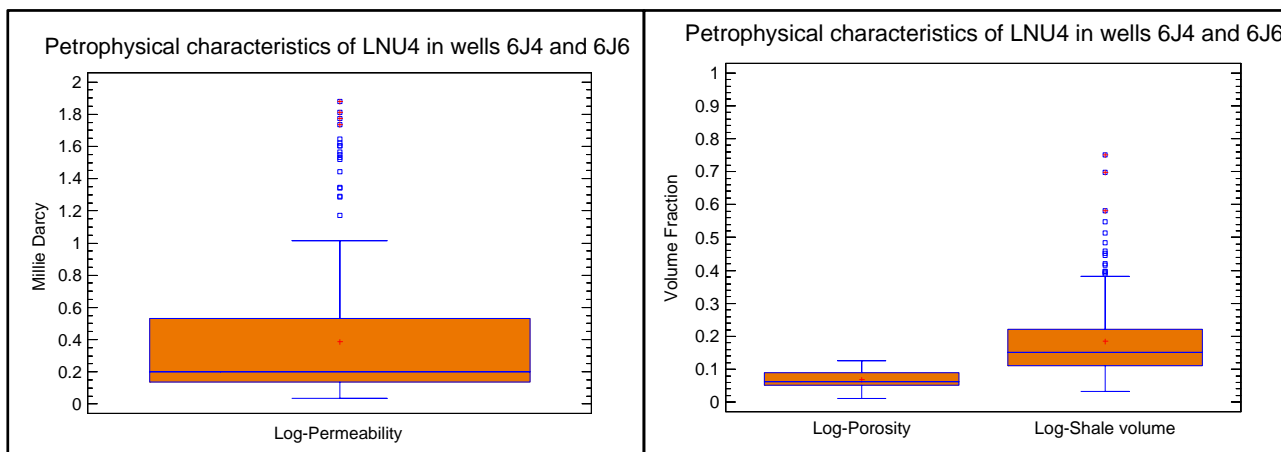
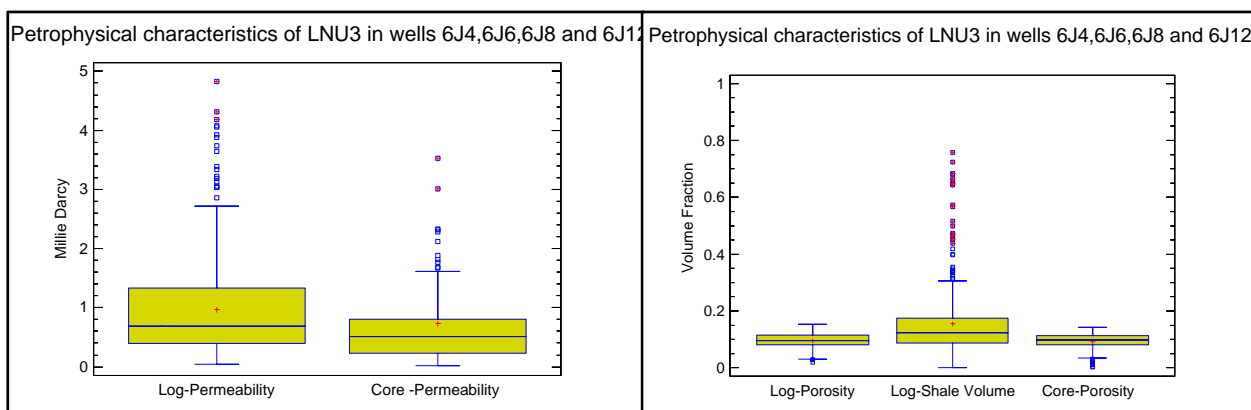


Fig. 4.4-6 Petrophysical characteristics of Lower Nubian Upper layer 4

#### 4.4.1.7 Reservoir Zone LNU3:

This zone is cored in three wells, 6J4, 6J8 and 6J12 (**Table 4.4-1**). It is comprised of a sequence of braided stream sandstones, the channel facies in well 6J4, exhibits core porosity average (.09v/v) and core permeability average (.88 md), the shale volume average is (.13v/v) (**Fig. 4.4-7**).



**Fig. 4.4-7 Petrophysical characteristics of Lower Nubian Upper layer 3**

#### 4.4.1.8 Reservoir Zone LNU2:

This zone also is cored in three wells, 6J4, 6J8 and 6J12 (**Table 4.4-1**). The sequence in these wells is dominated by braided facies, the channel sandstone in 6J4 has thickness of 90.5 ft, and shows, porosity average of (.11 v/v) and permeability average (.97 md), the shale average is (.13v/v) (**Fig. 4.4-8**).

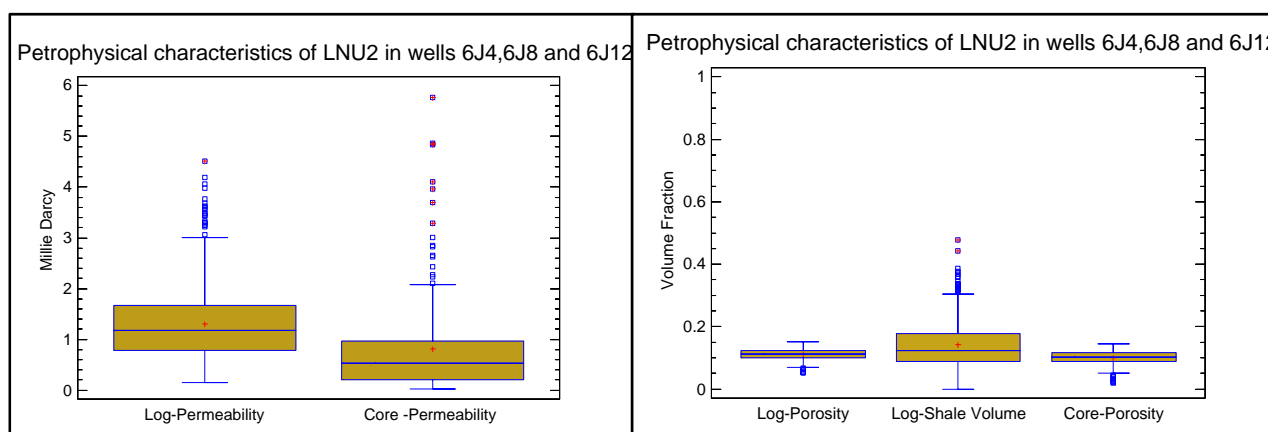


**Fig. 4.4-8 Petrophysical characteristics of Lower Nubian Upper layer 2**

#### 4.4.1.9 Reservoir Zone LNU1:

This is the lowermost zone is cored in well 6J12 (**Table 4.4-1**). It has a thickness of 80.5 ft, of braided stream channel. This zone exhibits moderate both porosity (.077v/v) and permeability (.741 md). The petrophysical characteristics are strongly controlled, by shale volume variation (average .11v/v) (**Fig. 4.4-9**).

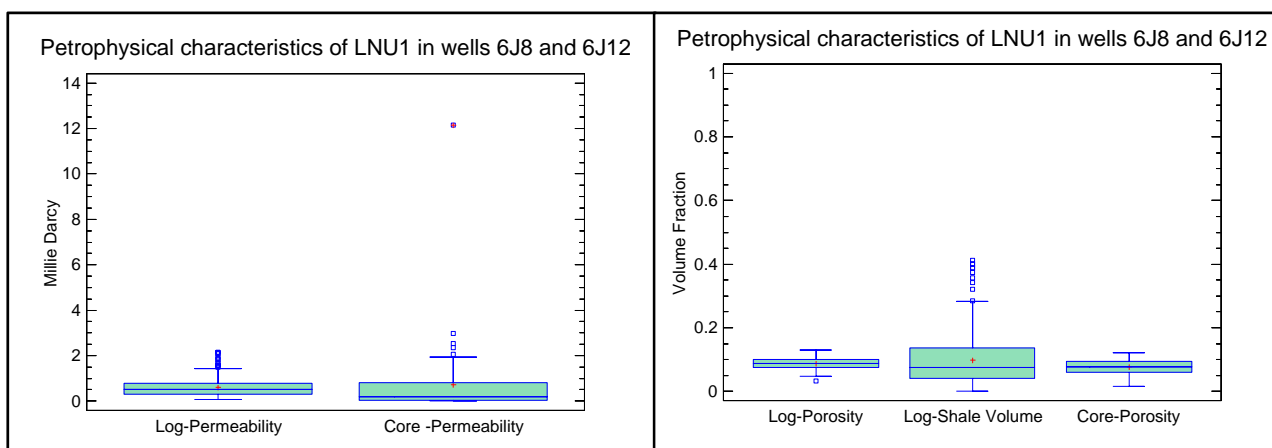


Fig. 4.4-9 Petrophysical characteristics of Lower Nubian Upper layer 1

#### 4.4.2 Middle Unite

##### 4.4.2.1 Reservoir Zone LNM4:

This is the uppermost zone of the Lower Nubian middle unite, is penetrated in two of cored wells, 6J8 by 83.5ft thick and 6J12 by 57.5ft thick (**Table 4.4-1**). It was cored only in well 6J8, where the 21.5ft of fluvial sequence dominated by overbank sandstone with, core porosity average (.046v/v), core permeability average (.087 md) and shale average(0.32v/v) (**Fig. 4.4-10**).

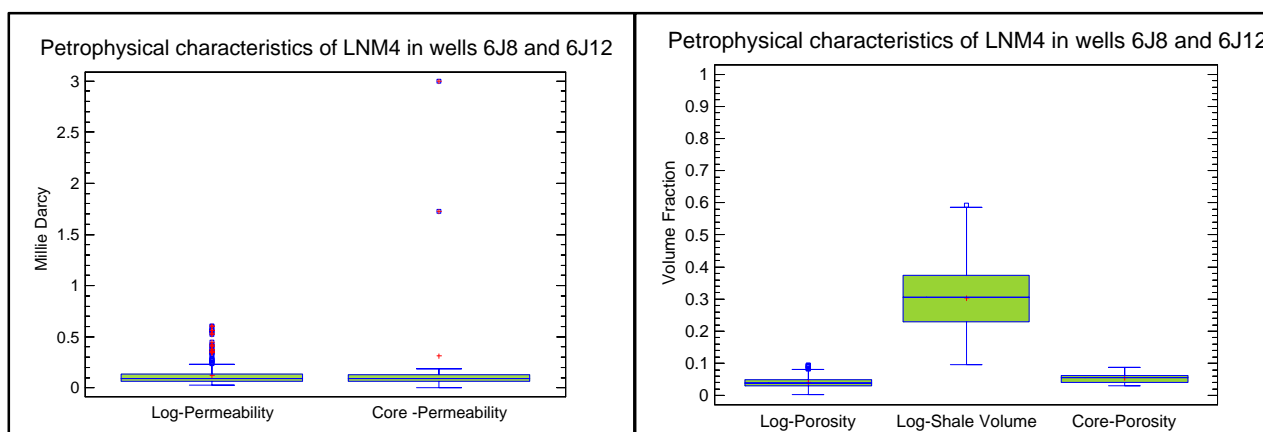
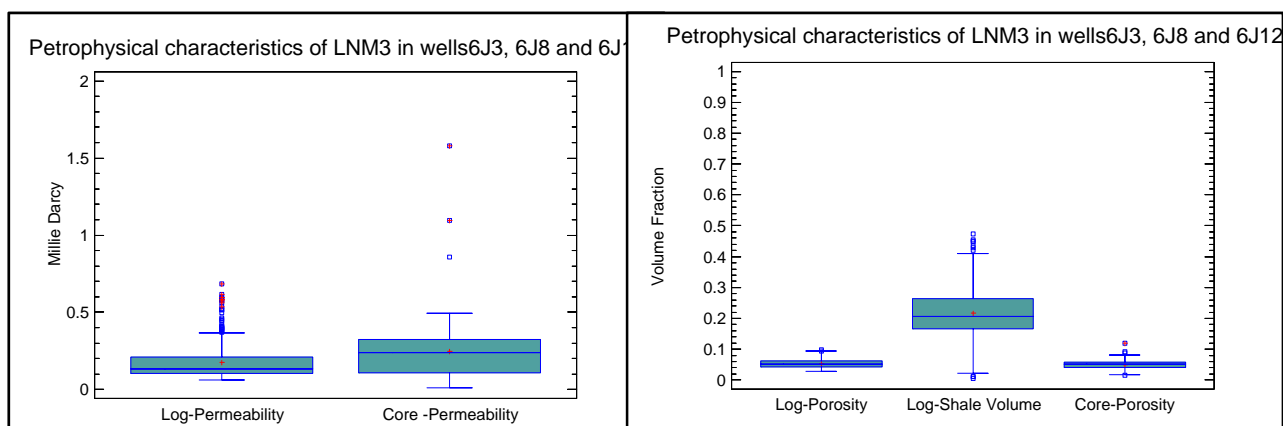


Fig. 4.4-10 Petrophysical characteristics of Lower Nubian Middle layer 4

#### 4.4.2.2 Reservoir Zone LNM3:

This reservoir zone is the most cored interval among the other zones. It is present in 6J3 with 82.5ft, 6J8 with 92ft, and in 6J12 with 92.5ft (**Table 4.4-1**). It consists mainly of channel sandstones. This channel facies described in well 6J3 (81ft) as braided sequence, in 6J8 (8.5ft) as fluvial crevassing channel and in 6J12 (51.5ft) as estuarine/deltaic channel/bar margin sediments. It characterized by average core porosity (0.054v/v), average core permeability (0.28 md).and average shale volume (0.24v/v) (**Fig. 4.4-11**).



**Fig. 4.4-11 Petrophysical characteristics of Lower Nubian Middle layer 3**

#### 4.4.2.3 Reservoir Zone LNM2:

It has drilled thickness of 96ft in well 6J3, 101ft in 6J8 and 94ft in well 6J12 **Table 4.4-1**. The cored thickness is 96ft in well 6J3 and 36.5ft in 6J12. It is comprised of a sequence of braided channel sandstones with average core porosity of (0.063v/v) and core permeability of (0.20 md). These sandstones are characterized generally by moderately shale volume with average of (0.15v/v) (**Fig. 4.4-12**).

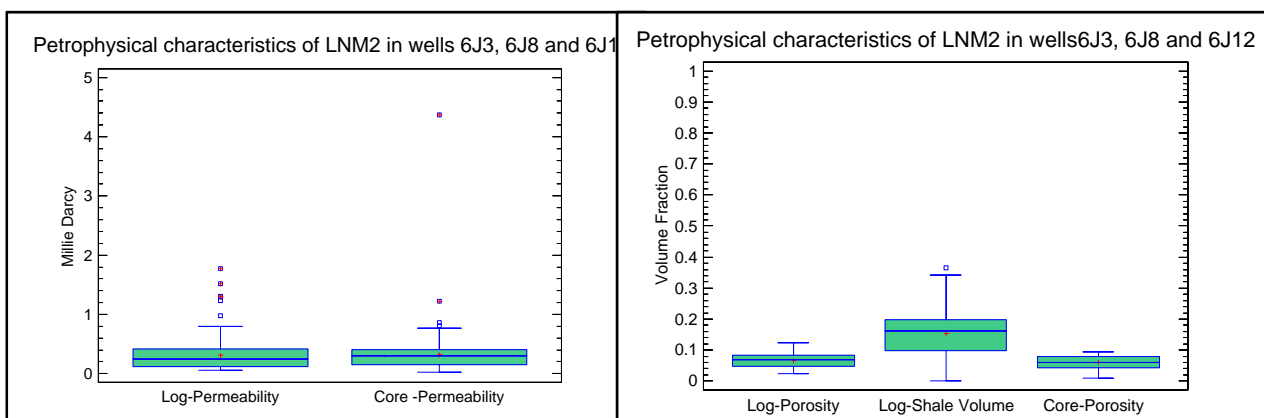


**Fig. 4.4-12 Petrophysical characteristics of Lower Nubian Middle layer 2**



#### 4.4.2.4 Reservoir Zone LNM1;

This Lower most zone of the Middle Unit is reached by three wells, 6J3 (39ft) and 6J8 (50ft) and well 6J12 (79ft) (**Table 4.4-1**). But there is only one cored: well 6J3 (39ft). The interval sequence in this well is dominated by channel sandstones, of the braided stream environment, which has average cored porosity of (0.08v/v), permeability of (0.345md) and average shale volume of (0.2v/v) (**Fig. 4.4-13**).

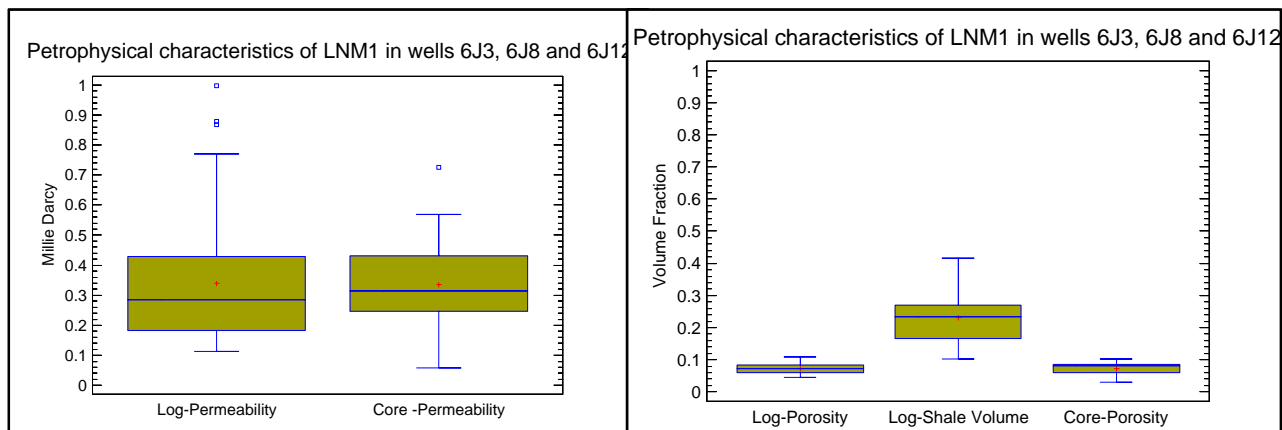


Fig. 4.4-13 Petrophysical characteristics of Lower Nubian Middle layer 1

#### 4.4.3 Base Unit

##### 4.4.3.1 Reservoir Zone LNB:

The LNB zone is representing the entire Lower Nubian Base Unit, it is determined by the braided channel facies cored in well 6J3 (32.5ft) (**Table 4.4-1**). It exhibits the cleanest sandstone sequence (shale volume average, 0.028v/v), comparing to the all above mentioned zones. In contrary it has poor porosity (0.042v/v) and permeability (0.065md) (**Fig. 4.4-14**).

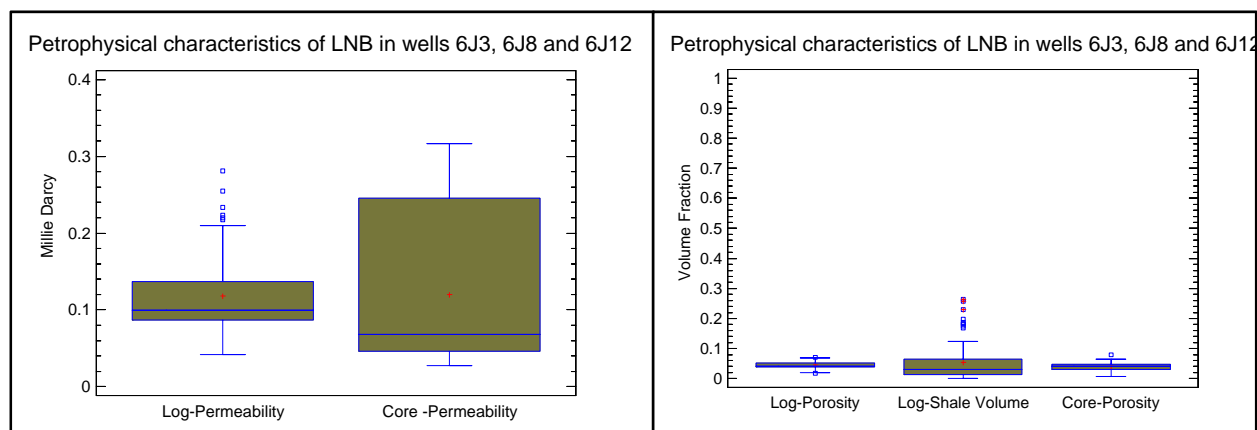


Fig. 4.4-14 Petrophysical characteristics of Lower Nubian Base

#### 4.5 CORED INTERVALS WITHIN THE ROCK BODY

The cored intervals of five wells (6J3, 6J4, 6J6, 6J8, and 6J12) give information about depositional facies building up the Lower Nubian Base, Middle and Upper Units. The information of the cored intervals can be seen in **Table 4.5-1**.

According to the detailed core description studies eight depositional facies have played significant roles in the accumulation of these sediments. They have been categorized into three main facies associations. The stratigraphic position and thickness of these facies associations are reported in **Table 4.5-2**.

**Table 4.5-1: Depth intervals of the cores.**

Well name	Core N.	Cored interval		Footage ft	Rec. %	Unite name	Well name	Core N.	Cored interval		Footage ft	Rec. %	Unite name
		From	To						From	To			
6J3	2	11252	11282	30	100	LNM	6J12	2	11037	11097	60	100	LNU
	3	11282	11312	30	100	LNM		3	11097	11157	60	100	LNU
	4	11312	11341	29	98.3	LNM		4	11157	11217	60	100	LNU
	5	11341	11371	30	100	LNM		5	11217	11277	60	100	LNU
	6	11371	11401	30	100	LNM		6	11277	11297	20	100	LNU
	7	11401	11431	30	98.3	LNM		7	11297	11328	31	100	LNU
	8	11431	11491	60	100	LNM/LNB		8	11450	11510	60	100	LNM
6J4	7	12359	12407	48	80.2	LNU							
	8	12568	12628	60	100	LNU							
	9	12628	12629	1	30	LNU							
	10	12629	12689	60	100	LNU							
	11	12689	12730	41	100	LNU							
6J6	8	12107	12167	60	100	LNU							
	9	12519	12577	58	100	LNU							
6J8	3	10734	10794	60	100	LNU							
	4	10794	10854	60	98.3	LNU							
	5	10854	10886	32	93.7	LNU							
	6	11072	11102	30	100	LNM							

**Table 4.5-2: The stratigraphical positions and thicknesses of the three facies associations**

Well name	Fluvial Facies		Thick. .ft	Braided Stream Facies		Thick. ft	Esturrian/Deltic Facies		Thick. ft
	From	To		From	To		From	To	
6J3	11260	11299	39	11299	11459.5	160.5			
	11459.5	11479.5	20	11479.5	11509	29.5			
6J4				12378	12414.5	36.5			
				12587.5	12749.5	162			
6J6							12163	12184.5	21.5
							12532.5	12590	57.5
6J8	11095.5	11125.5	30	10754	10905.5	151.5			
6J12				11113.5	11351.5	238	11480	11499.5	19.5
				11479	11480	1			
				11499.5	11538	38.5			

## 1. Braided Stream Facies Association (BR)

This facies group occurs in the base, middle and upper Unites of the Lower Nubian Member, which are penetrated in wells (6J3, 6J4, 6J8 and 6J12). It has been subdivided into three main facies: channel deposits, sand flat deposits and abandoned channel deposits (**Fig. 4.5-1, 4.5-2**).

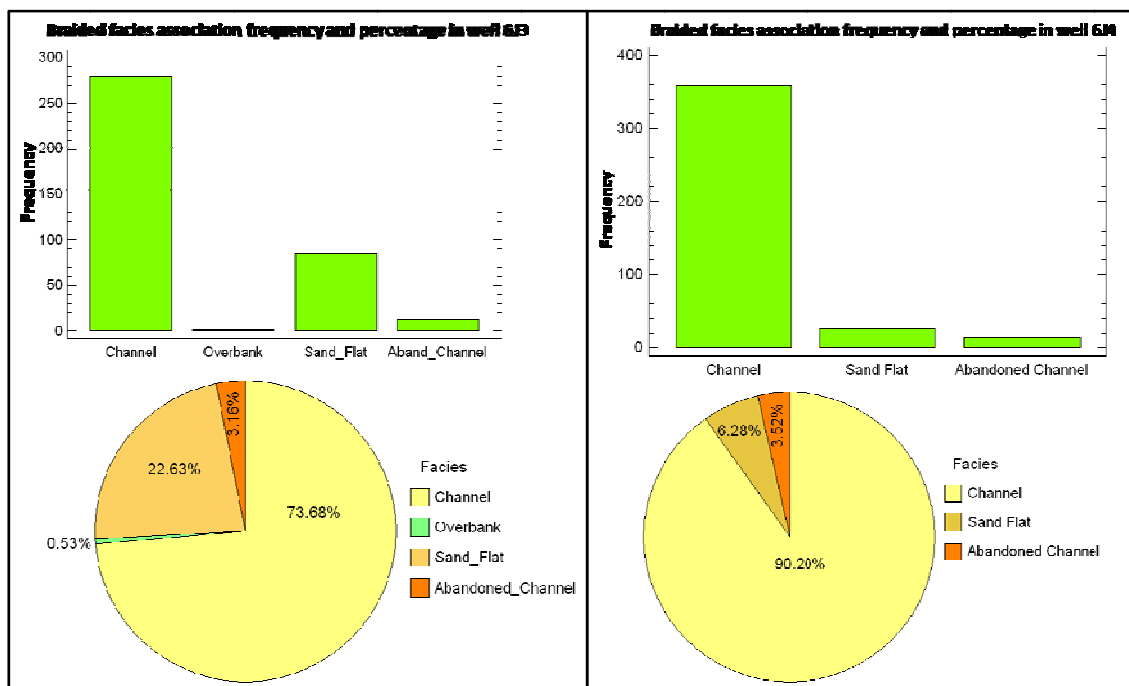


**Fig. 4.5-1 Braided facies frequency and percentage controlled by well location**

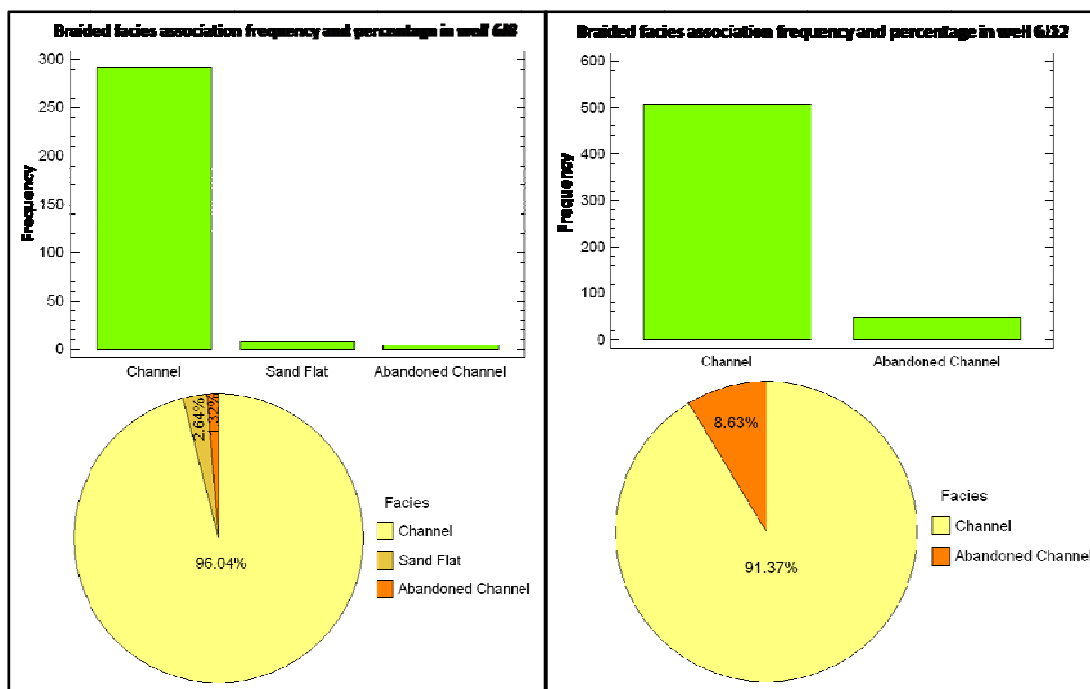


Fig. 4.5-2 Braided facies frequency and percentage controlled by well location

## 2. Estuarine/Deltaic Facies Association (ED)

This facies group is cored in wells (6J6 and 6J12) and occurs in middle and the upper Unites of Lower Nubian. It has been subdivided into four main facies: channel deposits, mouth bar deposits, abandoned channel deposits and channel /bar margin deposits (sand flat, splay). (Fig. 4.5-3).

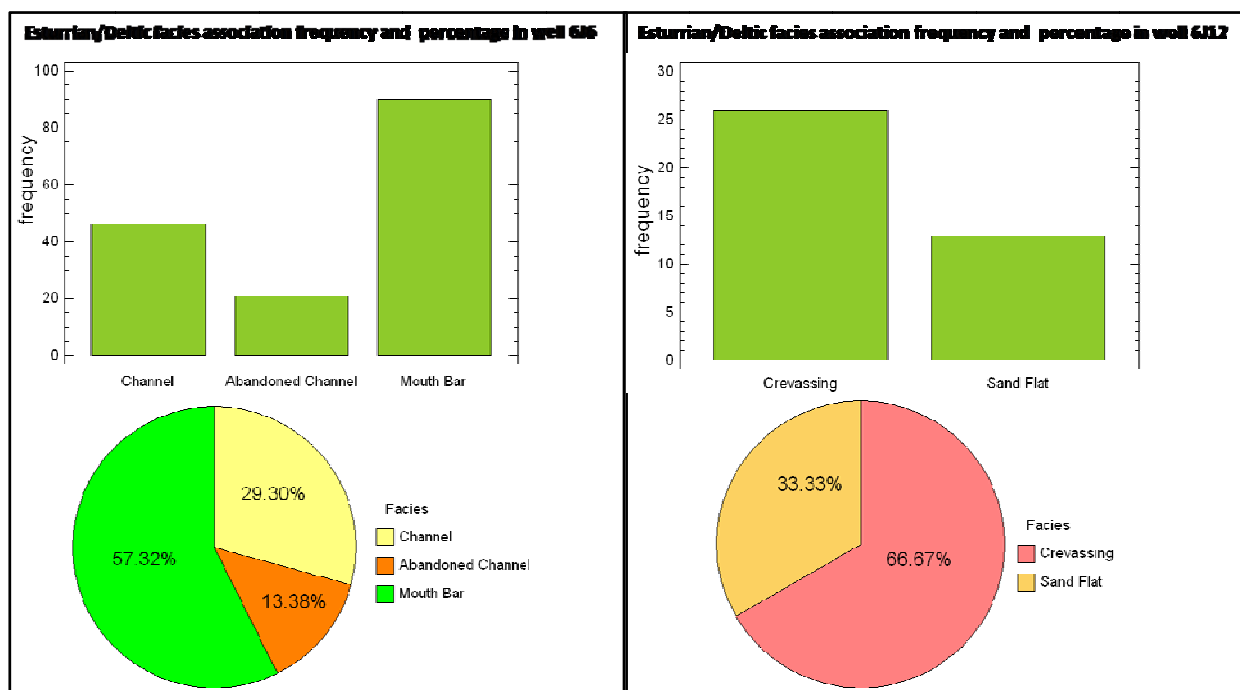


Fig. 4.5-3 Estuarine/Deltaic facies frequency and percentage controlled by well location

### 3. Fluvial Facies Association (FL)

In 6J3 and 6J8 well, a fluvial facies group occurs in the middle Unit of the Lower Nubian Member. It has been subdivided into five main facies: channel deposits, crevasse splays deposits, lake/overbank deposits, abandoned channel deposits and debris flow deposits. (Fig. 4.5-4)

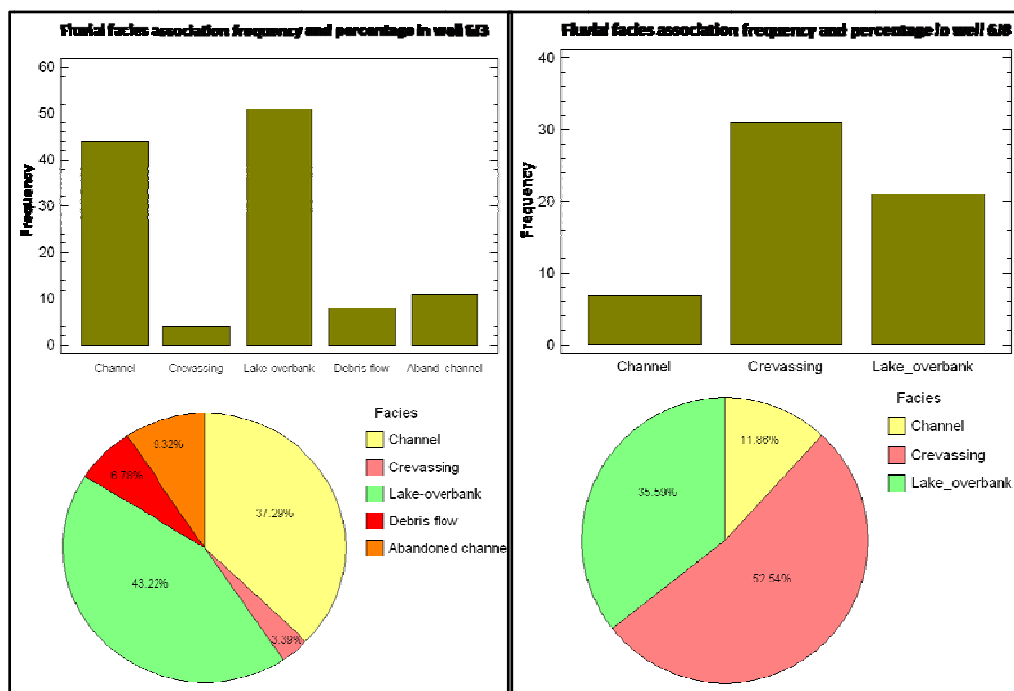


Fig. 4.5-4 Fluvial facies frequency and percentage controlled by well location

### 4.6 PETROPHYSICAL RESULTS

The quantitative well log analysis of the study area composed of eleven wells selected from the North Gialo oil field and seven wells from Farigh oil field. The wells were logged in different time periods. The suites of the measured well logs are rich and the applied logging tools are of good quality and reliability in North Gialo oil field. However, in Farigh oil field the available logs are limited. The available well logs are as follows: Sonic Log DT [ $\mu\text{sec}/\text{feet}$ ], Short Normal, and Lateral Resistivity Logs, Spontaneous Potential SP and Caliper log. The other kind of input information was a rich core analysis namely porosity, air permeability and rock grain density were measured on the cored intervals along the Lower Nubian formations from the North Gialo wells. However, no core data were available from Farigh wells. The available core data were used for calibrating the porosity and permeability evaluation. Moreover, the grain densities were utilized in the lithology evaluation. The interpretation was performed by utilizing all the available information (wire line

logs, core Data) see **Table 4.6-1** and by using Petrolog program methods, which correspond to deterministic quantitative analysis. This will give finally Porosity, Shaliness, and the net thickness for the processed intervals.

The objective of the log analysis is to identify the main reservoirs in each processed intervals. Reservoir characterization concerns the interpretation of lithology (sand shale ratio) and petrophysical characteristics (effective porosity, Permeability). The scope of this work consists of carrying out quantitative well log interpretations in the reservoirs of the Cretaceous Lower Nubian which have been penetrated in the selected well.

More precisely the different tasks are defined as follows:

1. To determine the rock composition: effective porosity, volumetric shale fraction and sand fraction, to determine the petrophysical parameters such as Permeability,
2. To determine the net thickness and the mean effective porosities and Permeabilities corresponding to selected cut-off.

The Farigh wells were drilled during the sixties. They thus have a limited set of logs with only resistivity logs available for all the wells, and Gamma Ray and porosity logs available in a few wells. The North Gialo wells are recently drilled with rich logs suit the logs are SGR, CGR pb,  $\phi_n$ , Pe, Th, K,  $\Delta t$ , Caliper, Induction deep and Induction medium. Eighteen wells have been selected and extracted from the project database to carry out quantitative log interpretation. The selection is based on the drilling date, the richness of logging records, and the total depth drilled. The selected wells are considered as key wells in the studied area with the objective of being used as data samples for stochastic modeling of the different reservoir properties, namely average porosity, permeability, shale volume,

Part of the available logs is used quantitatively for the petrophysical interoperation such as: Gamma-Ray (GR, CGR), Density (RHOB), Neutron (NPHI), Sonic DT, Photoelectric absorption coefficient- PEF, Gamma Ray Spectroscopy NGT components (Potassium-POTA, Thorium-THOR),, Resistivity log (D, M), Other logs Caliper (Cal), Spontaneous Potential (SP) were qualitatively used or quantitatively for occasional interpretations.

Conventional core analysis data from nine wells were used for matching porosities and permeabilities from core analysis and log interpretation.

Table 4.6-1 Available Log and Core data

Well no	Core Analysis	Bit Size inch	Mud	Year of logging	Wire line Logging Suite										
					GR	SP	Caliper CALI	NGS	Neutron NPHI	Density R HOB	Photo electric PEF	Sonic DT	Deep resistivity	Medium resistivity	Shallow resistivity
6J1	+	6	WBM	2002	+	+	+	+	+	+	+	+	+	+	+
6J3	+	8.5	OBM	2002	+		+	+	+	+	+	+	+	+	+
6J4	+	6	OBM	2003	+		+	+	+	+	+	+	+	+	+
6J6	+	6	OBM	2003	+		+	+	+	+	+	+	+	+	+
6J7	+	8.5	OBM	2003	+		+	+	+	+	+	+	+	+	+
6J8	+	8.5	OBM	2003	+		+	+	+	+	+	+	+	+	+
6J11	+	8.5	OBM	2004	+		+	+	+	+	+	+	+	+	+
6J12	+	8.5	OBM	2004	+		+	+	+	+	+	+	+	+	+
A1		6	OBM	2003	+		+	+	+	+	+	+	+	+	+
4C1		8.5	WBM		+	+	+			+		+	+		+
4E2A		6	WBM		+	+	+		+	+		+	+		+
2A1		6	WBM	1969	+	+	+					+	+		+
2A2		8.625	WBM	1969	+	+						+	+		+
2A4		8.5	WBM	1969	+	+	+					+	+		+
2A5		8.625	WBM	1969	+	+	+					+	+		+
2A6		8.625	WBM	1969	+	+	+					+	+		+
2A7A		8.625	WBM	1969	+	+	+					+	+		+

#### 4.6.1 Depth shifts

For comparison of core porosity and permeability with the derived log porosity and permeability, the core-log depth matching process was performed. Core data was depth shifted when necessary, and this was made on the basis of core surface gamma ray and downhole log gamma ray. No single plugs were shifted relative to each other, only complete cores were shifted. Shifted data are documented in **Table 4.6-2**.

**Table 4.6-2 Core to Log depth Shift**

Well	Core no	Core depth interval	Shift amount	Well	Core no	Core depth interval	Shift amount
6J1	3	11999.00 - 12030.00	+14.5	6J8	3	10734.00 - 10794.00	+20
	4	12030.00 - 12061.00	+14.5		4	10794.00 - 10853.00	+20
	5	12649.00 - 12679.00	+13.5		5	10853.00 - 10884.80	+20
6J3	2	11252.00 - 11282.00	+7.5		6	11072.00 - 11101.82	+23
	3	11282.00 - 11312.00	+7.5	6J7	1	11091.00 - 11133.60	+4.5
	4	11312.00 - 11340.50	+7.5	6J11	1	11475.00 - 11535.00	+19
	5	11341.00 - 11371.00	+7.5		2	11535.00 - 11595.00	+19
	6	11371.00 - 11401.00	+7.5		3	11595.00 - 11655.00	+19
	7	11401.00 - 11430.50	+7.5		4	11655.00 - 11715.00	+19
	8	11437.00 - 11491.40	+7.5		5	11715.00 - 11746.00	+19
	9	11491.40 - 11500.70	+7.5	6J12	2	11037.00 - 11097.00	+24
6J4	7	12359.00 - 12407.00	+17		3	11097.00 - 11157.00	+24
	8	12568.00 - 12628.00	+17.5		4	11157.00 - 11217.00	+23
	9	12628.00 - 12629.00	+17.5		5	11217.00 - 11277.00	+22
	10	12629.00 - 12689.00	+17.5		6	11277.00 - 11297.00	+22
	11	12689.00 - 12730.00	+17.5		7	11297.00 - 11328.00	+21
6J6	8	12107.00 - 12167.00	+16		8	11450.00 - 11510.00	+28
	9	12519.00 - 12577.20	+16				



#### 4.6.2 Log Headings

All the logs were recorded from Kelly Bushing (KB). Log headings give information about Bottom Hole Temperature (BHT). They also give mud characteristics namely, mud resistivity ( $R_m$ ) at measured temperature, mud cake resistivity ( $R_{mc}$ ) and particularly ( $R_{mf}$ ) resistivity of mud filtrates (in case of Oil Base Mud 'OBM', no such parameters will be available). Examples of such data are reported in the **Table 4.6-3**

**Table 4.6-3 Log heading information**

Well no	KB Log Ft	GL Log Ft	Run no	btm Log Ft/KB	Max Temp F	RHOM lb/gl	Rmc ohmm	Tmc F	Rm ohmm	Tm F	Rmf ohmm	Tmf F
6J1	365	335	5	13370	275	10.6	3.76	68	1.424	68	1.034	65
6J4	361	335	4	12750	295	10.7	OBM		OBM		OBM	
6J6	362	336	4	12771	290	10.4	OBM		0.007	290	OBM	
6J7	364	344	3-A	11343	260	10.27	OBM		OBM		OBM	
6J8	357	327	3	11546	252	10.6	OBM		OBM		OBM	
6J12	348	318	3	12130	260	10.9	OBM		OBM		OBM	

#### 4.6.3 Quantitative Interpretation Parameters

Different cross-plots were built in order to distinguish the main lithology facies and fluid content of the processed intervals and to determine the formation matrix. The parameters of the matrix point and shale point were determined by using the following cross-plots:

CGR vs RHOB, CGR vs NPHI, CGR vs  $R_d$ , CGR vs CAL, CGR vs PEF, RHOB vs PEF, RHOB vs NPHI, PEF vs NPHI. Cross-plot on (**Fig. 4.6-1**) presents the basic Formation measured rock densities vs. the neutron porosity (RHOB vs NPHI) used for this purpose in Lower Nubian. In the upper left corner of the cross-plot the constructed straight line is the theoretical line of the quartz (sandstones). A great number of points are located above this line which is an evidence for rugosity and caving out effect exerted on the density measurement. Really the caliper log shows frequent caving outs especially in the Upper interval but also in the other two intervals. All the basic logs, which used

were corrected to the environment effect. This analysis is reported in **Appendix 2**, which illustrate all the cross-plots containing the picked parameters used in our interpretation for the processed intervals from Lower Nubian Formation.

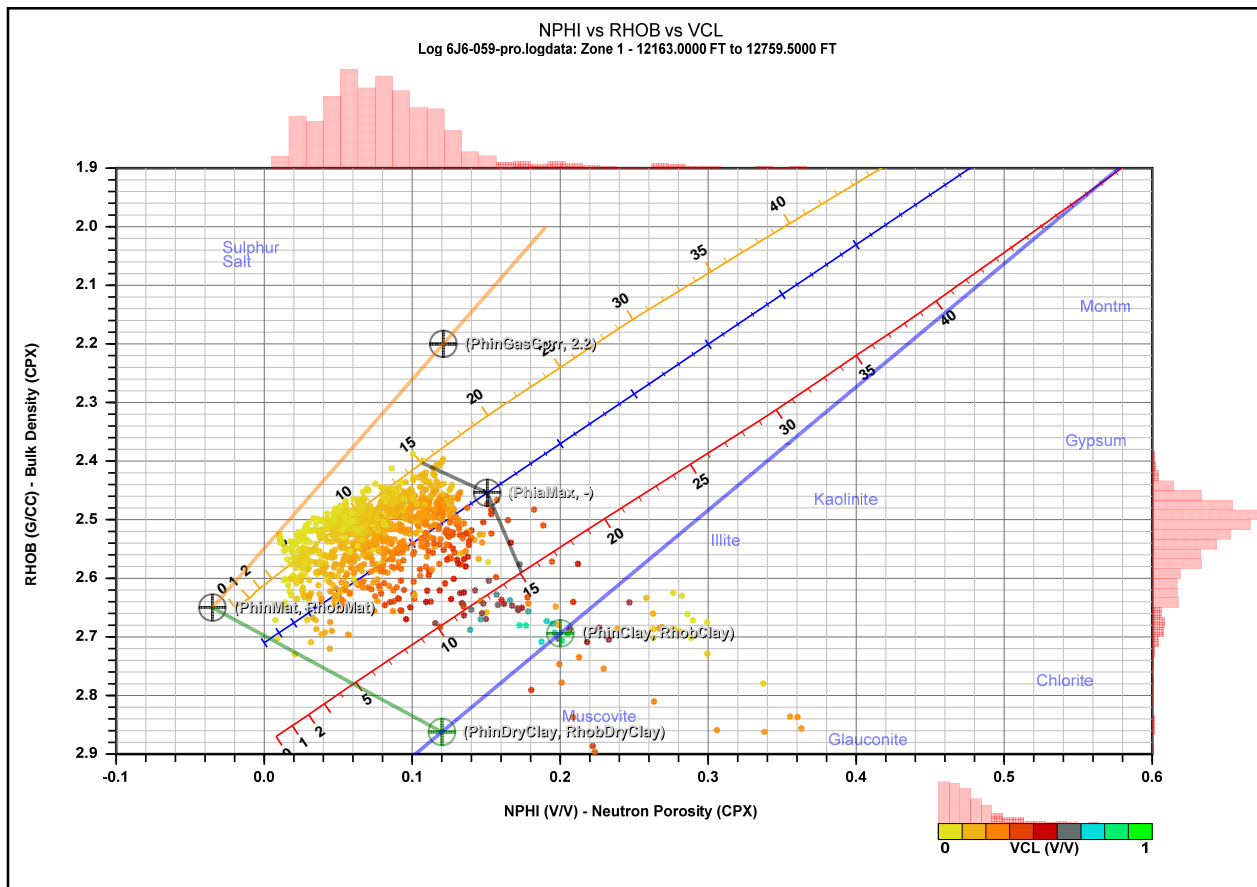


Fig. 4.6-1 Density versus Neutron crossplot, coded by shale volume, used for picking the zone parameters of matrix and shale point

#### 4.6.4 Quantitative evaluation of lithology in the Lower Nubian Formation

The Nubian sandstone is of continental development belonging to the Lower Cretaceous period. It features a typically sandwich-like development where sandstone and shale laminae change each other what is characteristic for fluvial and braided stream sediment developments. The interval can be distributed into 3 units:

- Lower Nubian **Upper** with average gross thickness of 524 ft.(min.283 ft and max. 864 ft)
- Lower Nubian **Middle** with average gross thickness of 299 ft.(min.190 ft and max.360 ft)
- Lower Nubian **Base** with average gross thickness of 109 ft.(min.30 ft and max.260 ft)

The highest shaliness was observed in the Lower Nubian Middle. The Lower Nubian Upper and the Lower Nubian Bottom are less shaly. The petrophysical properties of the Nubian sandstones are controlled by poorly sorted grain size and pore-size distribution. The results of lithology evaluation are shown on the composite integrated log, which generally composed of four striplogs (**Fig. 4.6-2**), each strip is titled according to its content as follows:

**Input Striplog:** shows all the involved input logs after necessary corrections were made.

**Core description Striplog:** whenever the cores are available presenting the main core description results including lithology, facies and environment of deposition.

**Output Striplog:** with results of calibrated deterministic lithology analysis and the main evaluated petrophysical quantities.

**Reservoir zoning Striplog:** with net thickness intervals distribution, and petrophysical Layering.

In the left side track of the output striplog the bulk rock composition is illustrated with effective bulk porosity  $\phi$ , followed by the sand fraction  $V_{SD}$  and by the shale  $V_{SH}$ .

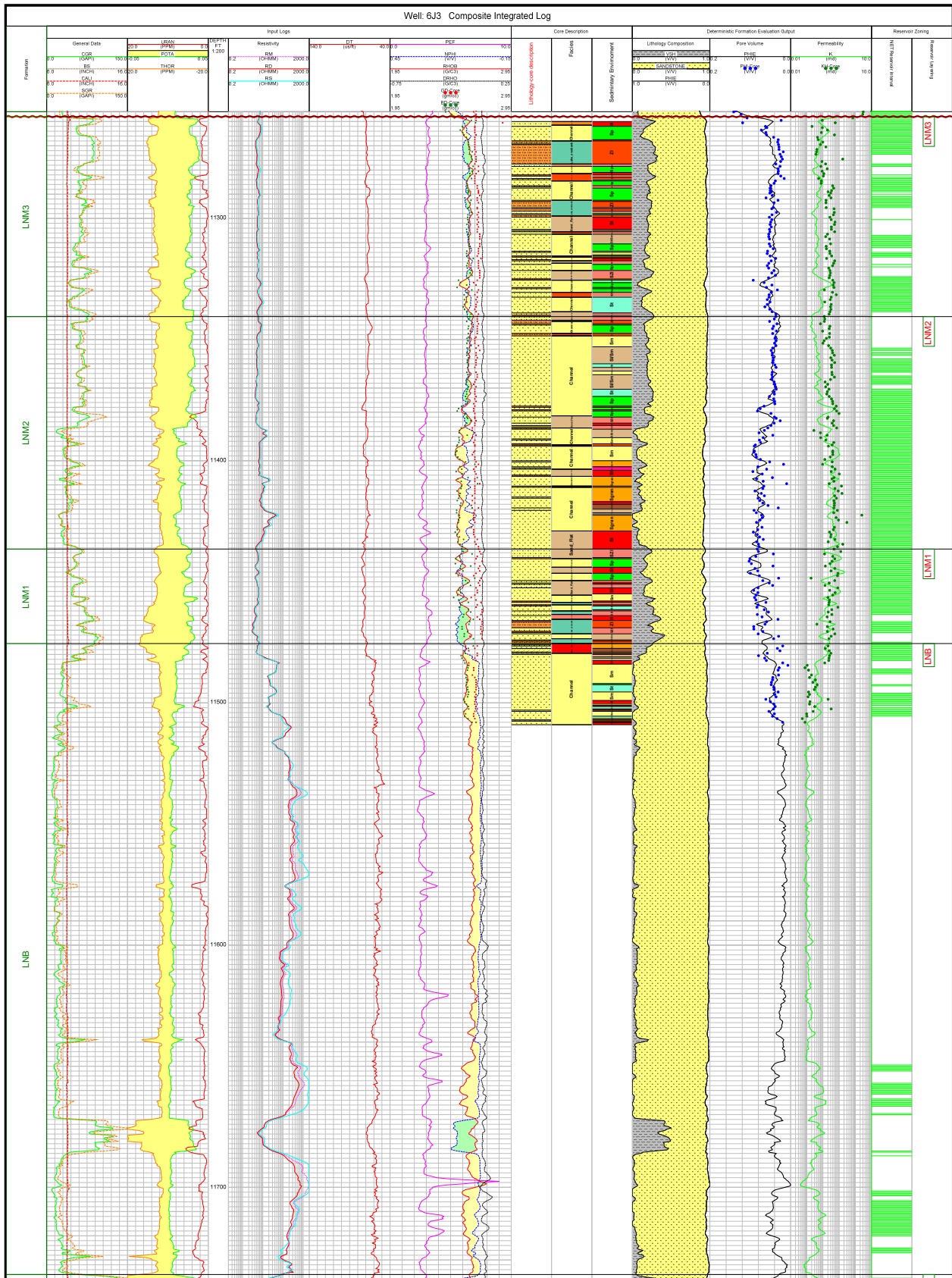
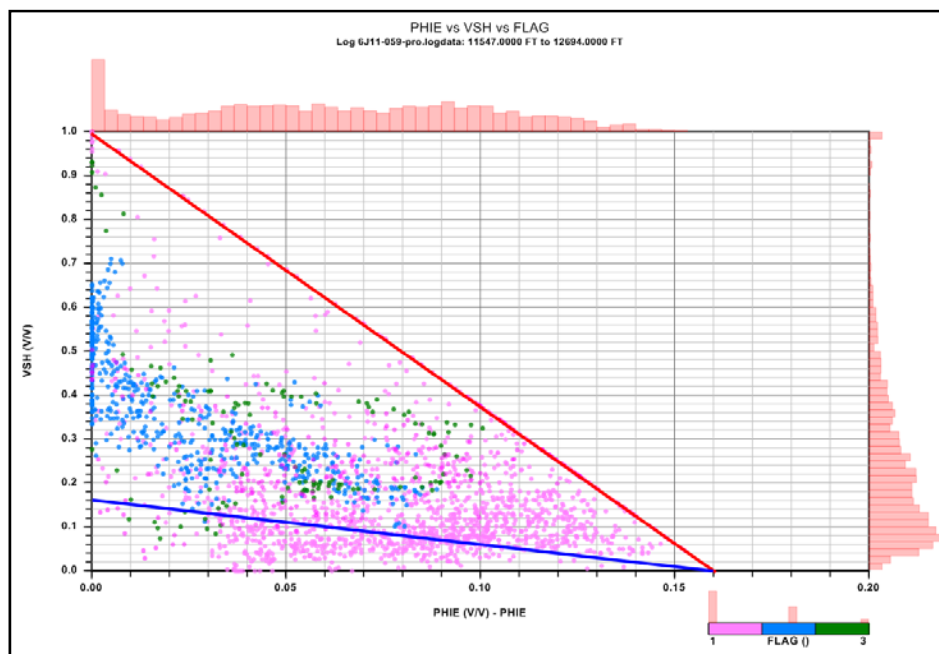


Fig. 4.6-2 Composite integrated log, consist of, input logs, core description, interpretation output, and reservoir zones.

The quality of lithology evaluation is high which is approved by the pattern of the point distribution on the shaliness vs. effective porosity cross-plot. All the points are located within a triangle which is limited from upwards by a tangent straight line started from the zero porosity and unit shaliness point and drawn as a tangent of the cloud of points from above. This straight line intersects the porosity abscissa at the original maximum porosity. This was the starting porosity of the Nubian sandstones at the end of sedimentation before higher degree chemical diagenesis started which reduced more or less the effective porosity at the different depth sites. On the cross-plot of **Fig. 4.6-3**, a second slanting straight line is also drawn from the original porosity place, which intersects the ordinate axis at shaliness where the dispersed shale fills up completely the original porosity. This straight line distributes the large triangle into two parts. The amplitude below the second slanting straight line indicates the magnitude of the dispersed pore-filling shale content, while the amplitude between the two slanting straight lines indicates the volume fraction of the laminated shale content of the rock. Those points which are located below the lower straight line show rock developments, which are isotropic without any shale laminae interbeddings. The cross-plot shows that in upper unit of Lower Nubian a great part of the rock is isotropic without containing shale laminae, while the Middle unite of Lower Nubian is characterized by more frequent sandwich type development. In the base unit of Lower Nubian all the rocks show sandwich type development.



**Fig. 4.6-3.**Shale volume versus Porosity values used for the interpretation quality control

#### 4.6.5 Evaluation of petrophysical properties in the Nubian formation

The results of petrophysical evaluation are presented on the composite integrated log. The right hand track of the output striplog shows the air permeability of the Nubian sandstones along with the permeabilities measured on the cores. The air permeability has been estimated using an empirical formula. For the calibration of the methodology air permeabilities and effective porosities measured on core samples were used. **Fig. 4.6-4** presents the core permeabilities traced vs. core porosities. The cross-plot pattern shows very great variance of permeability at high core porosities above 0.1. The measured permeabilities vary within four orders of magnitude. This variance somewhat decreases to 2 orders of magnitude when the core porosity decreases. The high variance can be explained by high variance of equivalent pore throat sizes at a constant porosity level.

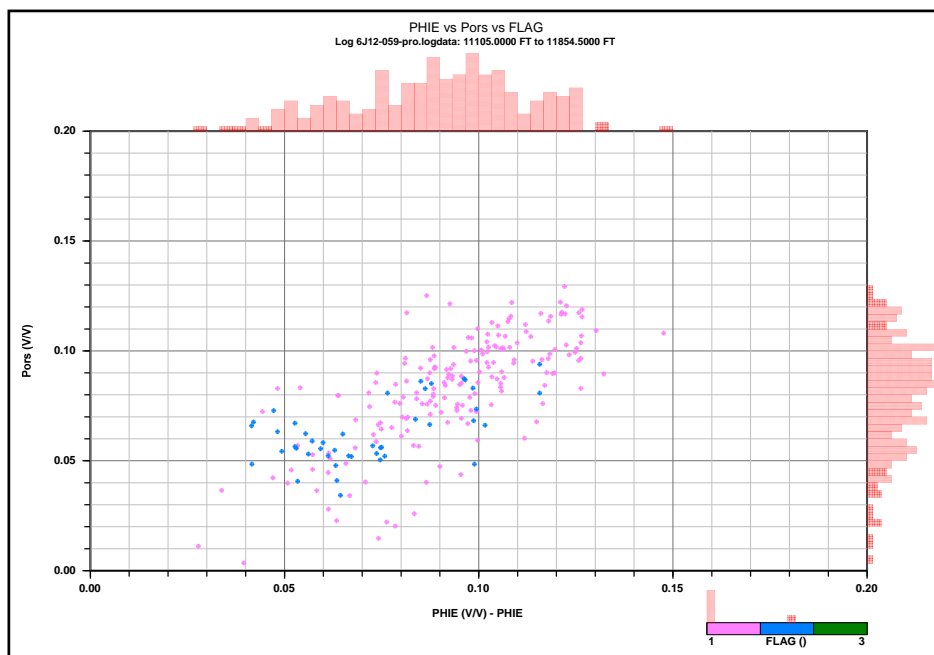


**Fig. 4.6-4.**Core porosity versus Core permeability used for calibrating the estimated permeability

The middle track of the output striplog presents the effective pore volume of the sand. Core data are used as a quality control on porosity derived from the well logs. **Fig. 4.6-5** depicts the correlation of log derived porosity on core porosity.

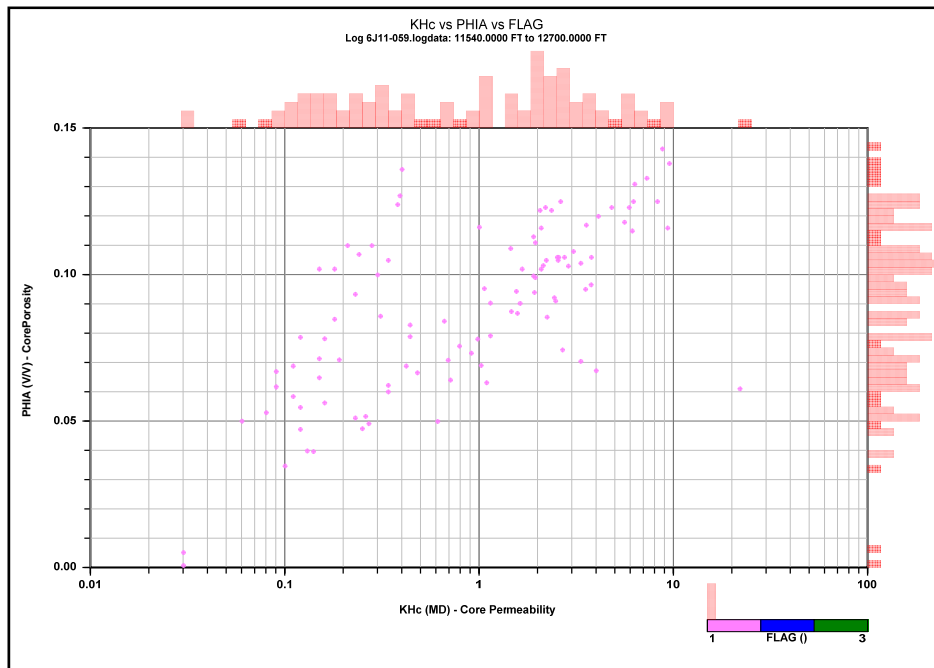


Fig. 4.6-5. Core porosity versus log derived porosity used for calibrating the estimated porosity

#### 4.6.5.1 Selection of cutoff parameters

The main goal of this petrophysical study was to provide porosity, permeability, and shale volume averages, obtained from log analysis, which could be used to generate stochastic models. This needs determination of the net thickness from the gross thickness of the Lower Nubian processed intervals in each well and this in contrary needs to set cutoff values for the interpretation output results namely porosity, permeability, and shale volume. The selection of the cutoff values was made applying some conventional statistics analysis by which we obtained cumulative frequency distribution for the subject properties (**Fig. 4.6-6**). On the bases of the net thickness distribution, the average values of the different reservoir properties were evaluated.

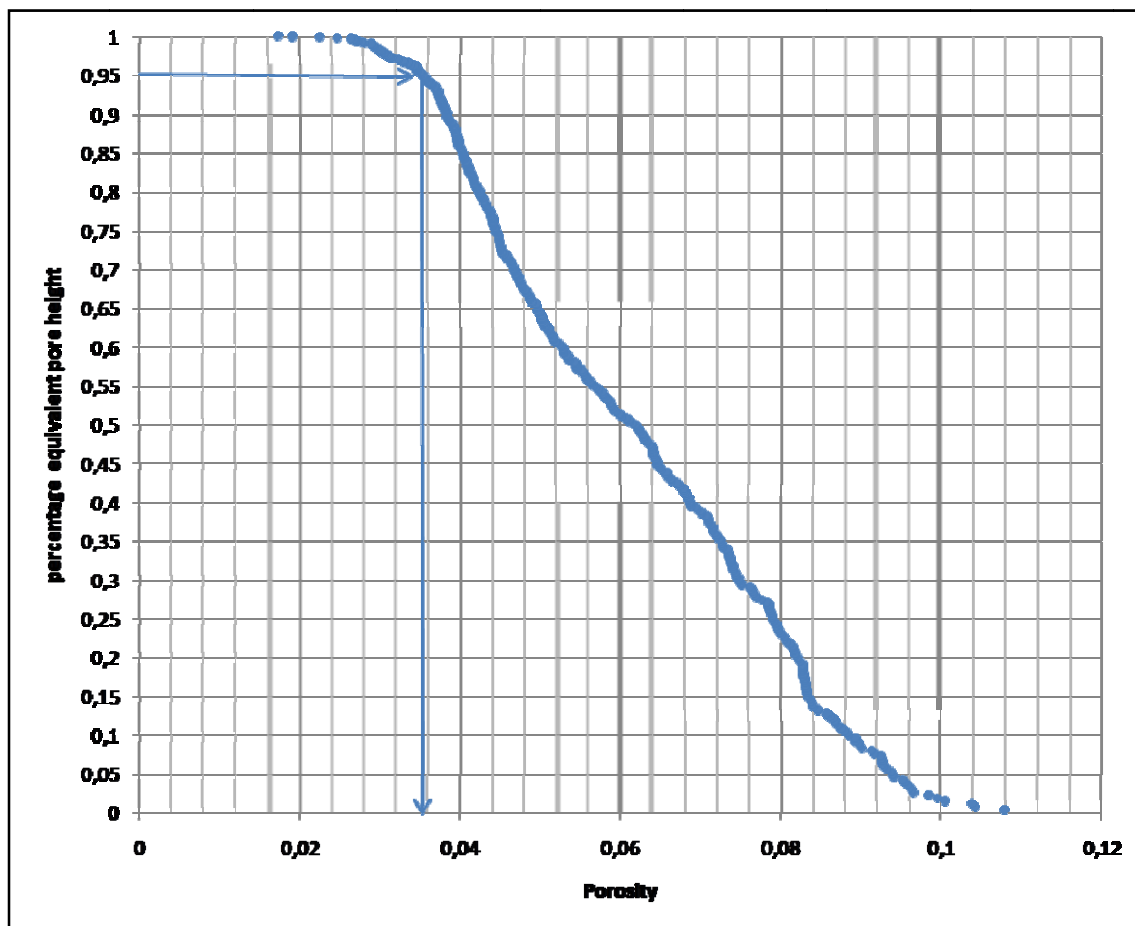


Fig. 4.6-6 Equivalent pore height Cumulative frequency, used for determination of porosity cutoff value

#### 4.6.5.2 Distribution of the reservoirs into lithofacies and/or hydraulic units

When all the necessary lithological and petrophysical properties of the rocks were evaluated in the selected depth interval of the borehole or well, then the log analyst has to distribute the total depth interval into lithofacies and/or hydraulic units. Thus for example into shaly sandstone intervals, sands and shales should be distinguished from each other in creating the different lithofacies units. Regularly there is a good correspondence between the lithological units and the hydraulic units. However, sometimes there are great differences in some petrophysical characteristics, thus in permeability within a common lithological unit. In such cases the lithofacies unit should be further distributed into hydraulic units.

The distribution of the geological sequence into lithological and hydraulic units is performed mostly by mental evaluation made by the well log analyst sometimes together with geologists and reservoir engineers who deal with the related reservoirs. Depending on lithology and



petrophysical evaluation results, each formation unit were divided into several layers from which the most important sand body reservoirs could be distinguished. Accordingly, on the bases of the net thickness distribution, the characteristics of the potential reservoir intervals from Lower Nubian are summarized in the **Table 4.6-4, 4.6-5 , 4.6-6**, and also presented on the reservoir layering striplog(**Fig. 4.6-2**). These results consist of gross thickness, net thickness, porosity average, shale average and permeability average.

**Table 4.6-4 Summary of the selected reservoirs characteristics**

Well name	Formation unite	Strata Name.	Start Depth ft	End Depth ft	Gross thickness ft	NET thickness ft	PHIE average %	VSH average %	K average md
6J1	LNU	LNU9	11996	12086	90	61.5	0.067	0.113	0.2353
		LNU8	12086	12181	95	94	0.088	0.059	0.4949
		LNU7	12181	12279	98	94.5	0.096	0.039	0.665
		LNU6	12279	12316	37	34.5	0.108	0.074	0.9859
		LNU5	12316	12438.5	122.5	104.5	0.097	0.1	0.6712
		LNU4	12438.5	12544.5	106	96.5	0.095	0.095	0.6362
		LNU3	12544.5	12656	111.5	109	0.12	0.08	1.503
		LNU2	12656	12769.5	113.5	110	0.096	0.05	0.654
		LNU1	12769.5	12860	90.5	90.5	0.102	0.067	0.8156
	LNM	LNM4	12860	12912.5	52.5	34.5	0.089	0.201	0.5192
		LNM3	12912.5	13047.5	135	116	0.087	0.125	0.4769
		LNM2	13047.5	13156.5	109	93.5	0.074	0.13	0.3078
		LNM1	13156.5	13215.5	59	59	0.094	0.187	0.6028
	LNB	LNB	13215.5	13330.2	114.7	53	0.105	0.027	0.9011
6J3	LNM	LNM3	11258	11340.5	82.5	54.5	0.051	0.193	0.1347
		LNM2	11340.5	11436.5	96	79.5	0.068	0.134	0.243
		LNM1	11436.5	11475.5	39	33.5	0.076	0.208	0.3266
	LNB	LNB	11475.5	11736	260.5	54.5	0.049	0.041	0.1293
6J4	LNU	LNU9	11982.5	12080	97.5	34	0.072	0.18	0.2883
		LNU8	12080	12175.5	95.5	84.5	0.08	0.094	0.3761
		LNU7	12175.5	12287	111.5	102	0.084	0.091	0.4342
		LNU6	12287	12323	36	26.5	0.075	0.08	0.3139
		LNU5	12323	12443.5	120.5	86	0.086	0.114	0.4649
		LNU4	12443.5	12547.5	104	85	0.072	0.147	0.2826
		LNU3	12547.5	12657	109.5	104.5	0.088	0.124	0.4984
		LNU2	12657	12750	93	72.5	0.109	0.126	1.0381
6J6	LNU	LNU9	12163	12250	87	38.5	0.068	0.12	0.2508
		LNU8	12250	12345.5	95.5	82	0.1	0.12	0.7464
		LNU7	12345.5	12441	95.5	90.5	0.084	0.1	0.4324
		LNU6	12441	12467	26	25	0.085	0.086	0.4435
		LNU5	12467	12587	120	86.5	0.082	0.128	0.4086
		LNU4	12587	12675.5	88.5	67	0.087	0.127	0.4795
		LNU3	12675.5	12771	95.5	68.5	0.089	0.089	0.508
6J7	LNB	LNB	11087	11190	103	2.5	0.049	0.115	0.1266

Table 4.6-5 Summary of the selected reservoirs characteristics

Well name	Formation unite	Strata Name.	Start Depth ft	End Depth ft	Gross thickness ft	NET thickness ft	PHIE average %	VSH average %	K average md
6J8	LNU	LNU3	10740	10832	92	83.5	0.112	0.111	1.1619
		LNU2	10832	10941	109	105	0.122	0.133	1.6116
		LNU1	10941	11033	92	91	0.095	0.088	0.626
	LNM	LNM4	11033	11116.5	83.5	31	0.065	0.233	0.224
		LNM3	11116.5	11222	105.5	90	0.072	0.185	0.2813
		LNM2	11222	11323	101	71	0.077	0.199	0.3356
		LNM1	11323	11373	50	4.5	0.067	0.283	0.2353
	LNB	LNB	11373	11403.5	30.5	20.5	0.069	0.224	0.2592
6J11	LNU	LNU7	11547	11655	108	79.5	0.079	0.111	0.3656
		LNU6	11655	11690	35	34.5	0.075	0.081	0.315
		LNU5	11690	11810.5	120.5	92	0.075	0.113	0.3208
		LNU4	11810.5	11905	94.5	57.5	0.065	0.099	0.221
		LNU3	11905	12014	109	61	0.094	0.128	0.6035
		LNU2	12014	12155	141	127	0.111	0.122	1.1131
		LNU1	12155	12252	97	91	0.101	0.124	0.7744
	LNM	LNM4	12252	12339.5	87.5	0	0	0	0
		LNM3	12339.5	12451.5	112	37.5	0.062	0.228	0.2028
		LNM2	12451.5	12552.5	101	52	0.058	0.197	0.1766
		LNM1	12552.5	12612	59.5	42	0.086	0.235	0.4558
	LNB	LNB	12612	12690.5	78.5	25	0.07	0.211	0.2618
6J12	LNU	LNU3	11113.5	11130.5	17	11.5	0.09	0.179	0.5253
		LNU2	11130.5	11247.5	117	110.5	0.104	0.136	0.8816
		LNU1	11247.5	11351.5	104	100	0.083	0.093	0.4223
	LNM	LNM4	11351.5	11409	57.5	22	0.048	0.18	0.1238
		LNM3	11409	11501.5	92.5	66.5	0.064	0.18	0.2138
		LNM2	11501.5	11595.5	94	55	0.088	0.197	0.4915
		LNM1	11595.5	11674.5	79	0	0	0	0
	LNB	LNB	11674.5	11854.5	180	0	0	0	0
A1	LNU	LNU9	12317	12419	102	44.5	0.066	0.155	0.2273
		LNU8	12419	12512.5	93.5	69	0.062	0.111	0.202
		LNU7	12512.5	12629	116.5	100.5	0.06	0.063	0.1851
		LNU6	12629	12661	32	31	0.058	0.063	0.1751
		LNU5	12661	12706	45	6	0.079	0.066	0.3649
4C1	LNU	LNU4	11366.5	11462	95.5	31	0.078	0.12	0.3563
		LNU3	11462	11582.5	120.5	38.5	0.053	0.075	0.1459
		LNU2	11582.5	11706.5	124	87	0.067	0.097	0.2426
		LNU1	11706.5	11794	87.5	22.5	0.052	0.087	0.1409
	LNM	LNM4	11794	11844	50	41.5	0.11	0.167	1.0679
		LNM3	11844	11929.5	85.5	70.5	0.094	0.145	0.6037
		LNM2	11929.5	11962	32.5	32.5	0.089	0.124	0.5083
		LNM1	11962	11984	22	21	0.059	0.142	0.1793
4E2A	LNU	LNB	11984	12046.5	62.5	44.5	0.068	0.068	0.2472
		LNU4	10530	10623	93	81.5	0.096	0.066	0.6545
		LNU3	10623	10742.5	119.5	116	0.079	0.061	0.3621
		LNU2	10742.5	10860	117.5	115	0.133	0.072	2.39
		LNU1	10860	10991.5	131.5	131.5	0.123	0.072	1.6988
	LNM	LNM4	10991.5	11033	41.5	22	0.069	0.184	0.2527
		LNM3	11033	11101.5	68.5	45	0.08	0.19	0.3712
		LNM2	11101.5	11204.5	103	22.5	0.063	0.23	0.2104
		LNM1	11204.5	11259	54.5	10.5	0.073	0.238	0.2955
	LNB	LNB	11259	11301.5	42.5	16.5	0.045	0.137	0.1124

Table 4.6-6 Summary of the selected reservoirs characteristics

Well name	Formation unite	Strata Name.	Start Depth Ft	End Depth ft	Gross thickness ft	NET thickness ft	PHIE average %	VSH average %	K average md
2A1	LNU	LNU8	12168	12179	11	7.5	0.071	0.196	0.273
		LNU7	12179	12298.5	119.5	96	0.082	0.108	0.3989
		LNU6	12298.5	12341	42.5	42	0.097	0.106	0.6763
		LNU5	12341	12460	119	117	0.104	0.089	0.8715
		LNU4	12460	12580	120	87	0.088	0.138	0.5047
2A2	LNU	LNU3	12580	12601	21	21	0.156	0.099	5.3896
		LNU9	12720	12819.5	99.5	77	0.088	0.208	0.4963
		LNU8	12819.5	12935.5	116	93.5	0.088	0.177	0.5041
		LNU7	12935.5	13039.5	104	78.5	0.06	0.086	0.1838
2A3	LNU	LNU6	13039.5	13063	23.5	24	0.064	0.104	0.2142
		LNU9	12256	12343	87	63	0.067	0.214	0.2396
		LNU8	12343	12445.5	102.5	97	0.094	0.166	0.6134
		LNU7	12445.5	12560.5	115	110	0.082	0.106	0.3997
		LNU6	12560.5	12600	39.5	38	0.088	0.103	0.5016
		LNU5	12600	12722	122	119	0.099	0.128	0.7279
		LNU4	12722	12833.5	111.5	109	0.101	0.092	0.793
2A4	LNU	LNU3	12833.5	12960	126.5	102	0.116	0.053	1.3446
		LNU8	11776	11886	110	104	0.087	0.142	0.4905
		LNU7	11886	11996	110	96	0.097	0.074	0.6837
		LNU6	11996	12035	39	37.5	0.098	0.094	0.7148
		LNU5	12035	12156	121	84	0.093	0.149	0.5983
		LNU4	12156	12271.5	115.5	99	0.092	0.146	0.5673
		LNU3	12271.5	12382	110.5	105.5	0.105	0.12	0.9152
		LNU2	12382	12477.5	95.5	92	0.092	0.103	0.575
	LNM	LNU1	12477.5	12539	61.5	55.5	0.072	0.092	0.2865
		LNM4	12539	12643	104	73.5	0.079	0.286	0.3646
		LNM3	12643	12751	108	80	0.076	0.304	0.3319
		LNM2	12751	12843.5	92.5	82	0.089	0.173	0.5205
		LNM1	12843.5	12880	36.5	9	0.081	0.258	0.3873
2A5	LNU	LNU8	12040	12155	115	96.5	0.106	0.139	0.9348
		LNU7	12155	12265	110	91	0.076	0.062	0.3317
		LNU6	12265	12308	43	36.5	0.104	0.084	0.8803
		LNU5	12308	12438.5	130.5	92.5	0.098	0.14	0.695
		LNU4	12438.5	12552	113.5	105	0.096	0.133	0.6684
		LNU3	12552	12655	103	96.5	0.117	0.104	1.3857
		LNU2	12655	12675	20	20	0.093	0.192	0.5836
2A6	LNU	LNU9	12670	12754.5	84.5	80	0.071	0.225	0.2794
		LNU8	12754.5	12849	94.5	84	0.073	0.095	0.2985
		LNU7	12849	12934	85	84.5	0.076	0.028	0.3262
2A7A	LNU	LNU6	12207	12235.5	28.5	19	0.115	0.09	1.3299
		LNU5	12235.5	12356.5	121	102	0.098	0.14	0.7027
		LNU4	12356.5	12475.5	119	68.5	0.081	0.16	0.3895
		LNU3	12475.5	12576	100.5	80.5	0.103	0.132	0.8263
		LNU2	12576	12700	124	106.5	0.107	0.137	0.9824

## **4.7 RESULTS OF WELL LOG CORRELATIONS**

Well logs were obtained for as many wells as was possible. The majority of the wells were concentrated in the North Gialo(6J) area operated by the Waha Oil Company, but also included wells from Farigh area that were available on open files. The final database consists of about 30 wells (**Fig. 4.1-1**) including key wells around the study area margin and records 14 potential layers cuts for each well occasionally. The well logs were extracted from Waha archive. The digital wells database was checked against original paper copy well logs whenever possible. In particular, there was a focus on the stratigraphy of the Lower-Cretaceous sequence. All unit tops of Lower Nubian and their sub-sequences, which picked up from the log correlation were reduced to sea level datum.

### **4.7.1 Lower Nubian Formation: Stratigraphic succession and correlation**

The early Cretaceous, Lower Nubian Formation in the study area, can be subdivided into Base, Middle and Upper units. It is overlain by Nubian Middle shale (**MN**) wherever not eroded by the Pre-Upper Cretaceous unconformity (**PUK**) surface. It is rested on **El Abd** Formation, which is effectively a weathered zone to underlying granitic **basement**. The top and bottom surfaces of Lower Nubian formation were defined by log correlation according to the well location as follows: Bottom surface is the total depth drilled (**TDD**) value when it is partially penetrated, the top of **El Abd** Formation when it is not eroded elsewhere the basement. However, the top surface is the **PUK** surface depth value when it is partially eroded. Elsewhere the bottom surface of the Nubian Middle (**MN**) shale was considered. The Lower Nubian Formation has a maximum measured thickness in well logs of 1104 ft in well 2A4 in the extreme northwest of the study region. In the central parts of the study area a maximum thickness of 1334.2 ft is encountered in the well 6J1. In the south western part the maximum thickness of 771.5 ft was measured in well 4E2A. The average Lower Nubian thickness is 506.7 ft. The lower Nubian gross thickness distribution is shown by **Fig. 4.7-1**. In the study area the thicknesses for the LNB unit of between 30.5 and 114.7 ft. The lower Nubian Base gross thickness distribution is shown on **Fig. 4.7-2**. For the LNM unit between 190 and 360 ft, lower Nubian Middle gross thickness distribution is shown on **Fig. 4.7-3**, and up to 864 ft for the LNU unit, lower Nubian Upper gross thickness distribution is shown on **Fig. 4.7-4**. The complete Lower Nubian sequence as measured in wells (6J1, 6J8, 6J11, and 6J12) in the study area attains a maximum thickness of 1334.2 ft, with an average thickness of about 970.6 ft.





#### **4.7.2 Flow-unite concept**

The Lower Nubian stratigraphic sequence described above has been interpreted as flow units. A flow- unit is an informal unit that groups together stratigraphic layers of similar materials that are adjacent. That is, contiguous units of predominantly sand would come together to form one flow-unit that would be thought of as a reservoir. Likewise, layers of shale that were arranged such that they formed a contiguous fine layer of low permeability would be lumped together to form a barrier. For example, the Upper part of the Lower Nubian sequence is comprised of several layers that are predominantly sandy – the lower Nubian. Facies and lithologic descriptions tend to indicate that these layers have small proportions of low permeability material associated with them, and it is probably possible to trace permeable sandstones on a reservoir scale basis. This is not to say that the layers are only composed of sandstones. On the contrary, the sequence may have persistent shale interbeds. However, overall one might expect that a lumped flow- unit such as this would display similar hydraulic properties and pressures at the broad reservoir scale. This broad reservoir flow unite approach is different to that within reservoir characteristics approach, which are measured at a very fine scale, and small differences in hydraulic properties are seen as indications of different types of materials(petro-types). These flow units were correlated by well logs in several directional trends overall the study area. Correlation was performed on reference datum which can be marker surface seen on all the wells traced by the correlation profile, it said hanged cross section (**Fig. 4.7-5**). The correlation was achieved by applying gamma ray and resistivity logs which were correlated very well overall the study area. For distinguishing the subject tops, differentiating the LNM, from the overlaying LNU, and underlying LNB, is made by its relative high gamma ray and low resistivity levels .This is because the LNM is more shaley succession than the other two successions.

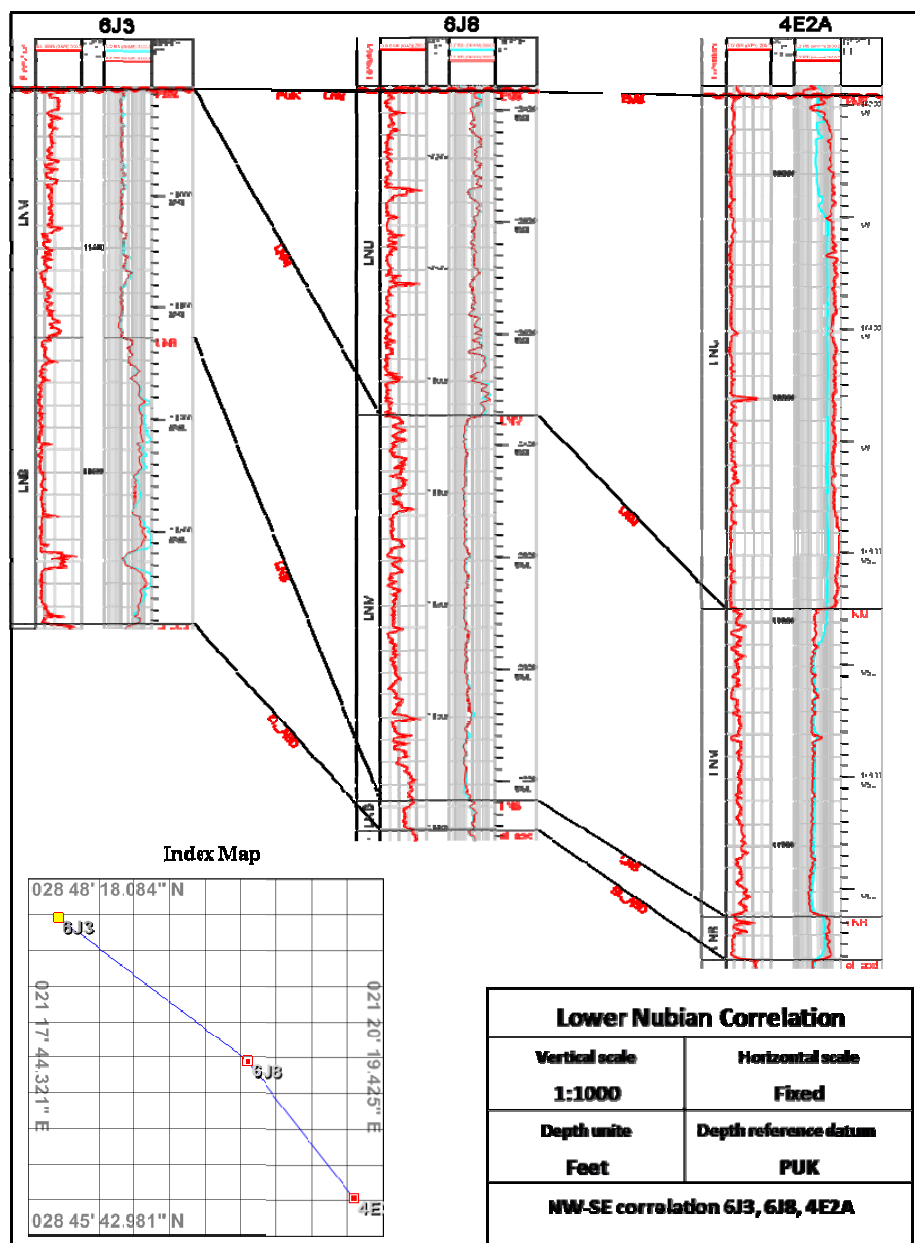


Fig. 4.7-5 Well log correlation section hanged on PUK surface

### 4.7.3 Petrophysical zoning concept

The Base, Middle and Upper units of Lower Nubian stratigraphic sequence described above has been further interpreted into a series of petrophysical zones or layers, according to the petrophysical results provided by well log analysis; i.e. porosity, permeability and shale volume values. The determination of such petrophysical layer is controlled by, the density on neutron, and thorium on potassium, overlay separation and by the net thickness intervals distribution which is consequent of gross thickness cutoff, using the values of motioned petrophysical parameters. The



zoning process had ended into three packages of petrophysical layers belonging to each of the Base, Middle and Upper units of Lower Nubian, as it will be described below:

#### **4.7.3.1 Base and Middle units -Petrophysical layers package**

The base flow unit of the Lower Nubian is composed only of one petrophysical layer named LNB. It is penetrated by eight wells, the complete thickness was measured in wells 4C1, 4E2A, 6J1, 6J3, 6J8, 6J11 and 6J12. With maximum gross thickness of 260.5ft and 54.5 ft net thickness measured in well 6J3. While the Middle flow unit is distributed into four petrophysical layers named, LNM4, LNM3, LNM2, and LNM1. These layers are encountered in eight wells. The complete thickness was measured in wells 2A4, 4C1, 4E2A, 6J1, 6J8, 6J11, and 6J12. However, in well 6J3 the LNM4 layer was eroded by PUK surface. The tops of each layer were picked by the well log correlation (**Fig. 4.7-6**), which was performed in several profiles. Each layer can be distinguished depending on the separation distance defined by the mentioned overlies and lithology components (porosity, sand and shale fraction) estimated by log analysis. The picked tops and measured thicknesses are given by **Table 4.7-2**, and **Table 4.7-3, 4.7-4**.

#### **4.7.3.2 Upper unite- petrophysical layers package**

The total thickness of this unite was measured in well 6J1. It can subdivided into nine layers named LNU9, LNU8, LNU7, LNU6, LNU5, LNU4, LNU3, LNU2, and LNU1 with varieties of thickness regarding the location where they are encountered. Some of these layers were eroded by PUK surface. Specifically, LNU9 was present only in four wells (2A2, 2A3, 2A6, and A1), while LNU8 and LNU7 are missing in wells 2A7A, 4C1, 4E2A, 6J8 and 6J12. However, some of the layers was not reached by the total depth drilled in such wells (2A1, 2A2, 2A6, 6J4, 6J6, and A1). The tops which are reported in **Table 4.7-1**, gross and net thicknesses in **Table 4.7-3, 4.7-4**, was determined by several correlation profiles. **Fig. 4.7-7** illustrates an example of such correlation.

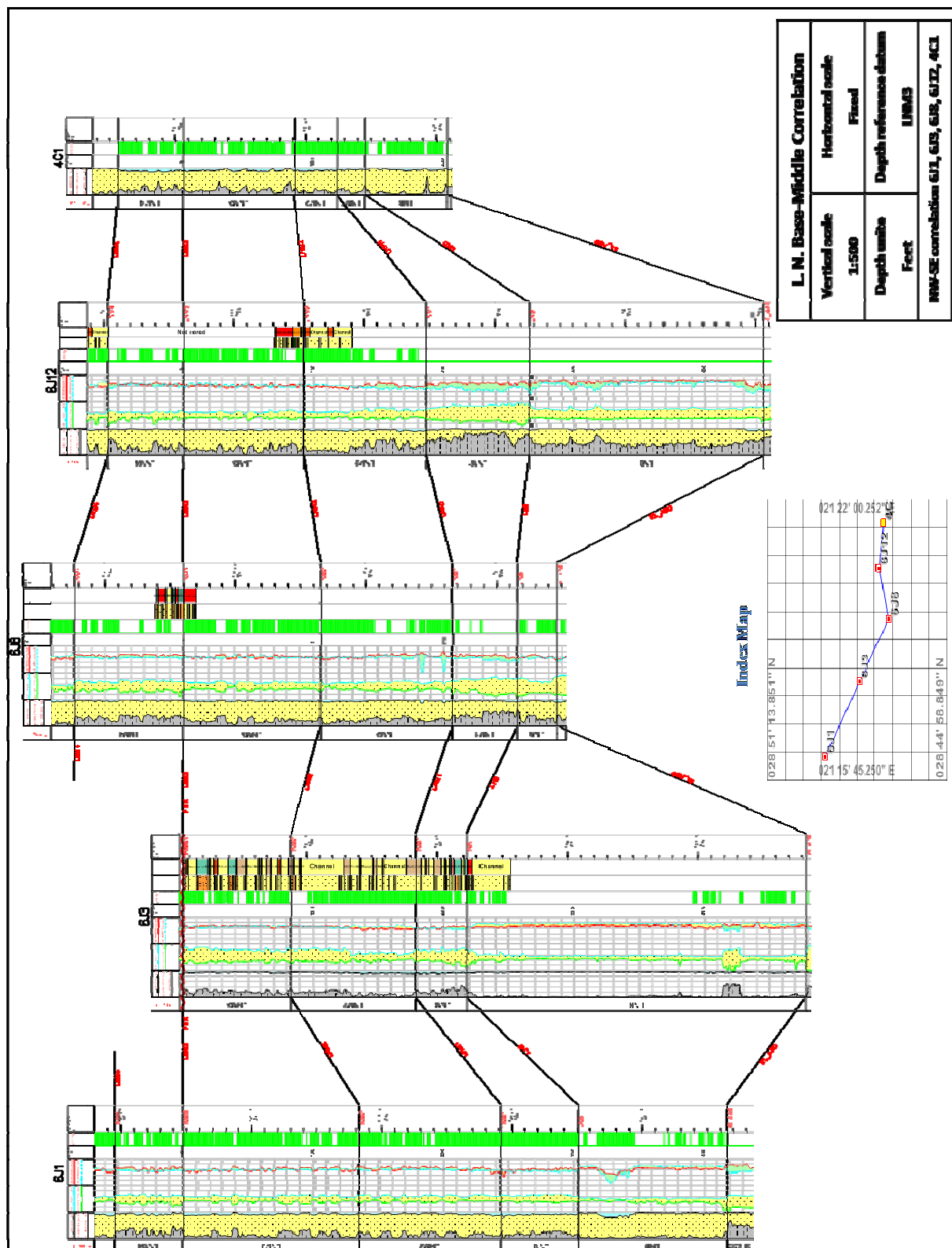


Fig. 4.7-6 Well log correlation section hanged on Lower Nubian Middle-3

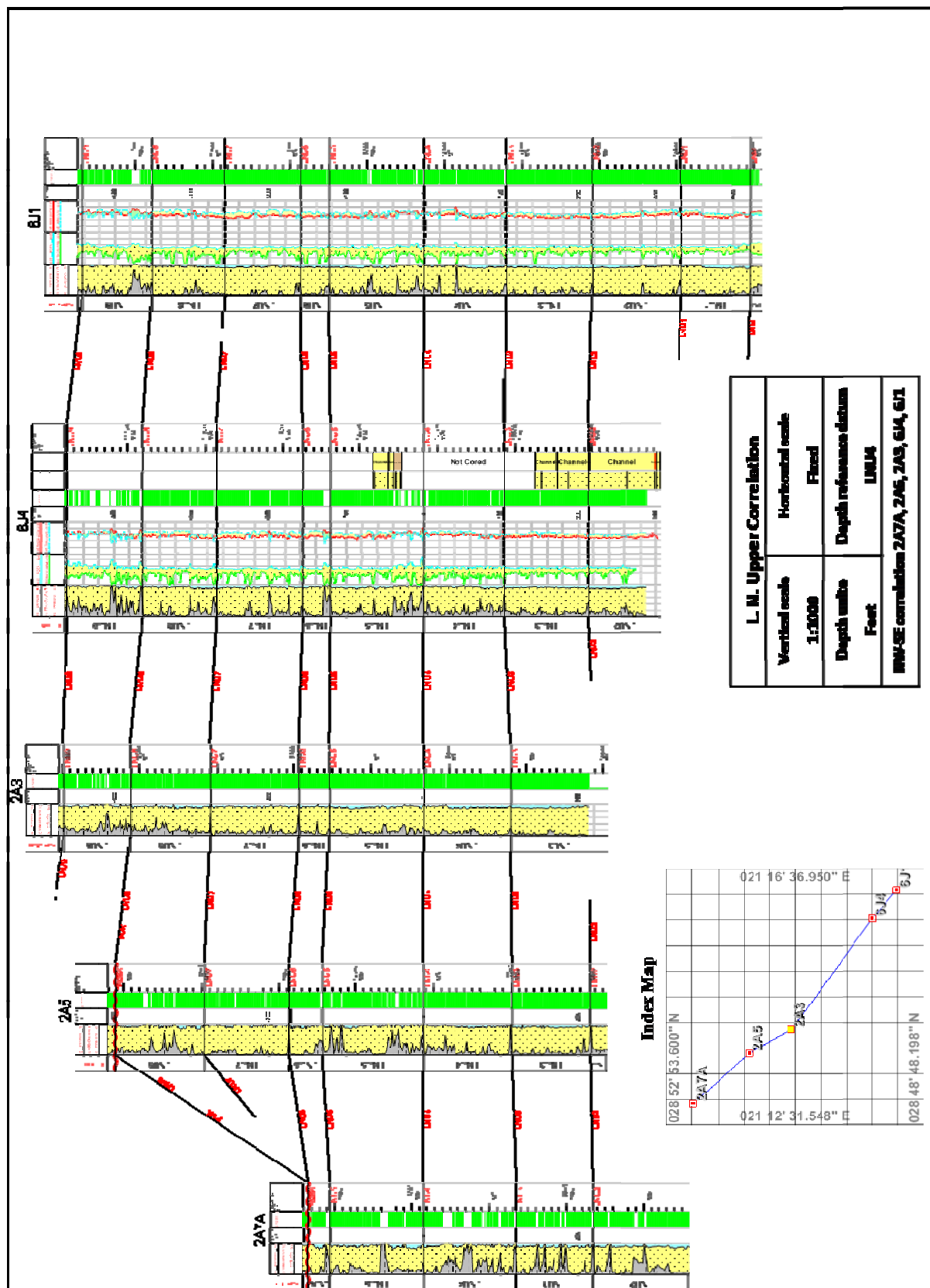


Fig. 4.7-7 Well log correlation section hanged on Lower Nubian Upper-4

Table 4.7-1 Lower Nubian(LNU) tops, measured depth from KB in feet

Well	Unconformity Surface	Lower Nubian Upper								
	PUK	LNU9	LNU8	LNU7	LNU6	LNU5	LNU4	LNU3	LNU2	LNU1
2A1	12168	ER	12168	12179	12298.5	12341	12460	12580	NR	NR
2A2		12720	12819.5	12935.5	13039.5	NR	NR	NR	NR	NR
2A3		12256	12343	12445.5	12560.5	12600	12722	12833.5	NR	NR
2A4	11776	ER	11776	11886	11996	12035	12156	12271.5	12382	12477.5
2A5	12040	ER	12040	12155	12265	12308	12438.5	12552	12655	NR
2A6	12670	12670	12754.5	12849	NR	NR	NR	NR	NR	NR
2A7A	12207	ER	ER	ER	12207	12235.5	12356.5	12475.5	12576	NR
4C1	11366.5	ER	ER	ER	ER	ER	11366.5	11462	11582.5	11706.5
4E2A	10530	ER	ER	ER	ER	ER	10530	10623	10742.5	10860
6J1		11996	12086	12181	12279	12316	12438.5	12544.5	12656	12769.5
6J3	11258	ER	ER	ER	ER	ER	ER	ER	ER	ER
6J4		11982.5	12080	12175.5	12287	12323	12443.5	12547.5	12657	NR
6J6		12163	12250	12345.5	12441	12467	12587	12675.5	NR	NR
6J7	11087	ER	ER	ER	ER	ER	ER	ER	ER	ER
6J8	10740	ER	ER	ER	ER	ER	ER	10740	10832	10941
6J11	11547	ER	ER	11547	11655	11690	11810.5	11905	12014	12155
6J12	11113.5	ER	ER	ER	ER	ER	ER	11113.5	11130.5	11247.5
A1		12317	12419	12512.5	12629	12661	NR	NR	NR	NR

Table 4.7-2 Lower Nubian (LNM andLNB) tops, measured depth from KB in feet

Well	Lower Nubian Middle				Lower Nubian Base	Bottom Surface	
	LNM4	LNM3	LNM2	LNM1	LNB	El_Abd	TD
2A1	NR	NR	NR	NR	NR	NR	12614
2A2	NR	NR	NR	NR	NR	NR	13082
2A3	NR	NR	NR	NR	NR	NR	12955
2A4	12539	12643	12751	12843.5	NR	NR	12899
2A5	NR	NR	NR	NR	NR	NR	12700
2A6	NR	NR	NR	NR	NR	NR	12956
2A7A	NR	NR	NR	NR	NR	NR	12700
4C1	11794	11844	11929.5	11962	11984	12046.5	12340
4E2A	10991.5	11033	11101.5	11204.5	11259	11301.5	11418
6J1	12860	12912.5	13047.5	13156.5	13215.5	13330.2	13370
6J3	ER	11258	11340.5	11436.5	11475.5	11736	12048
6J4	NR	NR	NR	NR	NR	NR	12750
6J6	NR	NR	NR	NR	NR	NR	12771
6J7	ER	ER	ER	ER	11087	11190	11343
6J8	11033	11116.5	11222	11323	11373	11403.5	11546
6J11	12252	12339.5	12451.5	12552.5	12612	12690.5	12972
6J12	11351.5	11409	11501.5	11595.5	11674.5	11854.5	12130
A1	NR	NR	NR	NR	NR	NR	12694

ER=Eroded

NR=Not reached

Table 4.7-3 Lower Nubian layers, net and gross thicknesses measured in feet.

Well name	Formation unite	Layer Name.	Gross thickness ft	NET thickness ft	Well name	Formation unite	Layer Name.	Gross thickness ft	NET thickness Ft
2A1	LNU	LNU8	11	7.5	6J1	LNU	LNU9	90	61.5
		LNU7	119.5	96			LNU8	95	94
		LNU6	42.5	42			LNU7	98	94.5
		LNU5	119	117			LNU6	37	34.5
		LNU4	120	87			LNU5	122.5	104.5
		LNU3	21	21			LNU4	106	96.5
2A2	LNU	LNU9	99.5	77			LNU3	111.5	109
		LNU8	116	93.5			LNU2	113.5	110
		LNU7	104	78.5			LNU1	90.5	90.5
		LNU6	23.5	24		LNM4	52.5	34.5	
2A3	LNU	LNU9	87	63		LNM	LNM3	135	116
		LNU8	102.5	97			LNM2	109	93.5
		LNU7	115	110			LNM1	59	59
		LNU6	39.5	38		LNB	LNB	114.7	53
		LNU5	122	119	6J3	LNM	LNM3	82.5	54.5
		LNU4	111.5	109			LNM2	96	79.5
		LNU3	126.5	102			LNM1	39	33.5
2A4	LNU	LNU8	110	104		LNB	LNB	260.5	54.5
		LNU7	110	96	LNU9		97.5	34	
		LNU6	39	37.5	LNU8		95.5	84.5	
		LNU5	121	84	LNU7		111.5	102	
		LNU4	115.5	99	LNU6	36	26.5		
		LNU3	110.5	105.5	LNU5	120.5	86		
		LNU2	95.5	92	LNU4	104	85		
		LNU1	61.5	55.5	LNU3	109.5	104.5		
	LNM	LNM4	104	73.5	LNU2	93	72.5		
		LNM3	108	80	6J6	LNU9	87	38.5	
		LNM2	92.5	82		LNU8	95.5	82	
LNM1		36.5	9	LNU7		95.5	90.5		
2A5	LNU	LNU8	115	96.5		LNU	LNU6	26	25
		LNU7	110	91	LNU5		120	86.5	
		LNU6	43	36.5	LNU4		88.5	67	
		LNU5	130.5	92.5	LNU3		95.5	68.5	
		LNU4	113.5	105	6J7	LNB	LNB	103	2.5
		LNU3	103	96.5	6J8	LNU	LNU3	92	83.5
		LNU2	20	20			LNU2	109	105
2A6	LNU	LNU9	84.5	80			LNU1	92	91
		LNU8	94.5	84		LNM	LNM4	83.5	31
		LNU7	85	84.5	LNM3		105.5	90	
2A7A	LNU	LNU6	28.5	19	LNM2		101	71	
		LNU5	121	102	LNM1		50	4.5	
		LNU4	119	68.5	LNB	LNB	30.5	20.5	
		LNU3	100.5	80.5					
		LNU2	124	106.5					

Table 4.7-4 Lower Nubian layers, net and gross thicknesses measured in feet.

Well name	Formation unit	Layer Name.	Gross thickness ft	NET thickness ft
6J11	LNU	LNU7	108	79.5
		LNU6	35	34.5
		LNU5	120.5	92
		LNU4	94.5	57.5
		LNU3	109	61
		LNU2	141	127
		LNU1	97	91
	LNM	LNM4	87.5	0
		LNM3	112	37.5
		LNM2	101	52
		LNM1	59.5	42
	LNB	LNB	78.5	25
6J12	LNU	LNU3	17	11.5
		LNU2	117	110.5
		LNU1	104	100
	LNM	LNM4	57.5	22
		LNM3	92.5	66.5
		LNM2	94	55
		LNM1	79	0
	LNB	LNB	180	0
A1	LNU	LNU9	102	44.5
		LNU8	93.5	69
		LNU7	116.5	100.5
		LNU6	32	31
		LNU5	45	6
4C1	LNU	LNU4	95.5	31
		LNU3	120.5	38.5
		LNU2	124	87
		LNU1	87.5	22.5
	LNM	LNM4	50	41.5
		LNM3	85.5	70.5
		LNM2	32.5	32.5
	LNB	LNB	22	21
4E2A	LNU	LNU4	62.5	44.5
		LNU3	93	81.5
		LNU2	119.5	116
		LNU1	117.5	115
	LNM	LNU1	131.5	131.5
		LNM4	41.5	22
		LNM3	68.5	45
		LNM2	103	22.5
	LNB	LNB	54.5	10.5
	LNB	LNB	42.5	16.5

## 4.8 GEOLOGICAL MODEL

The conceptualization described in the preceding sections was used to set up a numerical model of the study area. The numerical simulation was run through Rock Works.

### 4.8.1 Model Grid

The model was set up on a constant cell dimension of 500 ft by 500 ft in UTM coordinates. The model is 44 rows (East/West), 27 columns (North/South) and 30 vertical in dimension. The origin of the model was at (519000 easting, 3180000 northing) which lies near the centre of the North

Gialo field, close to 4P well outside the domain of the model. The south eastern boundary lies in the Uplift area. The north-eastern corner and the western corner lie in Farigh field.

#### 4.8.2 Layers

The model is composed of 14 layers. The approach to modeling has been to adopt a “true layer” approach. That is, wherever possible, the true layer thickness is represented. This means that the layer boundaries follow as closely to the true spatial position in nature as possible. Where a particular layer is missing, the layer is set to a minimum thickness of 1 ft and assigned the parameter values of the layer either immediately above or below. This preserves the integrity of the natural layering as well as ensures that the numerical stability of the model is retained. Layers were imported from the layer grids compiled and described in an earlier section. The model import function checks for internal integrity and resets any points where model layers cross over. The layers as generated were also checked against the various cross-sections. **Fig. 4.8-1** shows an example of a cross-section generated from the model.

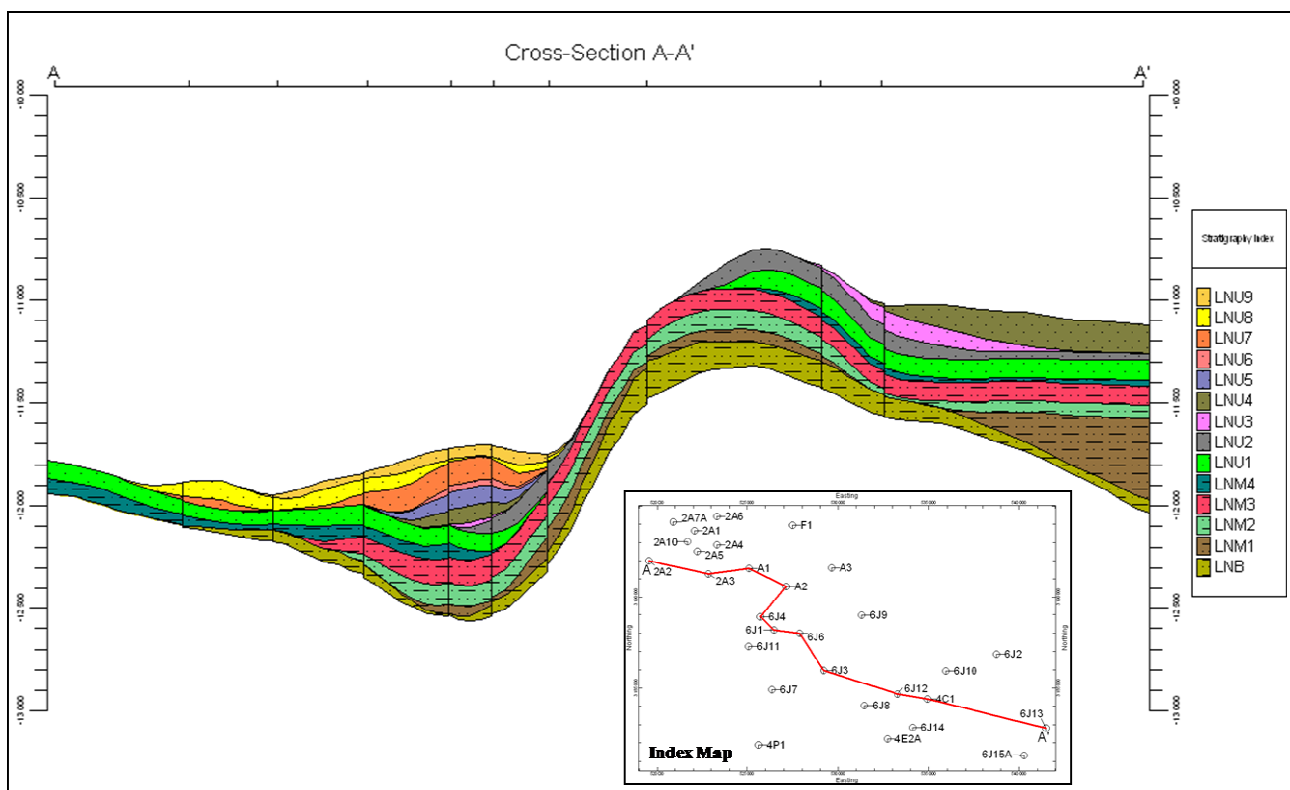


Fig. 4.8-1 Cross-section generated from the stratigraphy model

#### **4.9 RESULTS OF GEOSTATISTICAL APPROACHES**

The geostatistical analysis of the uncertainty of spatial distributions of the petrophysical properties belonging to the Lower Nubian sequences was achieved by generating 200 equally probable realizations using sGs approach. The simulation domain, laterally covers the study area, consists of 28 well data of well averaged porosities, permeabilities and shale fraction volumes. These averages are coming from quantitative well log analysis and related to the Lower Nubian net thickness. Since the frequency distributions were quite far from normality, normal score transformations were performed for each data-set. The experimental semivariograms of the transformed data were calculated in several directions using a proper angular increment and angular tolerance. This process ended by selecting three most characteristics directional semivariograms. The selected experimental semivariograms were approximated by nested theoretical models in the framework of VarioWin. During the numerical approaches we tried to reach the minimum values of Indicative Goodness of Fit (IGF, Panatier, 1996). The models were accepted when their variogram surfaces were like that of normal scores. Accordingly the Sequential Gaussian Simulation was performed on 10 m of grid resolution. For the analysis of uncertainty 200 stochastic realizations were generated. E-type grids show the most probable lateral distributions of the reservoir properties. The upper and lower confidence surfaces (on  $p=0.1$  level of significance) form the boundary of probability interval containing the point-wise E-type estimations. The thickness of this interval reflects the level of uncertainty in a particular location.

The general solution for any geostatistical reservoir description is to characterize individually the most significant zones of facieses or lithological sequences. However, in the case of this field, the total number of wells penetrating the whole Lower Nubian Sequence is only three (**Table 4.7-1 and 4.7-2.**). Only seven wells penetrated the Middle Lower Nubian Unit. This well control does not make reasonable to apply the above mentioned general solution. Instead, well averaged petrophysical properties were used in geostatistical analyses. It must be emphasized, that because of the above mentioned well controls, the results obtained can be valid mainly for the upper part of the Lower Nubian sequence.



#### 4.9.1 Original data distribution

The original data histograms of well-averaged porosities, permeabilities and shale fraction volumes (**Fig. 4.9-1, 4.9-2 and 4.9-3**) show that porosity and shale volume frequency have peaked-distributions (kurtosis,  $g_2 > 0$ ). Permeabilities could be characterized by heavily asymmetrical distribution. Consequently, prior to further steps, all data typed needed transformations for stabilizing the variances. The tool was the method of normal score transformation.

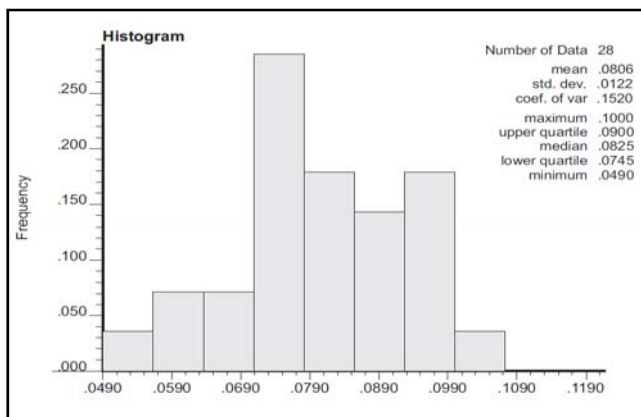


Fig. 4.9-2 Histogram of the original data for porosity

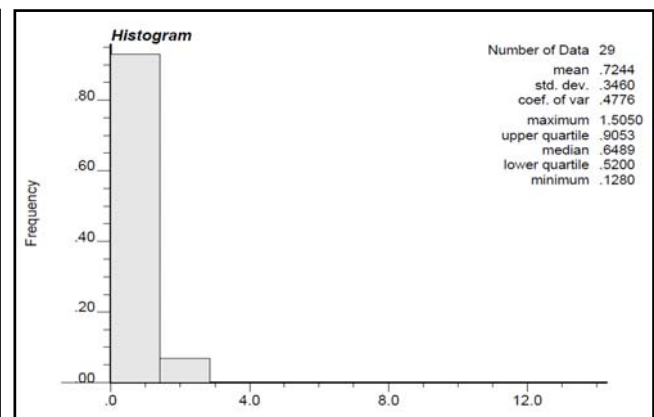


Fig. 4.9-1 Histogram of the original data for permeability

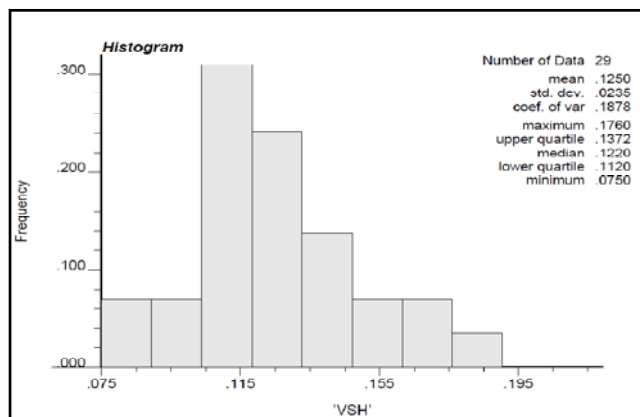
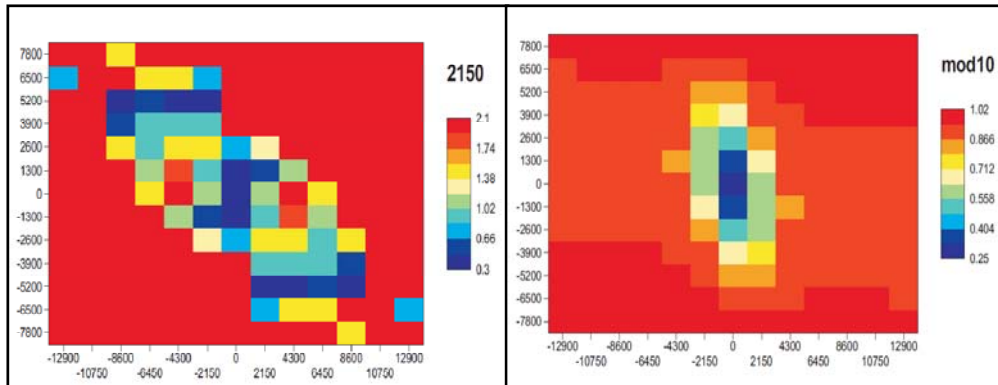


Fig. 4.9-3 Histogram of the original data for shale fraction volume

#### 4.9.2 Modeling of experimental variograms

The variogram surfaces of normal scores show the main directions of lateral continuities, that is the principal direction. The experimental variograms were calculated both in the principal and the perpendicular direction. Also, the goodness of their numerical approximations can be checked by comparing the experimental and theoretical variogram surfaces (**Fig. 4.9-4, 4.9-5 and 4.9-6**). For porosity and shale volume, the major continuity directions were 160° and 340° the minor ones were 90° and 180° respectively. In the case of permeability they were 140° and 90°. (**Fig. 4.9-4,**

**4.9-5 and 4.9-6)** show the matching of the experimental and model surfaces. The results of model-fitting processes can be seen on **(Fig.4.9-7.—4.9-9)**.



**Fig. 4.9-4** Experimental and model variogram surface of porosity

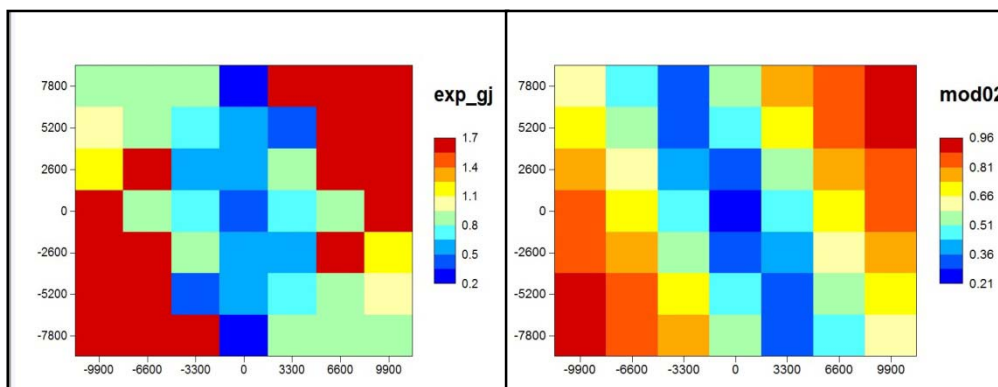


**Fig. 4.9-5** Experimental and model variogram surface of shale volume

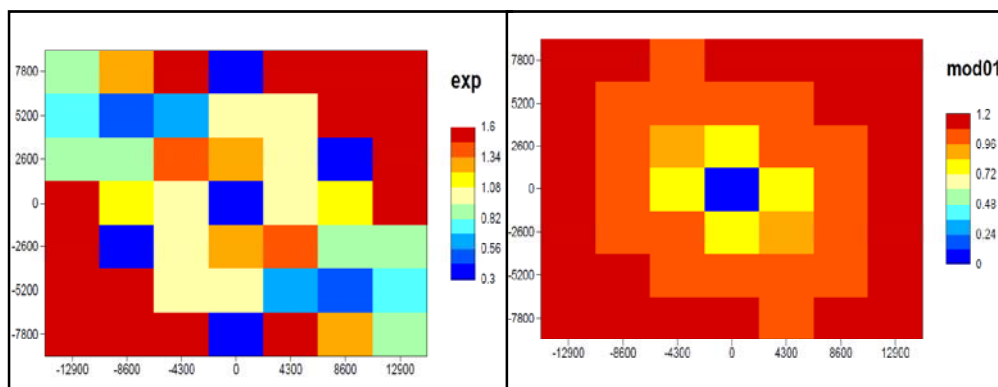


**Fig. 4.9-6** Experimental and model variogram surfaces of permeability

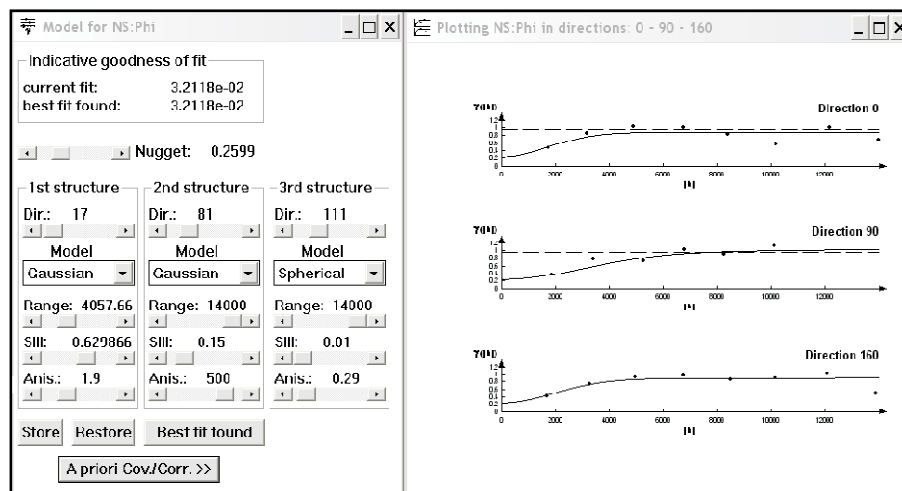


Fig. 4.9-7 Modeling the lateral heterogeneity of porosity

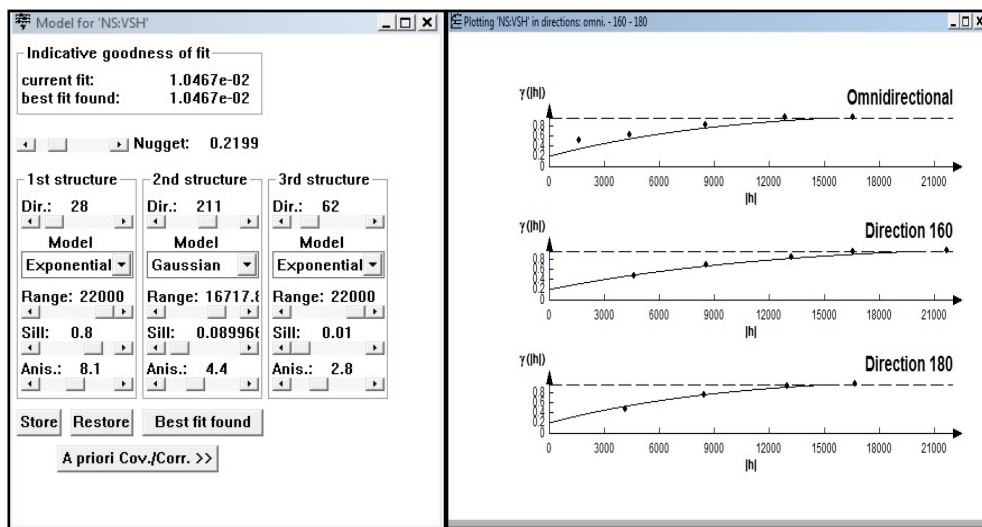


Fig. 4.9-8 Modeling the lateral heterogeneity of shale volume

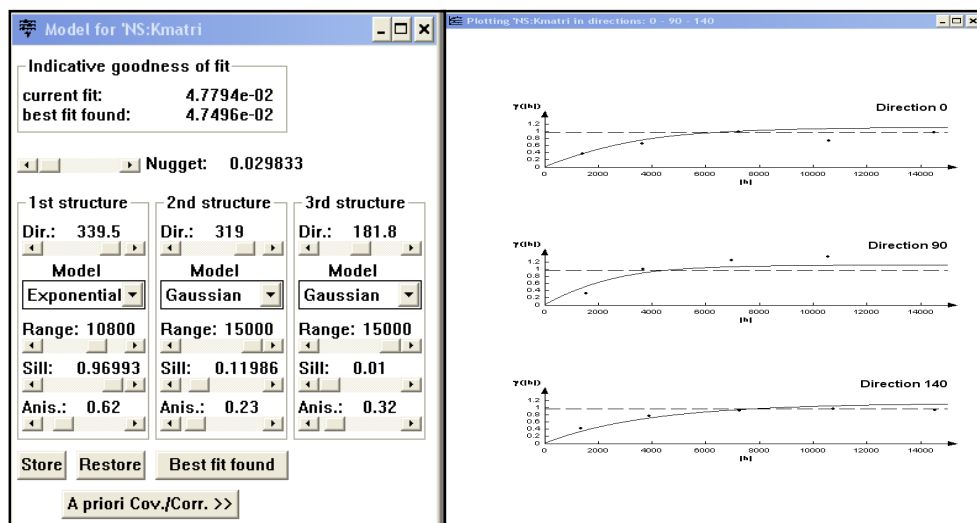
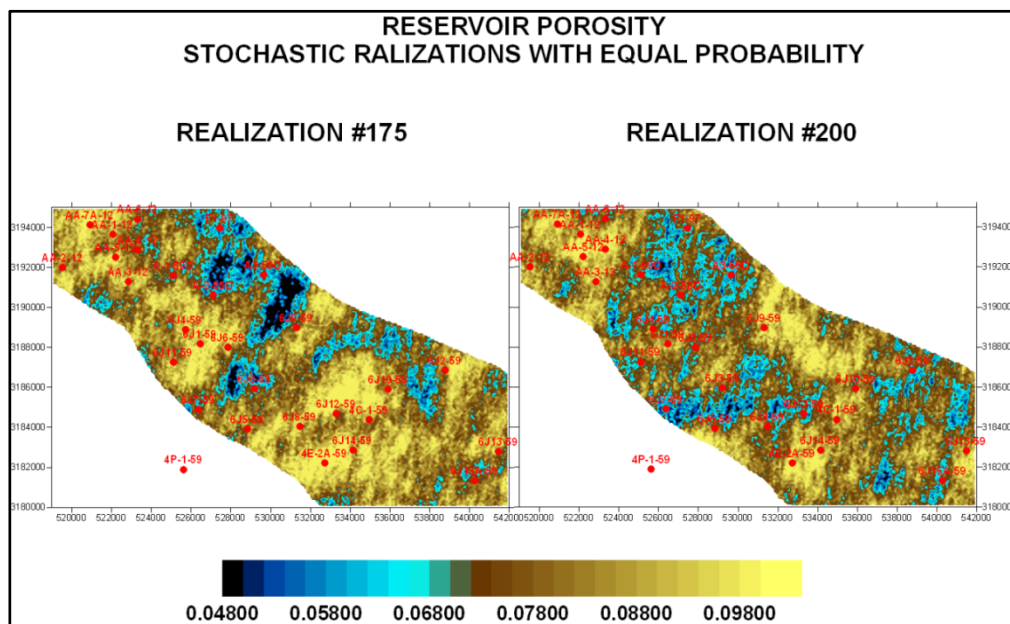


Fig. 4.9-9 Modeling the lateral heterogeneity of permeability

### 4.9.3 Stochastic realizations

Porosity and shale volume are basic rock properties, while permeability is strongly affected by the connectivity of pore network. Also, this latter one depends both on the pore-geometry and the volume of shale being in pores. This phenomenon can account for the similarity of spatial distributions of the estimated petrophysical values even in the different realizations. Two hundred realizations were provided in addition, the E-type expected values distribution map was elaborated. Arbitrary selected realizations, for each simulated parameter are given here by (Fig. 4.9-10, 4.9-11 and 4.9-12).



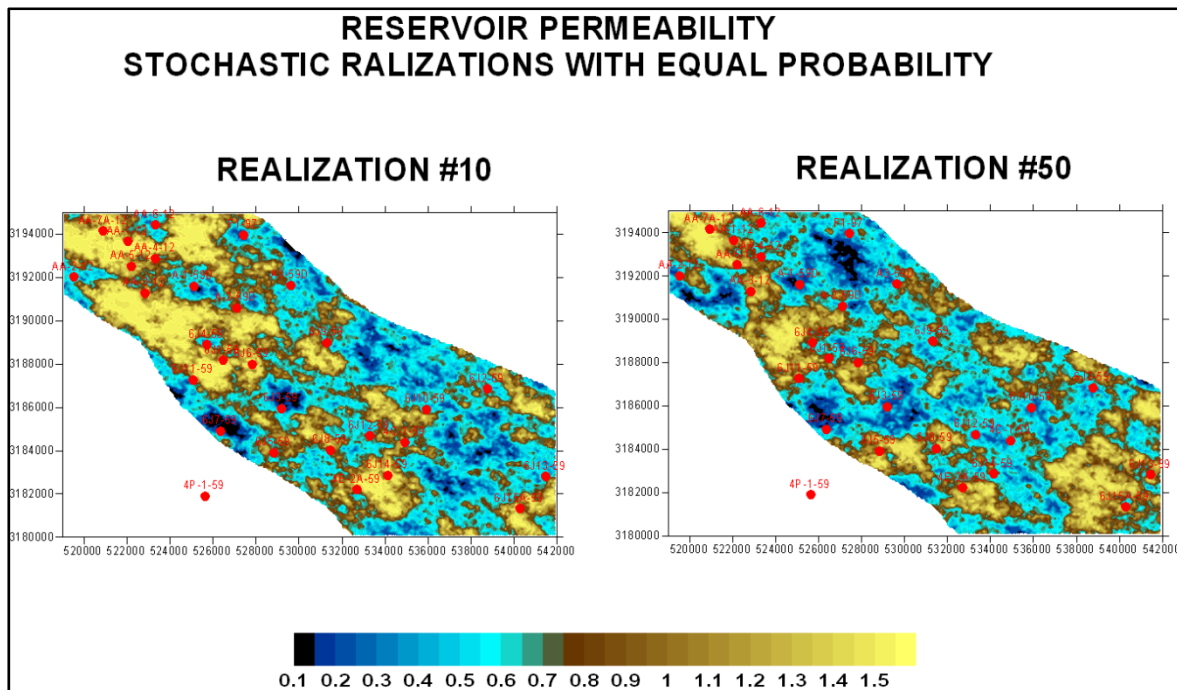


Fig. 4.9-12 Two of stochastic realizations for permeability

#### 4.10 UNCERTAINTY APPROACH

It is illogic and may be unrealistic to handle such number of fine-scale realizations, either it is hard to rank them to expect the loss one. The alternative way is attempting to characterize the uncertainty of the estimated values. Uncertainty can be associated with the variability of simulated values at a particular grid-node. or simulation pixel. This approach has been achieved by utilizing the probability distribution of the 200 estimated values at each simulation pixel. The uncertainty of the expected value at particular location can be quantified according to the width of their confidence intervals. A probability interval with total width of 0.1 offered by GSLIB has been proved to be equivalent to the 'traditional confidence interval with 0.1 level of significance

##### 4.10.1 Uncertainty of porosity

The porosity is considered to be as angle stone for the reservoir management due to its sensitivity role in evaluating the hydrocarbon reserve. It is essential to assess the uncertainty of its horizontal and vertical distribution over the reservoir domain. Three uncertainty levels could be defined from the lateral distribution of the width of confidence interval, which has been elaborated from the Et-type values and their associated confidence boundaries (**Fig. 4.10-1, 4.10-2**). These levels occur in wide spread also in the form of continuous lateral clusters. In the following the high level

uncertainty regions and their relations to the Lower Nubian reservoir characteristics are analyzed. Regions with high level of uncertainty

This uncertainty level (**Fig. 4.10-3**) occurs around the cored well location 6J3 where the Lower Nubian is represented by the LNB and LNM units. In this region the uncertainty may be related both to the source of small scale heterogeneity coming from the diagenetic process which altered the original porosity (quartz cementation in case of LNB), and presence of dispersed clay in the case of LNM. The high values of uncertainty have strip-like geometry. This can be related to presence of tectonic elements (large scale heterogeneity) like major and minor faults (**Fig. 4.10-4**). Also, it can be related to the interfingering of sedimentary facieses. This medium scale heterogeneity can be seen for instance between Fluvial Braided facies (Well 6J3) and Estuarine/Deltaic facies (Well 6J6). The eastern part of the field has dominantly high uncertainty values. The zero or very small net thickness values can explain this fact (**Fig. 4.10-5**).

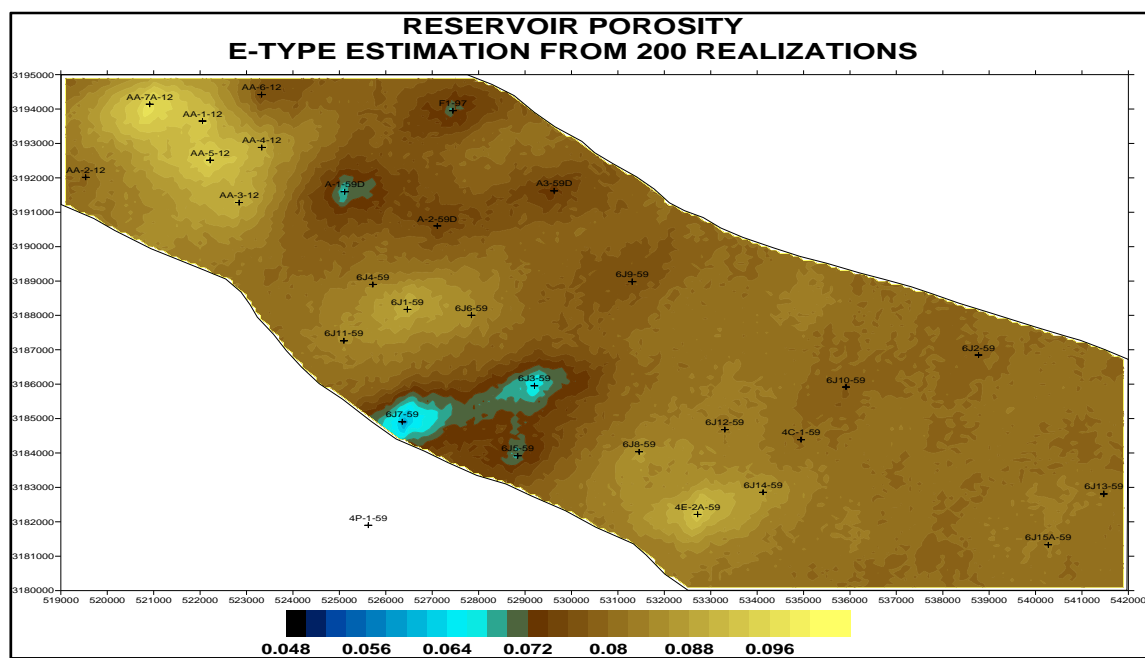
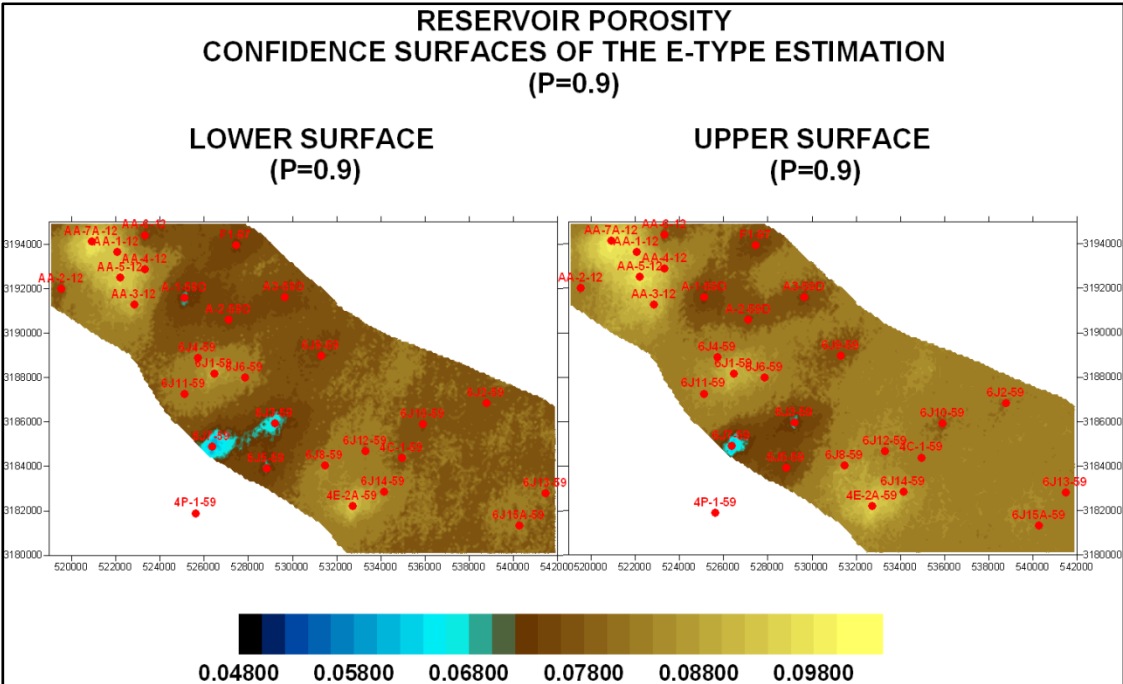
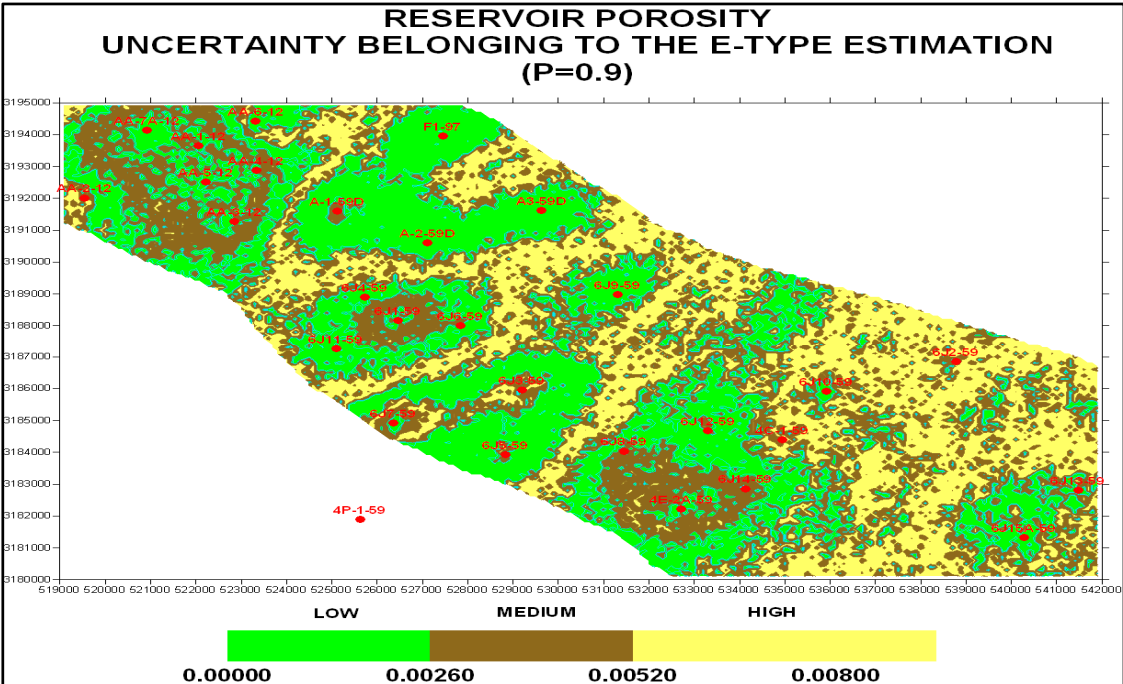


Fig. 4.10-1 E-type estimation of well-averaged porosity





(p=0.9)



**Fig. 4.10-3 Map of uncertainty for well-averaged porosity**

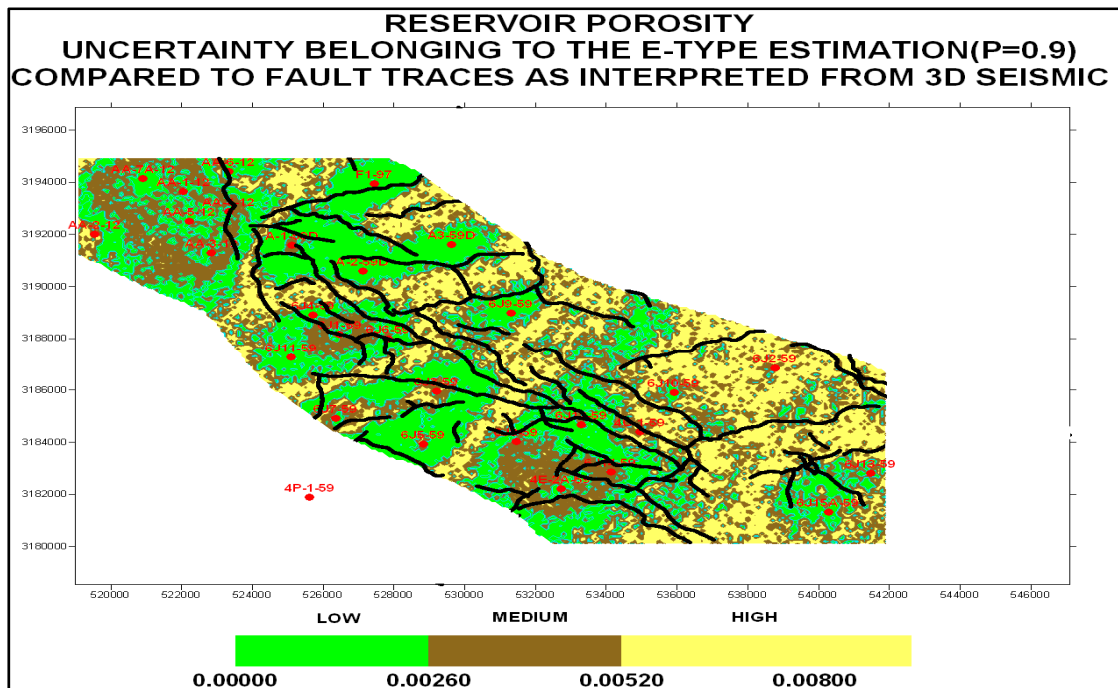


Fig. 4.10-4 Uncertainty related to Fault traces as interpreted from 3D seismic

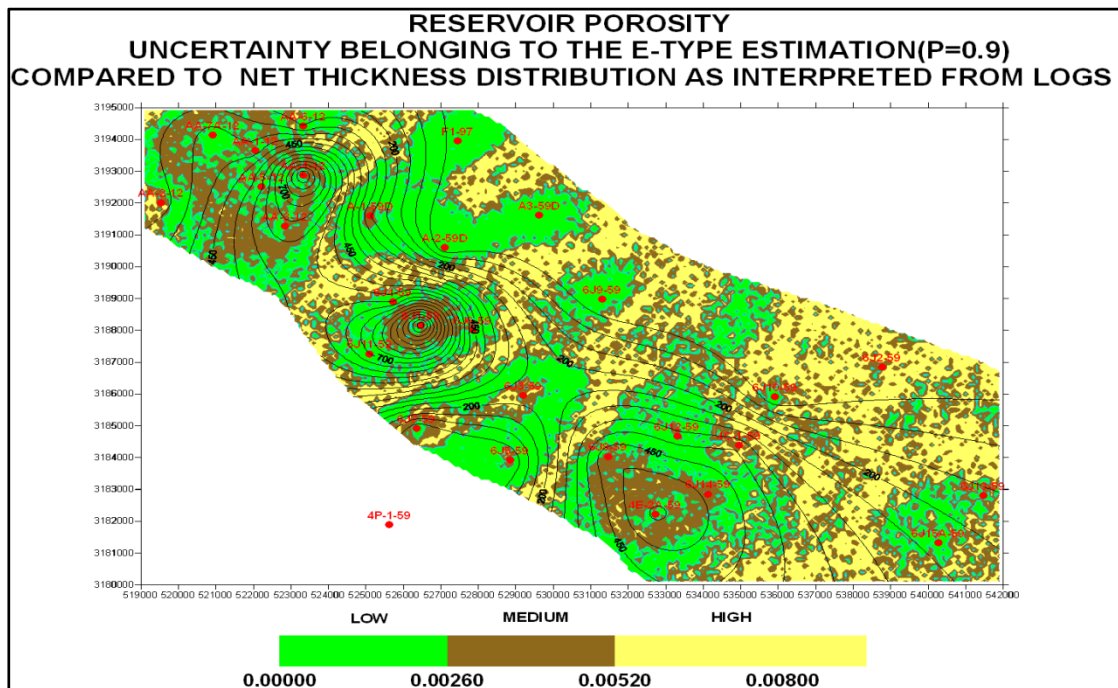


Fig. 4.10-5 Uncertainty related to Net thickness

#### 4.10.2 Uncertainty of permeability

Permeability is thought to be primarily controlled by matrix porosity and secondarily by natural fractures. Although it can also be the result of their complex effects. Usually in tectonic rift settings fractures are mostly of tectonic origin, where fracture intensity increases when getting



closer to faults. In other words it is fault-related fractures. It has been recently demonstrated that fracture intensity increases close to faults (Mueller, D., and Daly, C., 2004). However, in the area immediately adjacent to faults the high fracture intensity is associated with low production due to fault gouge. The best production occurs some distance away from faults in which the fracture intensity is still relatively high, but the influence of fault gouge is diminished. On the other hand, drilling-induced fractures are developed during drilling. The development of induced fractures is under the control of pre-existing mechanical anisotropy (natural fractures and bedding planes). These fractures are generally observed in the fine-grained and compacted rocks. When the permeability is related to the matrix porosity, it may be controlled by the larger grain sizes and cementation. The cementation may have reduced porosity in the large pores, and has caused a significant corresponding decrease in pore throat sizes and permeability, this can be explained by the porosity permeability correlation, those points demonstrating high permeability with low porosity values (**Fig. 4.10-9**).

#### **4.10.2.1 Regions with high level of uncertainty**

The map showing the general uncertainty of permeability (**Fig. 4.10-8**) which is the consequent of the E-type expected values, and its associated confidence boundaries given in (**Fig. 4.10-6, 4.10-7**). The uncertainty distribution map demonstrates, that the high uncertainty levels are generally related to small scale heterogeneities. This can be confirmed by the porosity –permeability relationship (Beard, D. and Weyl, P.1973) (**Fig. 4.10-9**). here the porosity permeability relation shows good correlation trend, which means that the permeability values are function of pore and pore throat size variation (small scale heterogeneity) and in (**Fig. 4.10-10**), which shows that the permeability values are controlled by the fraction volume of the authigenic (Pore-lining and pore-filling) clays (Wilson, M. J., and Pittman, E.D., 1977), this might be playing also a major role in creating such locations of permeability small scale heterogeneity. These sources of small scale heterogeneity are thought to be the primary reasons of high uncertainty. One of the other factors may be fracturing diagenetic processes, most of fractures; observed in core descriptions are mainly closed ones and filled by quartz or clay cements. It seems that the faults were acted as a conduit for the silica-rich fluids that contributed to diagenetic quartz cementation near the faults. (**Fig. 4.10-11**) shows the permeability values in some well locations, as a result of both DST and production tests. Those values are almost equal to the permeability values measured on cores or derived from logs (Corbett, P.W., Zheng, S., Piniseti, M., Mesmari, A. and Stewart, G., 1998). This

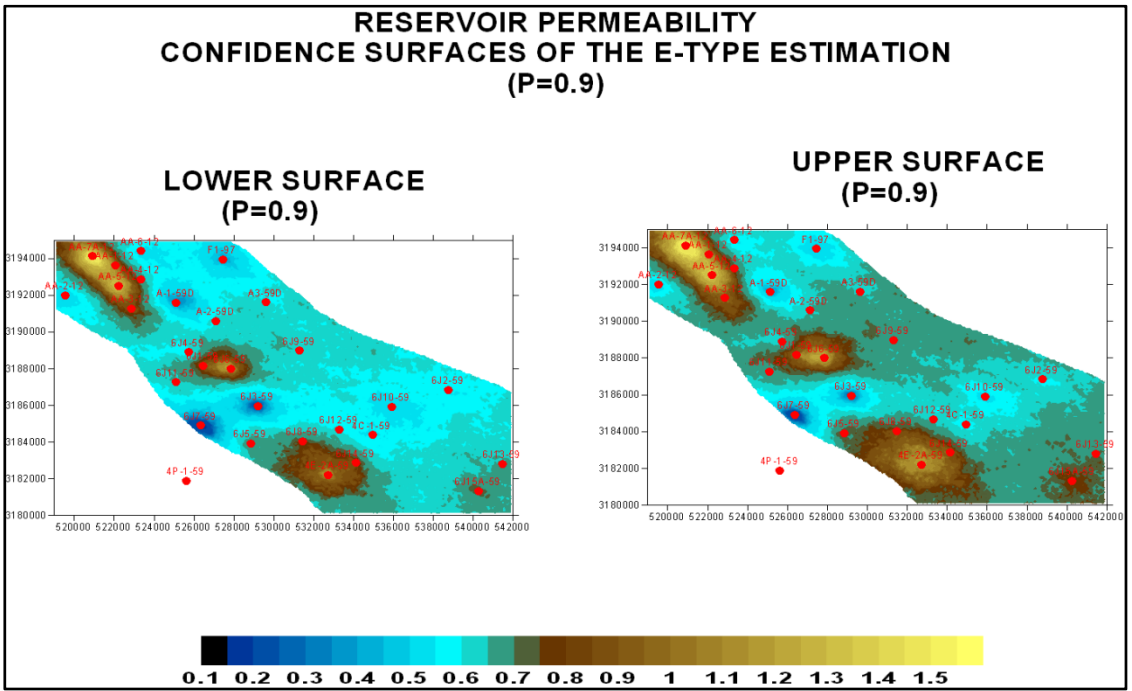
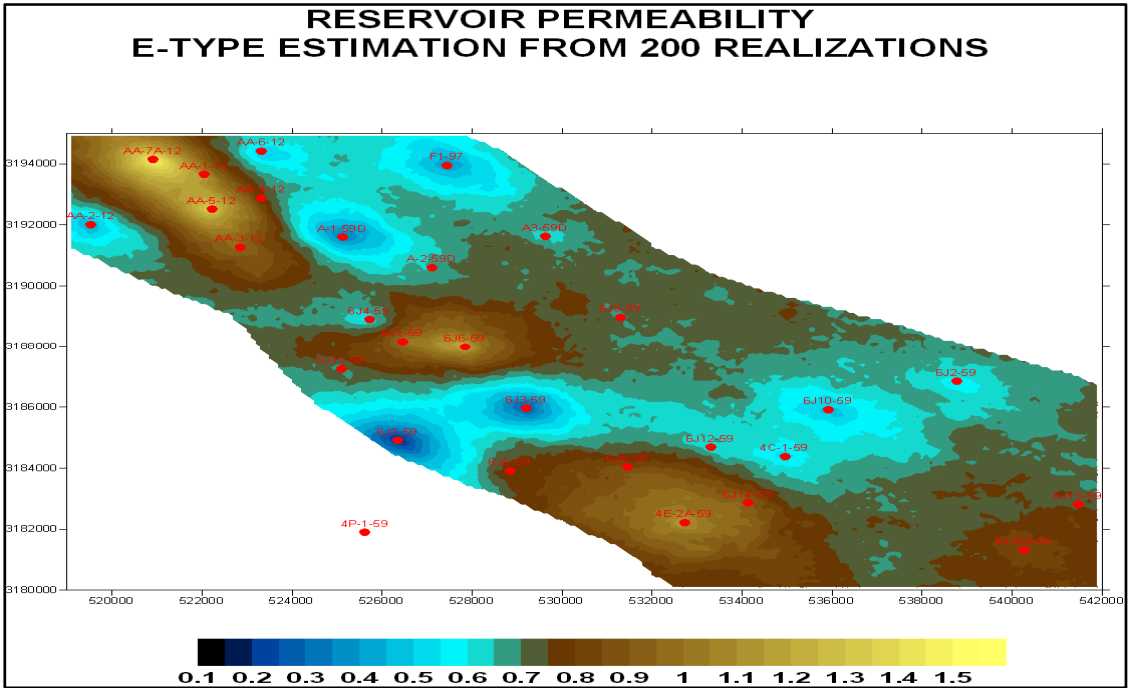


**Fig. 4.10-7 Upper and lower bounding surfaces of E-type estimation for permeability (p=0.9)**



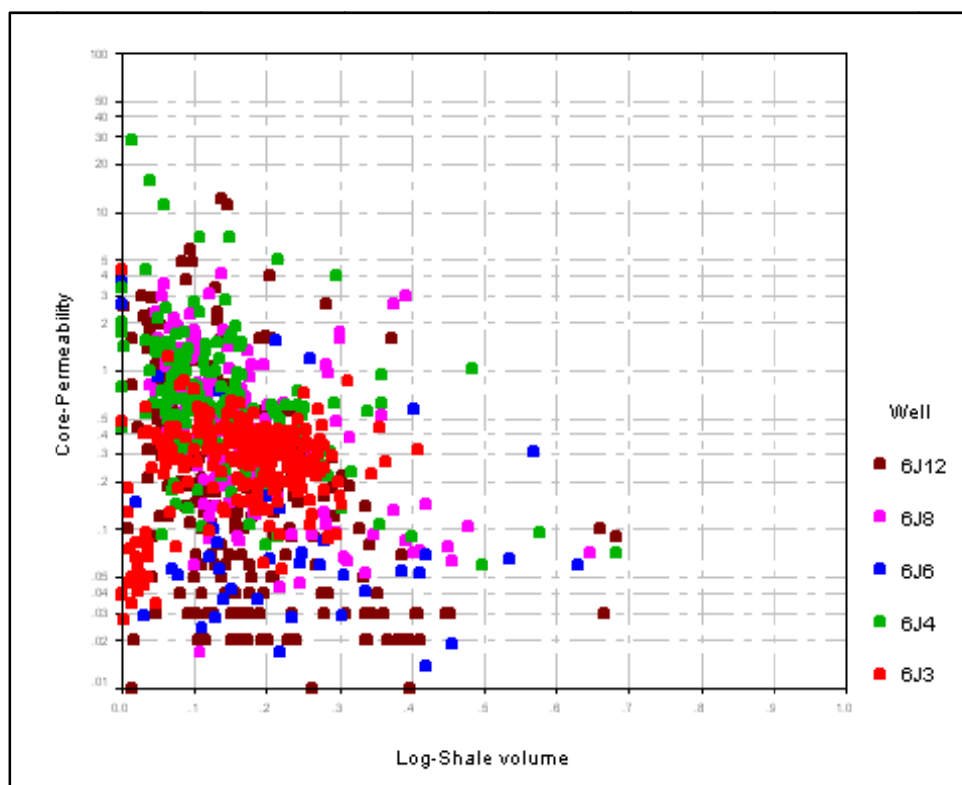


Fig. 4.10-10 Core permeability correlation with shale volume

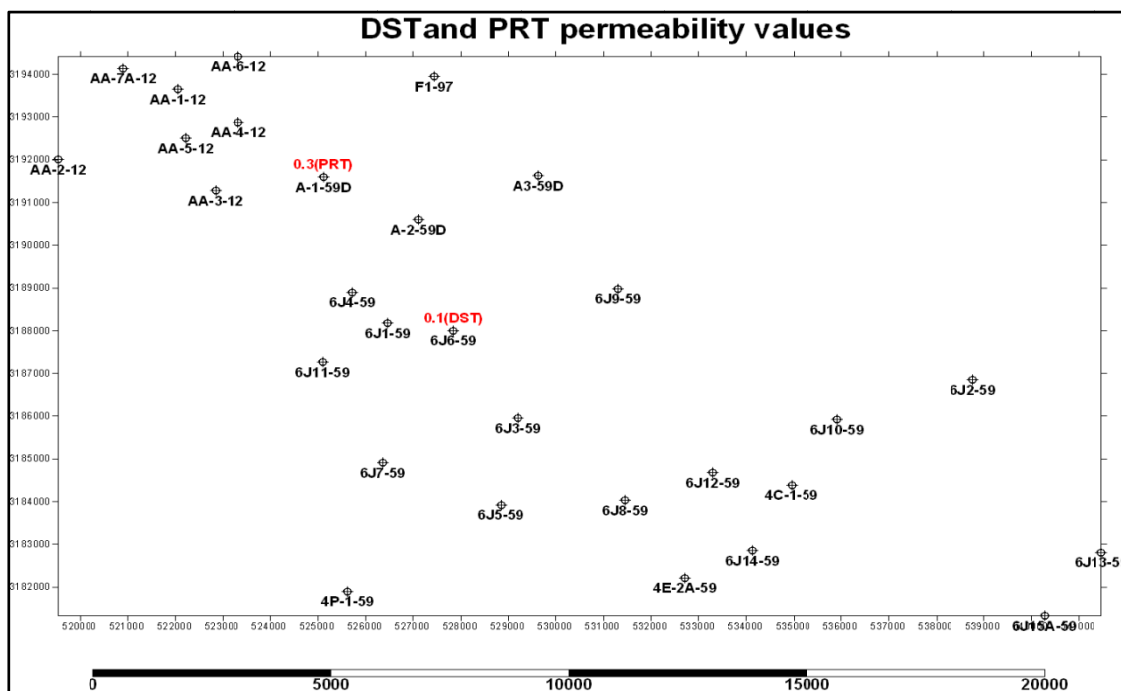


Fig. 4.10-11 Permeability values from production test in some locations

### **4.10.3 Uncertainty of shale volume**

The precipitation of clay or shale in reservoir sandstones can have an effect on the reservoir properties by reducing its hydrocarbon potential. Clay minerals in sandstones can be both of detrital and authigenic origin. In general clays in the reservoir sandstones can appear in two forms: laminated detrital or authigenic dispersed (disseminated). The laminated shale, if it has significant thickness and lateral continuity, will act as a connectivity barrier and impact the transmissibility of the reservoir sandstones. The authigenic clay can occur as pore filling (illite), grain coating (Chlorite) and booklet (Kaolinite). Clay minerals are extremely fine grained. They can impair, in varying degrees, permeability and porosity of the pore network where they reside. The shale volume of the Lower Nubian is thought to be of authigenic origin. This thought is drawn from correlations of shale volume versus porosity and permeability in cases of both core and log interpretation. The E-type map and the associated probability intervals are shown in **(Fig. 4.10-12, 4.10-13)**. It must emphasize that during the reservoir management understanding of the uncertainty levels related to the expected shale values is essential, especially in IOR stages. The following section will describe the background of the lateral appearance of high uncertainty levels.

#### **4.10.3.1 Regions with high level of uncertainty**

The map showing the lateral distribution of uncertainty **(Fig. 4.10-14)** provides definitive information on the reliability of expected values. The high-level-patches on the map of uncertainty may be connected to some small scale heterogeneity **(Fig. 4.10-15)**. It indicates, that the level zones of uncertainty can be related to a trend of decreasing net-to-gross thickness, which, can be related predominantly to diagenetic clay cementation process. , For example in case of well 6J7 core observations indicate strong diagenetic quartz cementation and the net-to-gross ratio is very low., while uncertainty level is Low, which can be considered as strong evidence, for relating the high uncertainty levels, to the net to gross ratio trend ,caused only by diagenetic clay cementation process.

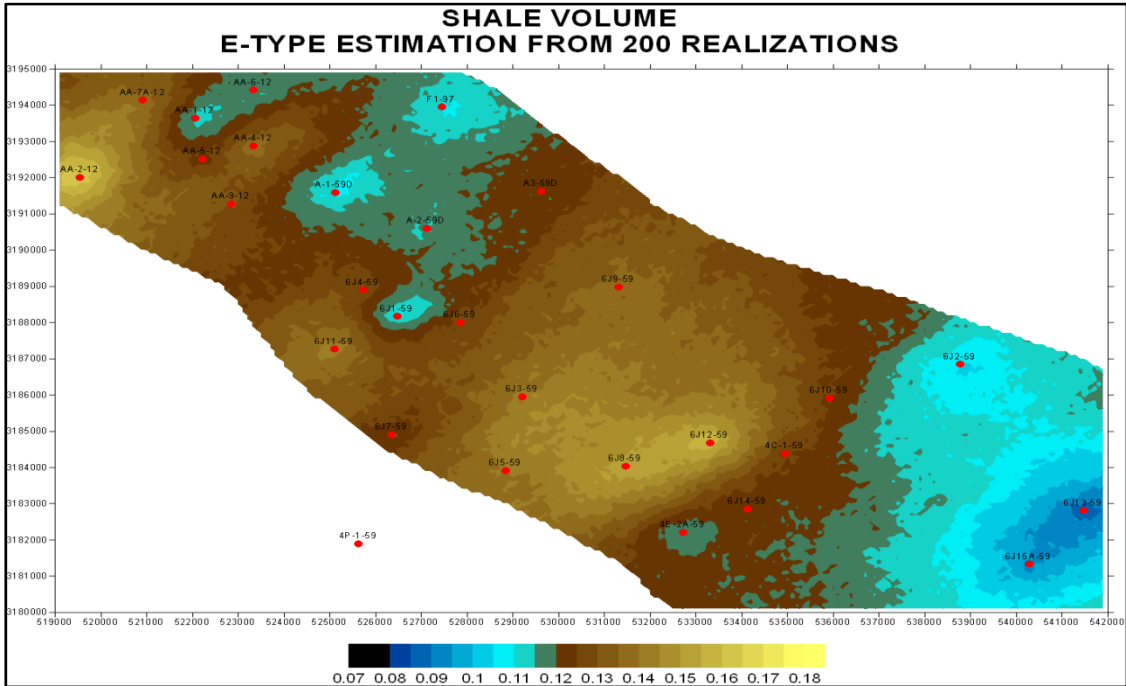


### Fig. 4.10-12 E-type estimation of shale volume

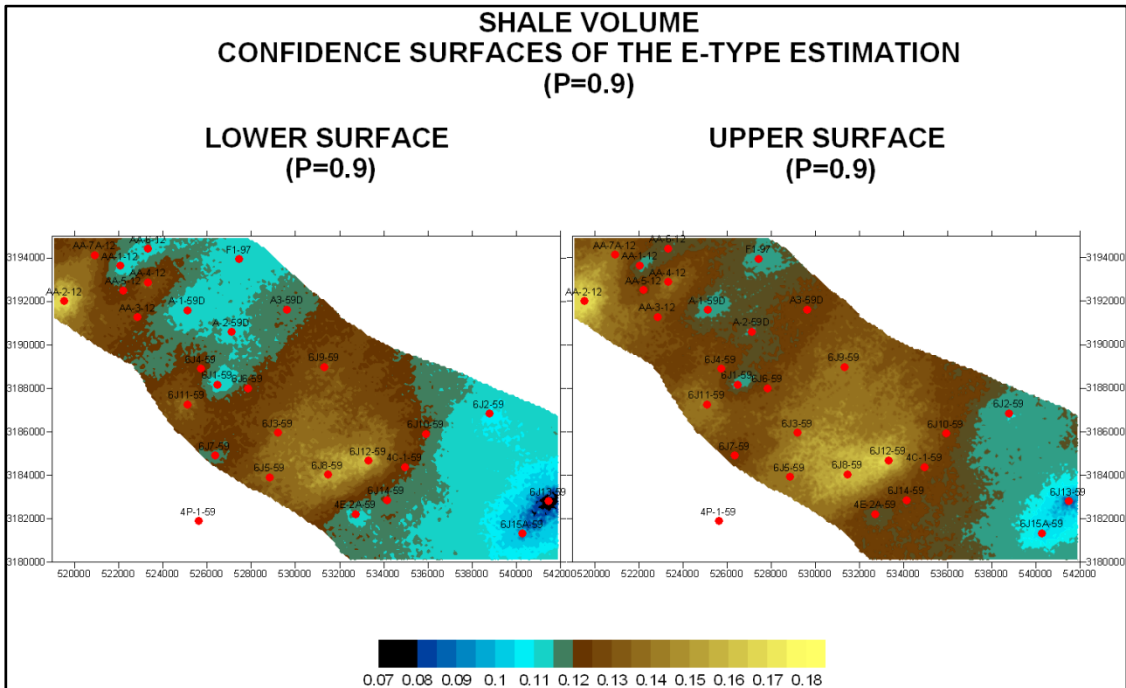
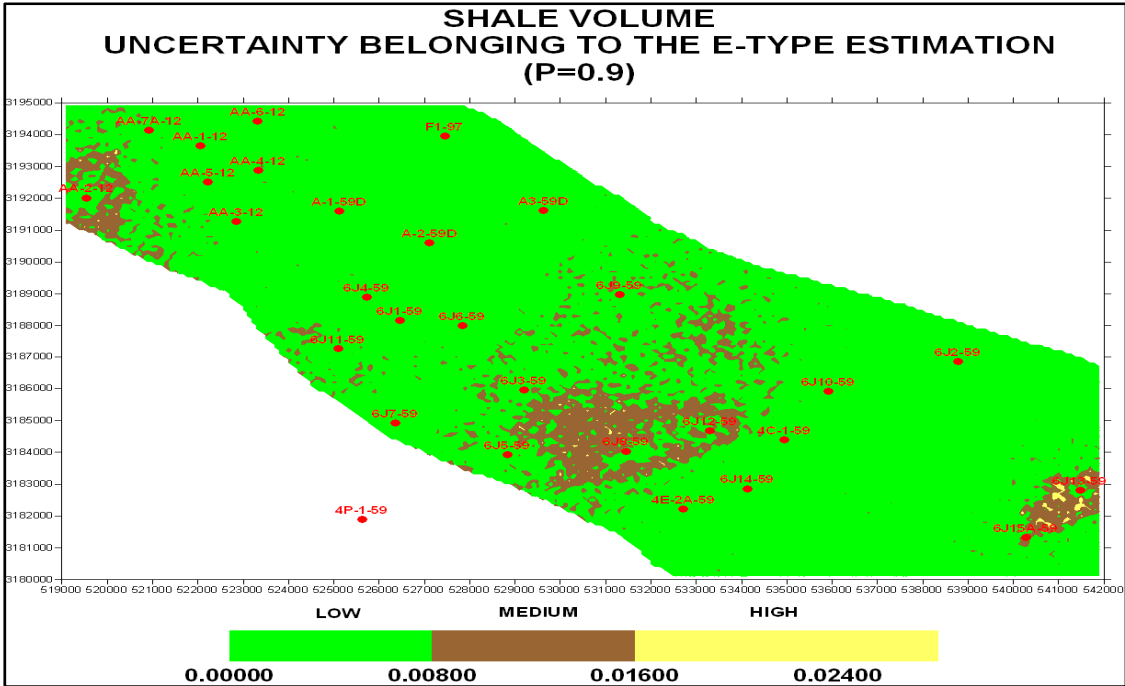
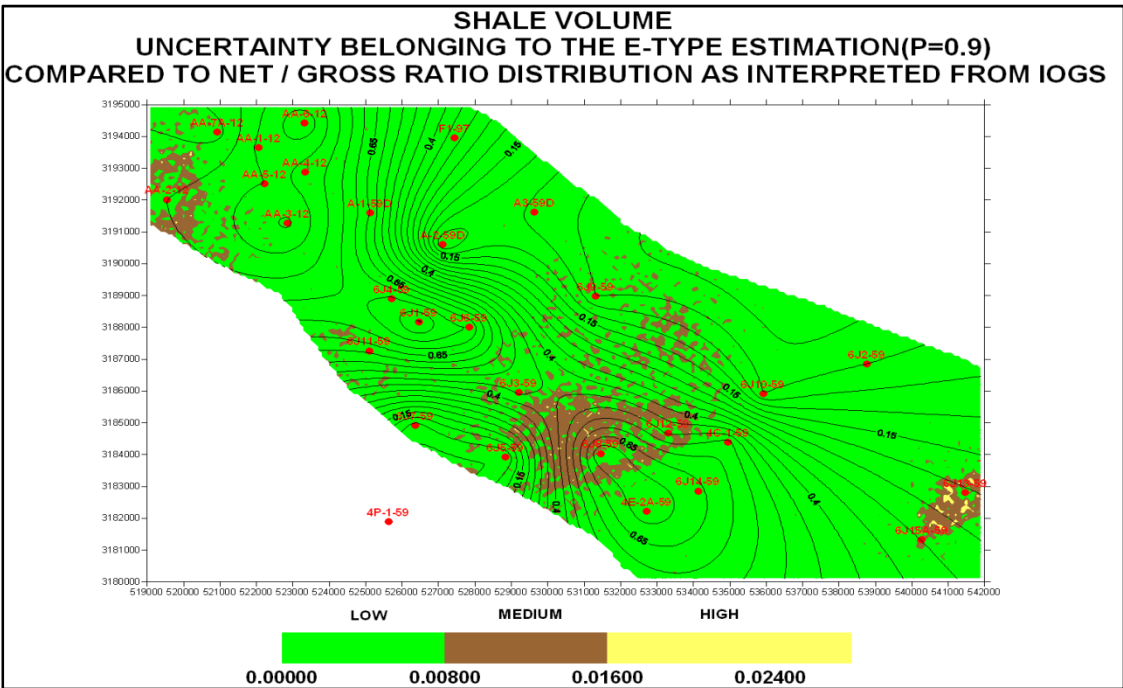


Fig. 4.10-13 Upper and lower bounding surfaces of E-type estimation for shale volume ( $p=0.9$ )



**Fig. 4.10-14 Map of uncertainty for well-averaged shale volume**



**Fig. 4.10-15 Net to gross thickness ratio in well locations**

## 5 DISCUSSION AND CONSLUSIONS

## 5.1 SEDIMENTARY CORE ANALYSIS

The studied Lower Nubian rock body has a high degree of variability throughout the reservoir section. The reservoir quality is a product of a complex interaction of primary (depositional) and

secondary (diagenetic) factors. The entire stratigraphic section has undergone pervasive diagenetic modifications to porosity and permeability.

There is no direct correlation between depositional facieses and core porosities and permeabilities. Majority of the Lower Nubian has been formed in braided fluvial channel environment. As a consequence, porosity-permeability trends display an extremely high degree of variability. **Fig. 5.1-1**

The core permeability and porosity data were used to perform the flow unit analysis in well 6J12. The results show, that roughly 78% of the total flow is coming from GHE (4.5.6), which provides only (30%) of the storage, whereas (22%) of the total flow is coming from GHE (2, 3), which provides (70%) of the storage capacity. On **Fig. 5.1-2**, the porosity-permeability trends display good clustering, if they are GHE coded. **Fig. 5.1-3**

The observed core does not exhibit any abundance of open fractures. Most of the fractures are closed, since they have been filled by quartz cementation and/or clay-minerals. This has been confirmed by the core measurements and quantitative log interpretation, too. Although production tests and DST indicated the same observation, the proving data sets are very limited. Nine reservoir layers have been identified in the LNU section, while four in LNM and one in LNB. These layers exhibit uniform lateral continuity, wherever they are not truncated by the erosion surface of PUK unconformity.

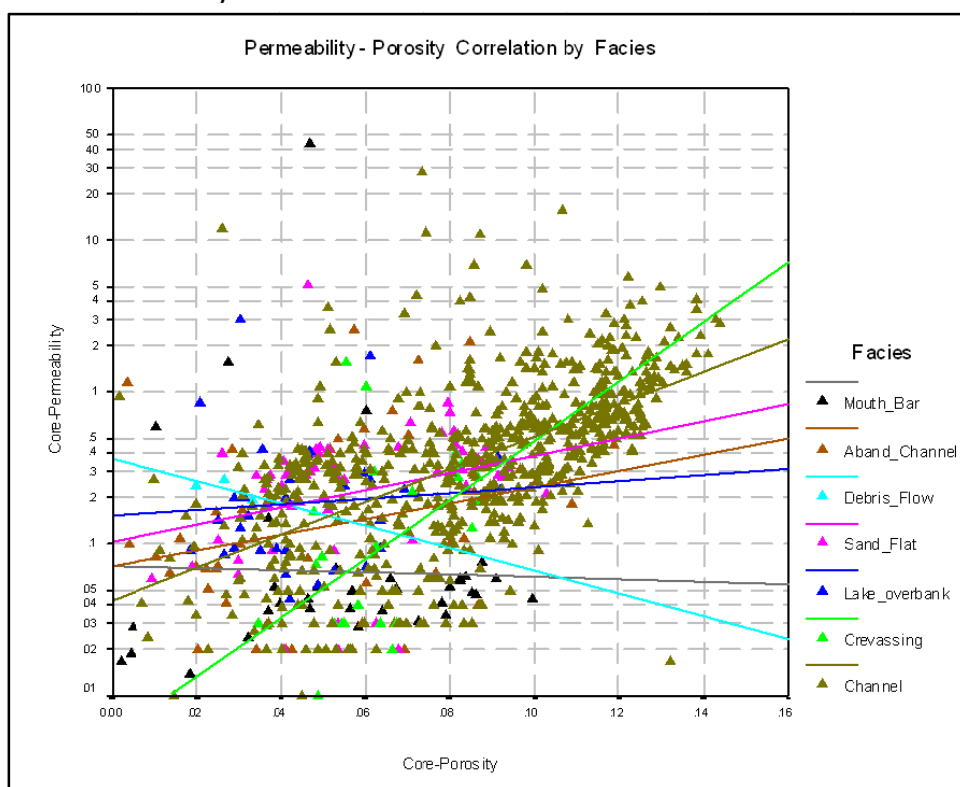


**Fig. 5.1-1 Porosity Permeability plots by facies**



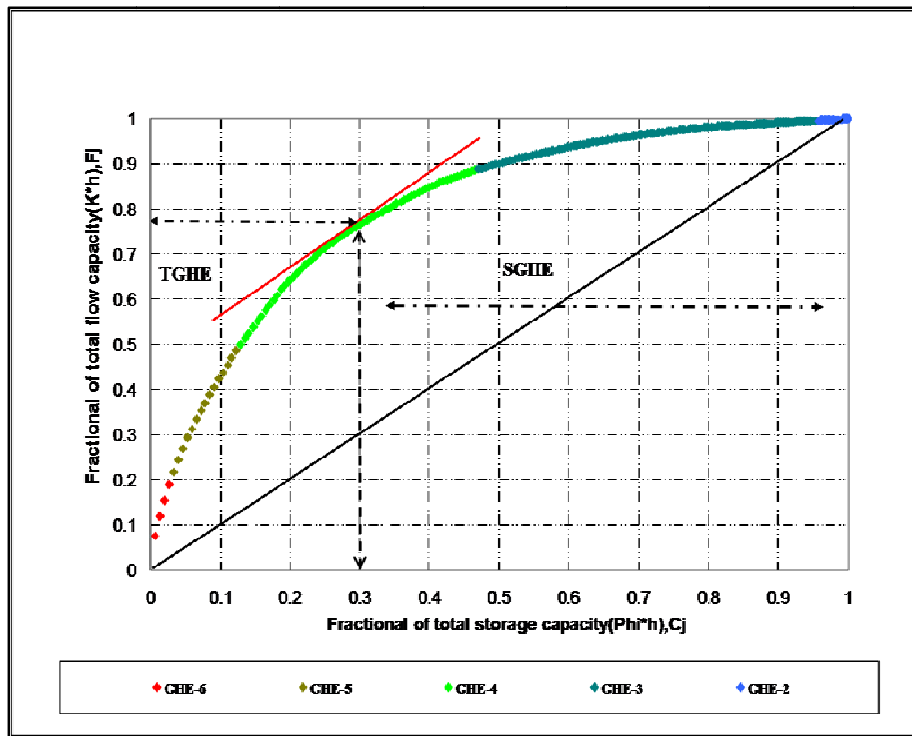


Fig. 5.1-2 Flow unite analysis using Lorenz plot

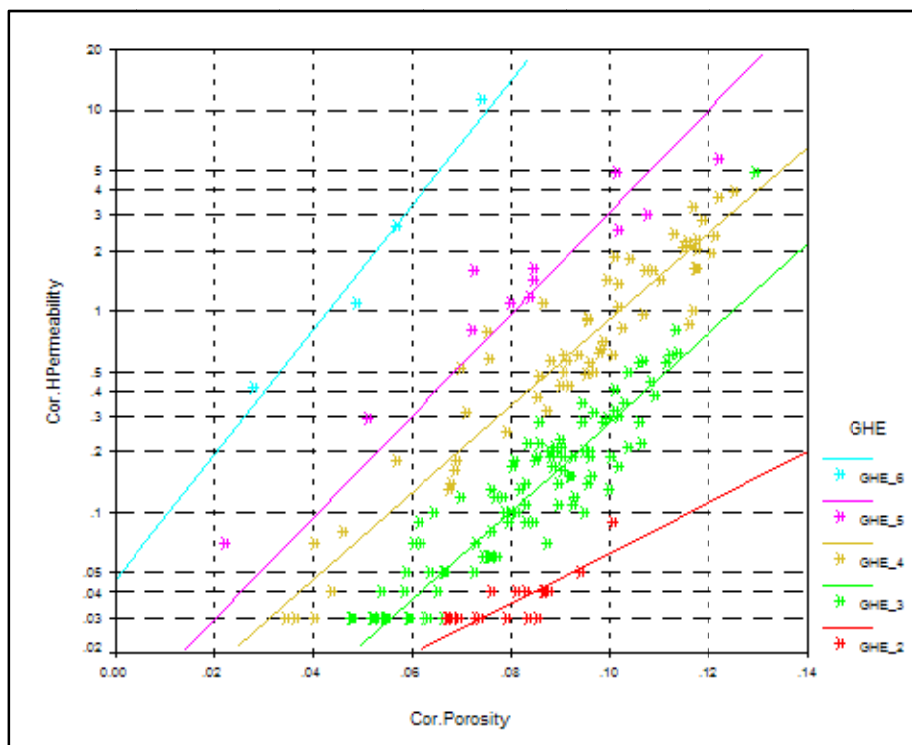


Fig. 5.1-3 Porosity permeability trends by flow units

## 5.2 LOG ANALYSIS

The resistivity curves, mainly (deep) and gamma ray (GR) ones, served excellent correlation **markers** for the Lowe Nubian sequences. (1) **PUK** surface appears with abrupt gamma ray readings. (2) **LNU-LNM** can be recognized as distinguishable boundary surface with resistivity -

gamma (right-left) cross over log shape. (3) **LNM-LNB** boundary surface show resistivity -gamma (left- right) cross over.

The **LNB** has high degree of heterogeneity and exhibit extremely low porosity and permeability values throughout the study area. This unite is characterized by smaller amount of clay content and exhibits higher sand fractions by comparing the overlying Nubian units. Reservoir quality appears to be highly variable throughout the interval.

The **LNM** has high GR and low resistivity levels, The highest shaliness content was observed from quantitative lithology evaluation (sand shale fractions). This unit is of typically sandwich-like development where sandstone and shale laminae change each other. The petrophysical properties of the sandstones are controlled by poorly sorted and variable grain size distributions.

The **LNU** sequence comprises of potentially good reservoirs. They can be characterized only on the basis of their porosity and permeability. In that way **LNU3**, **LNU2**, and **LNU1** are good, **LNU6**, **LNU5** and **LNU4** are weaker, however **LNU8**, **LNU7**, and **LNU9** are poor layers.

The **LNU** sequence in well **6J12**, where investigated on the basis of petro-type approach (Global Hydraulic Elements, GEH), The GHE variation was mapped against the observed facieses and results of log interpretation. The **LNU3**, **LNU2** and **LNU1** sections are dominated by GHE 3, 4 and 5. This is characteristic of moderate reservoir quality.

### **5.3 UNCERTAINTY ANALYSIS**

The estimation of uncertainties has been related to geological controls of heterogeneities. These controls, such as sedimentary facieses, diagenetic trace prints, and thicknesses variation can provide a detailed description of uncertainties. These results are very close to the natural phenomenon of petrophysical properties.

The regions of high uncertainty of the E-type estimations of permeability and shale volume appear mostly in three locations of the study area. They can be recognized on the basis of the highest parameter-fluctuations. This indicates that the effect of higher uncertainty in permabilities is masked by the high uncertainty in shale fraction.

In general, uncertainties associated with the reservoir properties can be related to the small scale heterogeneities of the reservoir rocks. The different uncertainties of reservoir rock properties, namely porosity, permeability and shale fraction, can be used together to study the reservoir quality controls around the wells, and even up to certain distances apart from the wells.

## 6 REFERENCES CITED

- ALLEN, D., COATES, G. and Muller, P., Ayoub, J., et al**, 1988: Probing for Permeability: An Introduction to Measurements, The Technical Review, Schlumberger, volume. 36, no. 1, 20 P.
- ARCHIE, G.E.**, 1952: The electrical resistivity log as an aid in determining some reservoir characteristics: Transactions AIME, v. 146, PP. 54-62.
- ARKINSON, C.D., MCGOWEN, J.H., BLOCH, S., LUNDELL, L.L. and TRUMBLY, P.N.**, 1990: Braidplain and Delatic Reservoir, Prudhoe Bay Field, Alaska. : In Sandstone Petroleum Reservoirs. Edited by Barwis, G., Mcpherson, J., Studlick, R., Springer-Verlag, PP. 7-26
- BARLAI, Z.**, 2000: Permeability - Hydraulic Conductivity of porous rocks; Equivalent pore-throat size In: The Structure of "FlexInLog" Software, Edited by Barlai, Z. and Kelemen, Z., Libyan Petroleum Internal report, unpublished.
- BARLAI, Z., CZEGLEDI, I. and MULLER, P.**, 1973: A Review of the Status of the Basic Well Logging and Interpretation Methods Applied in Hungary, Presented in SPWLA, 14 Annual Logging Symposium, 6-9 May, 29 P.
- BEARD, D. AND WEYL, P.**, .1973: Influence of texture on porosity and permeability of unconsolidated sands, AAPG Bulletin. 57, pp. 349-369.
- BJORLYKKE, K.**, 1989: Sedimentology and Petroleum Geology, Springer-Verlag, PP.71
- BRAYSHAW, A.C., DAVIES, G.W. and CORBETT, P.W.M.**, 1996: Depositional Controls on Primary Permeability and Porosity at the Bed form Scale in Fluvial Reservoir Sandstones: advances in fluvial .Dynamics and Stratigraphy. Edited by Carling, P.A. and Dawson M.R., Wiley and Sons Ltd., 530P
- BRAYSHAW, A.C., DAVIES, G.W. and CORBETT, P.W.M.**, 1996: depositional Controls on primary Permeability and Porosity at the Bedform Scale in Fluvial Reservoir Sandstones In: advances in Fluvial Dynamics and Stratigraphy, Edited by Carling, P.A. and Dawson, M.R., Wiley and Sons Ltd, 530 P.
- BRIDGE, J.S.**, 2003: River and Floodplains: Forms, Processes, and Sedimentary Record, Blackwell Publishing, PP 74, PP 272 and PP 275.
- CANNON, D.E. and COATES, G.R.**, 1990: Applying Mineral Knowledge to Standard Log Interpretation, Presented in SPWLA 31st Annual Logging Symposium, Lafayette, 24-27 June, paper V.
- CHILES,J.P. AND DELFINER, P.** (1999): Modeling Spatial Uncertainty. John Wiley & Sons. Inc. New York.
- CORBETT, P., and MOUSA, N.**, 2010: Petrotype-based Sampling Applied in a Saturation Exponent Screening Study, Nubian Sandstone Formation, Sirt Basin, Libya, PETROPHYSICS, VOL. 51, NO. 4, 7P
- CORBETT, P., ELLABAD, Y., and MOHAMED, K.**, 2001: The Definition of Transmissive-Dominated Hydraulic units (THU) and Storage-Dominated units(SHU) and their role in understanding of Reservoir Dynamics, Presented in the EAGE 63<sup>rd</sup> Conference and Technical Exhibition, Amsterdam, 11-15 June, 4 P.
- CORBETT, P.W., ZHENG, S., PINISETTI, M., MESMARI, A. and STEWART, G.**, 1998: The Integration Of Geology and Well Testing for Improved Fluvial Reservoir Characterization, Society Petroleum Engineers, Inc., Papper no.SPE 48880, PP.471-488.
- COSKUN, S.B., WARDLAW, N.C. and HAVERSLEW, B.**, 1993: Effect of comaction, texture and diagenesis on porosity, permeability and oil recovery in sandstones. Journal of Petroleum Science and Engineering, 8, PP. 279-292.

- COSKUN, S.B., WARDLAW, N.C. and HAVERSLEW, B.**, 1993: Effects of compaction, texture and diagenesis on porosity, permeability and oil recovery in sandstones. *Journal of Petroleum Science and Engineering*, 8, PP. 279-292.
- CRAIN, E. R.**, 2000: The Future of Petrophysics in Reservoir Description, Presented in the 1st Annual Well Log Analysis / Formation Evaluation Conference, Tripoli, Libya, 29 – 31 October, 11P.
- DEUTCH, C.**, 2002: *Geostatistics Reservoir Modeling*, Oxford, New York, Oxford University Press, PP.31-71.
- DEUTCH, C.V. AND JOURNEL, A.G.**, 1997, *GSLIB: Geostatistical Software Library and User's Guide*, Oxford University Press, New York. 2nd edition. p 376.
- DOUGLAS, J.C.**, 1982: Fluvial Facies Models and Their Application: In *Sandstone Depositional Environments*. Edited by Scholle, P.A. and Spearing, D., AAPG, Memoir 31, PP 115-136.
- DULLIEN, F.**, 1979: *Porous Media Fluid Transport and pore Structure*, Academic Press, PP 75-150.
- EATON, T.**, 2006: On the importance of geological heterogeneity for flow simulation, *Sedimentary Geology*, Elsevier, 184 (2006) 187, 201P.
- EVERETT, R., HERRON, M. and PIRIE, G.**, 1983: Log Responses and Core Evaluation case study Technique Field and Laboratory Procedures, Presented in SPWLA, 24<sup>th</sup> Annual Logging Symposium, 27-30 June, 26 P.
- FARRELL, F.G.**, 2001: Geomorphology, facies architecture, and high-resolution, non-marine sequence stratigraphy in avulsion deposits, Cumberland Marshes, Saskatchewan, *Sedimentary Geology*, Elsevier, 139(2002)93,-150P.
- FRIEDMAN, G.M. AND SANDERS, J.E.**, 1978: *Principles of Sedimentology*, Wiley and Sons Ltd., PP 219-228
- GALLOWY, W.E., HOBDAI, D.K.**, 1983: *Terrigenous Clastic Depositional Systems: Applications to Petroleum, Coal and Uranium Exploration*, Springer-Verlag, PP, 64 and PP, 537
- GARDINER, S., THOMAS, D., BOWERING, D. and MCMINN, L.**, 1990: A Braided Fluvial Reservoir, Peco Field, Alberta, Canada. : In *Sandstone Petroleum Reservoirs*. Edited by Barwis, G., McPherson, J., Studlick, R. Springer-Verlag, PP. 31-54.
- GOOVAERTS, P.**, 1997: *Geostatistics for Natural Resources Evaluation*, Oxford, New York, Oxford University Press, PP.9-20.
- GOOVAERTS, P.**, 2006, Geostatistical modeling of the spaces of local, spatial and response uncertainty for continuous petrophysical properties, in Coburn, T.C., Yarus, J.M. and Chambers, R.L. (eds), *Stochastic Modeling and Geostatistics: Principles, Methods and Case Studies, Volume II.*, AAPG Computer Applications in Geology 5. p.59-81.
- GOOVAERTS, P.**, 1998, *Geostatistics for natural resources evaluation*, Oxford University Press, Oxford, 483 p.
- GUCCIONE, M.J.**, 1993: Grain size distribution of overbank sediment and its use to locate channel positions: In *Alluvial Sedimentation*. Edited by Marzo and Puigdefabregas, Blackwell Scientific Publication, International Association of Sedimentologists, Special Publication Number 17, PP. 185-194
- HIETALA, R.W. and CONNOLLY, E.T.**, 1984: *Well Log Analysis Methods and Techniques*, AAPG memoir 38.
- HIETALA, R.W.**, 1990: The Process and Value of Petrophysical Integration, Presented in 1st Archie Conference, Houston, 22-25 October.
- HOOK, J., R.**, 2003: An Introduction to Porosity, *PETROPHYSICS*, VOL. 44, NO.3, PP.205-212.
- ISAAKS, E. and SRIVASTAVA, R.**, 1989: *An Introduction to Applied Geostatistics*. New York, Oxford, Oxford University Press, PP. 11-39.

- JENSEN, J.L., LAKE, L.W., CORBETT, P.W.M., and GOGGIN, D. J.**, 2000: Statistical for Petroleum Engineers and Geoscientists. 2<sup>nd</sup> Edition, Elsevier, 338 P.
- JIA, L., ROSS, C.M and KOVSCEK, A.R.**, 2005: A Pore Network Modeling Approach to Predict Petrophysical Properties of Diatomaceous Reservoir Rock, Society of Petroleum Engineers Inc, paper no. SPE93806, 12 P.
- JOURNEL A.G.**, 1999: Past, present and future of petroleum geostatistics, Stanford University Special Report of the Stanford Center of Reservoir Forecasting.
- JOURNEL, A.G.** 1983: Non-parametric estimation of spatial distributions.—Journal of the International Association of Mathematical Geology. 15. 445-468
- KELEMEN, Z.**, 2000: Techniques for Corrections of input Well Logs, Presented in the 1st Annual Well Log Analysis / Formation Evaluation Conference, Tripoli, Libya, 29 – 31 October, 10P.
- KENNEDY, J., COX, A. and ALDRED, R.**, 2010: Using Quantified Model Based Petrophysical Uncertainty to aid in Conflict Resolution, Presented in the SPWLA 51<sup>st</sup> Annual Logging Symposium, Perth, Australia, 19-23 June, 12P.
- LARESNI, G. and CHILINGAR, G.**, 1979: Diagenesis in Sediments and Sedimentary Rocks, Elsevier Scientific Publishing Company, PP.31-90.
- MAYER, C. and SIBBIT, A.**, 1980: New Approach to Computer-Processed Log Interpretation, presented at the SPE Annual Technical Conference and Exhibition, Dallas, 21-24 September, paper SPE 9341.
- MIALL, A.D**, 1996: The Geology of Fluvial Deposits, Sedimentary Facies, Basin Analysis, and Petroleum Geology, Springer, PP 175 and PP.273-276.
- MJOS, R., WALDERHUGE, O., and PRETHOLM, E.**, 1993: Crevasse splay sandstone geometries in the Middle Jurassic Ravenscar Group of Yorkshire, UK: In Alluvial Sedimentation, Edited by Marzo and Puigdefabregas, Blackwell Scientific Publication, International Association of Sedimentologists, Special Publication Number 17, PP.167-184.
- MUELLER, D., and DALY, C.**, 2004, Characterisation and Modelling of Fractured Reservoirs: Static Model: presented in the European Conference on the Mathematics of Oil Recovery-Cannes, France, 30 August - 2 September
- MURRAY, C.**, 1994: Identification and 3-D Modeling of Petrophysical Rock Types: In Stochastic Modeling and Geostatistics Principles, Methods, and Case Studies. Edited by Yarush, J.M. and Chambers, R.L., AAPG Computer Applications in Geology, No.3, PP. 323-337.
- PANATIER, Y**, 1996, VARIOWIN Software for Spatial Data Analysis in 2D, Springer-Verlag New York, p.90
- PETTIJOHN, F., POTTER, P. and SIEVER, R.**, 1972: Sand and Sandstones, Springer-Verlag, PP 93-97.
- QUIREIN, J., KIMMINAU, S., LAVIGNE, J., SINGER, J. and WENDEL, F.**, 1986: Coherent Framework for Developing and Applying Multiple Formation Evaluation Models, Presented in SPWLA 27th Annual Logging Symposium, Houston, 9-13 June, paper DD.
- SELLEY, R.**, 1988: Applied Sedimentology, Academic Press, PP.63-71.
- SERRA, O. and ABBOT, H.T.**, 1980: The Contribution of Logging Data to Sedimentology and Stratigraphy, Society of Petroleum Engineers, paper no. SPE9270.
- SERRA, O.**, 1989: a Guide for Well Log Interpretation of Siliciclastic Deposits (Clay, Silt, Sand, Shales), Schlumberger Technical Services, 211 P.
- SERRA, O.**, 1989: Sedimentary environments from wireline logs: Schlumberger Technical Services, 234 p.

- SRIVASTAVA, R.M., 1994**, An overview of stochastic models for reservoir characterization, in Jarus, J.M. and Chambers, R.L. (eds), Stochastic modeling and geostatistics: Principles, methods and case studies. AAPG Computer Applications in Geology 3. p 3-16.
- THOMEER, J., 1983**: Air Permeability as a function of three pore-Network Parameters, Society of Petroleum Engineers of AIME, paper no. SPE 10922, PP. 809-814.
- TIMUR, A., 1968**: An Investigation of Permeability, Porosity, and Residual Water Saturation Relationships, Presented in SPWLA, 19<sup>th</sup> Annual Logging Symposium, 23-27 June, 18 P.
- VERLY, G. 1986**: MultiGaussian kriging—A computer case study. In R.V. Ramani, editor, Proceedings of the 19th International APCOM Symposium. pp.283-298. Littleton, CO. Society of Mining Engineers.
- WAHA OIL COMPANY, 2004**: Preliminary Data Assembly Report, Proprietary report.
- WAHA OIL COMPANY, 2005**: N. Gialo Field, Geology and Geophysics, Proprietary report.
- WAHA OIL COMPANY. 2008**: North Gialo Core Study Phase 1 Report v1, internal company document (Confidential unpublished)
- WEBSTER, R. and OLIVER, M., 2007**: Geostatistics for Environmental Scientists, John Wiley and Sons, Ltd, PP12-35.
- WILSON, M. J., AND PITTMAN, and E.D., 1977**: Authgenic clays in sand stones Recognition and influence on reservoir properties and palaeo-environments analysis, Journal of Sedimentary Petrology, 47. Pp, 3-31.
- WINGLE, W.L. AND POETER, E.P., 1993**, Uncertainty associated with semivariograms used for site simulation, Ground Water, v.31, p. 723-734.
- ZHENG, S., CORBETT, P.W., RYSETH, A., and STEWART, G., 2000**: Uncertainty in well test and core permeability analysis: A case study in fluvial channel reservoirs, Northern Sea, Norway, AAPG Bulletin, vol. 84, No12, PP.1929-1954

## 7 SUMMARY

The area studied is situated in the eastern portion of the Sirte Basin. The objective of this study was to reveal and measure uncertainties associated with micro-, macro- and megascale of the Lower Nubian reservoir rock heterogeneities by utilizing the application of geostatistics in clastic reservoir characterization. This has been solved via integration of all the available data (routine core analysis, log analysis, core description, etc) from two oil fields, namely North Gialo and Farigh. However, the focus was mostly on North Gialo (6J) area, owned by Waha Oil Company.

Cores of 1000 ft of total length come from five wells penetrated the Lower Nubian were described for identifying rock types building up the reservoirs, interpreting sedimentary structures and revealing the main depositional facies. Eight depositional facies have played significant roles in the accumulation of the reservoir rocks. Each facies represents a distinct association of lithology, grain-size, and sedimentary structures. They have been categorized into three main facies associations: Braided Stream, Estuarine/Deltaic and Fluvial Facies associations. The studied Lower Nubian rock body presents a high degree of variability throughout the reservoir section. The reservoir quality is a product of a complex interaction of primary (depositional) and secondary (diagenetic) factors. The entire stratigraphic section has undergone pervasive diagenetic modifications to porosity and permeability.

The quantitative well log analysis of eleven wells selected from the North Gialo oil field and seven wells from Farigh oil field was performed to identify the main Lower Nubian reservoirs in each processed intervals and to characterize them on the basis of lithological (sand/shale ratio) and petrophysical characteristics (effective porosity, permeability). The processed intervals were distributed into lithological and hydraulic units depending on the results of former lithological and petrophysical evaluations. Each formation unit were divided into several layers from which the most important sand body reservoirs could be identified. The LNB unit exhibits high degree of heterogeneity and it has extremely low porosity and permeability values throughout the study area. The unit LNM has the highest shale content as observed from quantitative lithology evaluation (sand shale fractions), while the LNU sequence comprises of potentially good reservoirs.

All unit tops of Lower Nubian and their sub-sequences were picked up from the log correlation. The Lower Nubian stratigraphic sequence has been interpreted as flow units, when stratigraphic

layers of similar materials that are adjacent. That is, contiguous units of predominantly sand are regarded to be one flow-unit that would be thought of as a reservoir. Likewise, layers of shale that were arranged such that they formed a contiguous fine layer of low permeability would be lumped together to form a barrier. The resistivity curves, mainly (deep) and gamma ray (GR) ones, served excellent correlation markers for the Lower Nubian flow units.

The Base, Middle and Upper units of Lower Nubian stratigraphic sequence has been further interpreted as series of petrophysical zones or layers. The zoning process had ended into three packages of petrophysical layers belonging to each of the Base, Middle and Upper units of Lower Nubian. The determination of such petrophysical layer was carried out by the overlaying separation of density being on neutron log, and thorium being on potassium log, and by the distribution of net thickness intervals. This latter one was that gross thickness cutoff belonging to the values of petrophysical parameters having been obtained from well log analysis.

The reservoir characteristics of the reservoir layers were discussed in terms of their petrophysical characteristics (observed from deterministic log analysis and core measurements) and the facieses contained. These properties were summarized for each of the nine reservoir zones of the Upper Unit (LNU), four reservoir zones of the Middle Unit (LNM) unit and one reservoir zone of the basal unit (LNB). In that way LNB and LNM are non reservoir intervals, meanwhile LNU3, LNU2, and LNU1 are good reservoirs, LNU6, LNU5 and LNU4 are weaker, however LNU8, LNU7, and LNU9 are poor layers.

Relationship between the core permeability and porosity was studied as function of depositional facieses. The results have showed that depositional environments have had not any affect on the porosity-permeability relation. However the porosity-permeability plot display good clustering, if they are GHE coded.

The geostatistical analysis of the uncertainty of spatial distributions of the petrophysical properties belonging to the Lower Nubian sequences was achieved by generating 200 equally probable realizations using sGs approach. The simulation domain, laterally covers the study area, consists of 28 well data of well averaged porosities, permeabilities and shale fraction volumes. These averages were obtained from quantitative well log analysis and related to the Lower Nubian net thickness. Because of the bottom elevations of the controlling wells, the uncertainty of spatial distributions can be characteristics mainly for the upper part of the Lower Nubian sequence. The



geological controls of heterogeneities, such as sedimentary facieses, diagenetic trace prints, and thicknesses variation can provide a detailed explanation of causes of uncertainties. Higher uncertainty in permeabilities is masked by the high uncertainty in shale fraction. The regions with higher uncertainty in porosity have been compared to trends of tectonic elements. The different degree of uncertainties of porosity, permeability and shale fraction, can reveal the reservoir quality.

## **8 SUMMARY in HUNGARIAN**

A vizsgált terület a Sirte-medence K-i részén helyezkedik el. A vizsgálat célja az Alsó Núbiai szénhidrogén tároló kőzetek mikro-, makro – és megaléptékű heterogenitásával kapcsolatos bizonytalanságok feltárása és mérése volt. Ennek során két olajmező a North Gialo és a Faraigh mezők összes rendelkezésre álló adatának (rutin magvizsgálatok, geofizikai lyukszelvény vizsgálatok, magleírások, stb.) integrálása útján geostatisztikai elemzések készültek. Az elemzés súlypontja a WAHA olajtársaság tulajdonában levő North Gialo (6J) terület volt.

A makroszkópos elemzések során az Alsó Núbiai sorozatot harántolt öt fúrás mintegy 1000 láb (kb. 330 méter) maganyagának feldolgozása történt. Az elemzés célja alapvetően az üledékes szerkezetek értelmezése és a tároló fontosabb üledékes fácieseknek meghatározása volt. Nyolc üledékes fácies játszott meghatározó szerepet a tároló üledékes sorozatának felhalmozódásában. Minden egyes fácies megkülönböztetett litológiai, szemcsemérete és üledékszerkezet sorozatot képvisel. Ezek a vizsgálatok során három fácies-asszociációba lehetett sorolni. Ezek a fonatos zóna, eszturium/delta, és meanderező folyóvízi sorozatok voltak.

A vizsgált kőzettest a tároló-kifejlődésekben nagy-fokú változékonyságot mutat. A tároló képesség az elsődleges (felhalmozódási) és másodlagos (diagenetikus) folyamatok komplex kölcsönhatásának eredményeként alakult ki. A teljes rétegtani sorozat a permeabilitás és porozitás erőteljes diagenetikus módosulásán ment át.

A kvantitatív karotázs értelmezés a North Gialo mező tizenegy és a Faraigh mező hat fúrására történt. Ennek célja az Alsó-Núbiai tárolórendszer egyes tároló zónáinak azonosítása és a zónák litológiai (homok-agyag arány), és kőzetfizikai (porozitás, permeabilitás) alapú jellemzése volt. Az egyes tároló szakaszokat a korábbi litológiai és kőzetfizikai értékelések alapján kőzettípus és hidraulikai zónákra bontottuk. Minden egyes ilyen zóna további rétegre lett felosztva amelyekből a

legfontosabb homokos tároló azonosítható volt. Az LNB egység nagyfokú heterogenitást mutat. A teljes területen extrém alacsony porozitás és permeabilitás értékekkel jellemezhető. Az LNM egységnek van a legmagasabb agyagtartalma a kvantitatív geofizikai szelvényértelmezés szerint. Az LNU egység tartalmazza a legjobb potenciális tárolót.

Az Alsó-Núbiai sorozatnak és valamennyi egységének tető-azonosítása a geofizikai szelvények korrelációjából származik. Az Alsó-Núbiai rétegtani sorozatot áramlási egységekként értelmeztük, minden olyan helyen, ahol hasonló kifejlődések érintkeztek. Azaz, a főleg homokkőből álló folytonos egységeket egy áramlási egységként és tárolóként kezeltük. Hasonlóképpen, a kis permeabilitású vékony, folytonos egységeiből álló rétegeket összevontuk és áramlási gátként értelmeztük. Az ellenállás (főként a mélybehatolású) és gamma (GR) szelvények jó korrelációs markereket biztosítottak az Alsó-Núbiai áramlási egységek korrelációjához.

Az Alsó-Núbiai rétegtani sorozat alsó, középső és felső egységeit a továbbiakban kőzetfizikai zónák vagy rétegek sorozataként értelmeztünk. A zonációs folyamat eredményeként az alsó, középső és felső egységeket a kőzetfizikai rétegek három csomagjára bontottuk. Az ilyen kőzetfizikai zónák meghatározása a sűrűség-neutron és tórium-kálium plotok egymásra helyezésével kapott átfedő zónák, valamint az effektív vastagság intervallumok eloszlása alapján történt. Ez utóbbi az a teljes vastagsági vágási érték, amely a geofizikai szelvényvizsgálatból származó kőzetfizikai paraméterhez tartozik.

Az üledékes rétegek tároló jellemzését kőzetfizikai (geofizikai értelmezések és magmérések) és üledékes fácies oldalról egyaránt megadtuk. A tulajdonságokat a Felső egység (LNU) kilenc, a Középső egység (LNM) négy és a Bazális egység (LNB) egy tároló zónájára összegeztük. Így módon az LNB és LNM egységek nem bizonyultak tárolónak, az LNU3, LNU2, és LNU1 egységek jó tárolók, az LNU6, LNU5 és LNU4 gyengébb tárolók, míg az LNU8, LNU7, és LNU9 gyenge tárolók.

A magon mért porozitások és permeabilitások közötti kapcsolatot az üledékes fácies függvényeként elemeztük. Az üledékes fáciesnek nincs közvetlen hatása a magon mért porozitás és permeabilitás kapcsolatra. Ugyanakkor a porozitás-permeabilitás digram jól csoportosuló pontokat mutat, ha a mintákat GHE kóddal látjuk el.

Az Alsó-Núbiai sorozat kőzetfizikai tulajdonságai térbeli eloszlása bizonytalanságának geostatisztikai elemzése Szekvenciális Gaussi szimulációval történt (sGs). Ennek során 200

azonosan valószínű realizációt állítottunk elő. A szimulációval vizsgált térrészen 28 fúrásból származó kútra átlagolt porozitás, permeabilitás és agyagtartalom adatot használtunk. Az átlagok a kvantitatív geofizikai értelmezés adatsoraiból származnak és átfogják a teljes Alsó-Núbiai sorozatot. A rendelkezésre álló fúrások talpértékei alapján a térbeli eloszlások bizonytalansága főként az Alsó-Núbiai sorozat felső részét jellemzik. A heterogentiás geológiai tényezők, mint pl. üledékes fácies, diagenézis és vastagság változatosság a bizonytalanság okainak részletes magyarázatát adják. A permeabilitás nagyobb bizonytalanságait elfedi az agyagfrakció térbeli bizonytalansága. A porozitás nagy bizonytalanságainak területi eloszlást összehasonlítottuk a tektonikai elemek trendjével. A porozitás, permeabilitás és agyagtartalom bizonytalanságának különböző foka a tároló minőséget erősen meghatározza.